PB88-132980

APPLICATION OF MECHANICS TO ROADSIDE SAFETY

Research, Development, and Technology
Turner-Fairbank Highway Research Center
6300 Georgetown Pike
McLean, Virginia 22101-2296

U.S. Department of Transportation
Federal Highway Administration

Report No.
FHWA-TS-87-228

February 1987

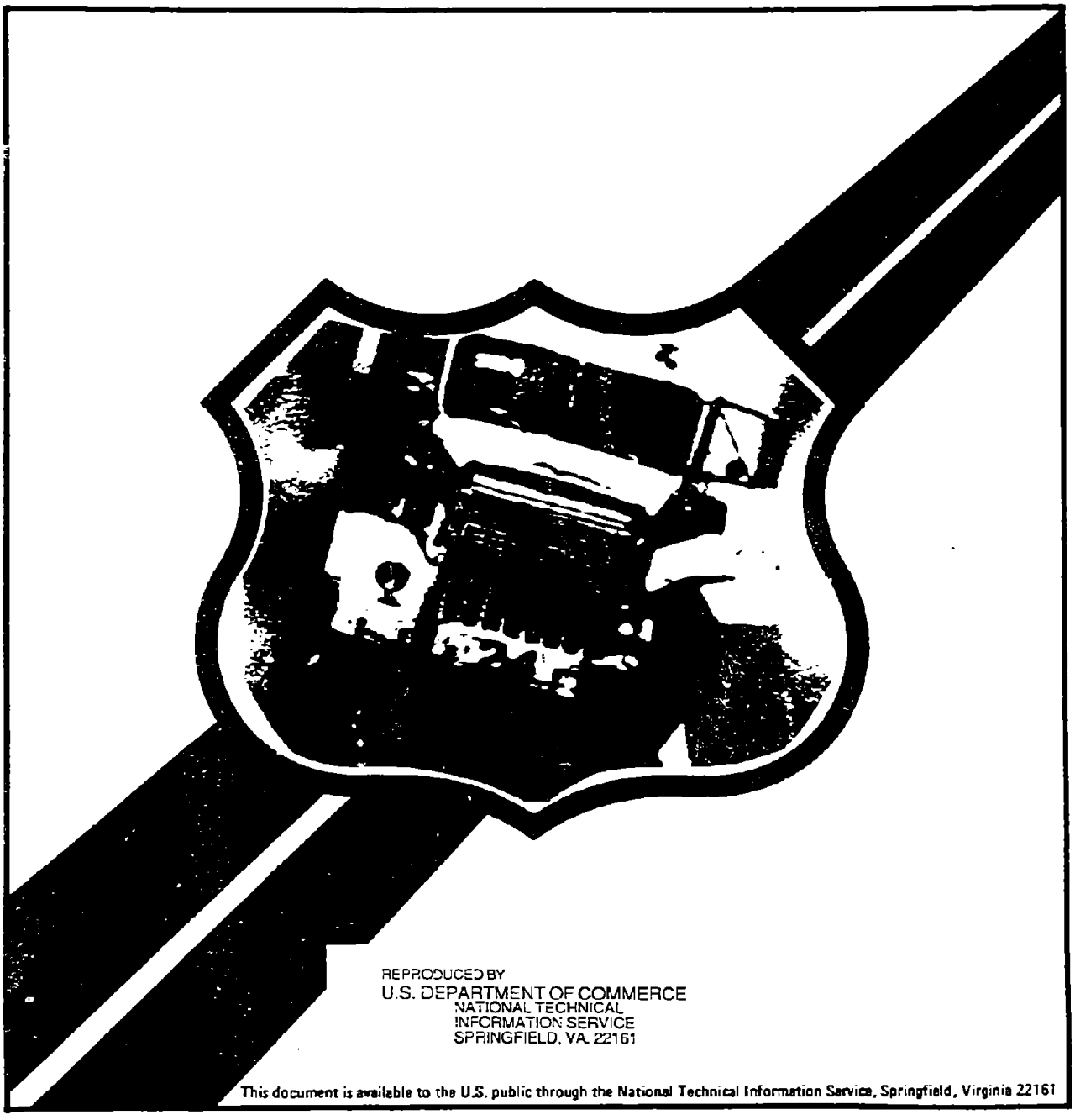

FOREWORD

This report describes the concepts of mechanics - system of units, Newton's second law, rigid body mechanics, friction, momentum, and energy and work - as they relate to roadside safety design. Following the review of the important concepts of mechanics, the report addresses vehicle characteristics, human injury criteria, and details of highway safety hardware design.

The report is written for readers who wish to increase their knowledge of highway appurtenances and their functions. It will be valuable to highway engineers and researchers who are initially becoming involved with highway safety.

Copies of this report are available from the National Technical Information Service, 5285 Port Royal Road, Springfield, Virginia (703) 487-4690.

NOTICE

Technical Report Documentation Page

1. Report No.	2. Government Accession No.	3. Recipient's Catalog No.
FHWA-TS-87-228	PB88 [illegible] GAS	

4. Title and Subtitle	5. Report Date
APPLICATION OF MECHANICS TO ROADSIDE SAFETY	February, 1987
	6. Performing Organization Code
	8. Performing Organization Report No.
7. Author(s)	5003-2
Raymond P. Owings	
9. Performing Organization Name and Address	10. Work Unit No. (TRAIS)
RHOMICRON, Inc. Box 404 Fairfax Station, VA. 22039	11. Contract or Grant No. DTFH61-85-C-00128
	13. Type of Report and Period Covered
12. Sponsoring Agency Name and Address	Final September, 1985 to February, 1987
Federal Highway Administration Office of Implementation 6300 Georgetown Pike McLean, VA 22101-2296	14. Sponsoring Agency Code

15. Supplementary Notes

Contracting Officer's Technical Representative:
Mr. James Wentworth

16. Abstract

This report summarizes the analysis procedures and concepts used by the highway research community to design roadside safety appurtenances. The concepts of momentum, kinetic energy and work are presented. Applications to the design of impact attenuators, breakaway hardware, and longitudinal barriers are discussed.

The objective of the report is to present the state of the practice in applying mechanics to the design of roadside safety appurtenances.

17. Key Words	18. Distribution Statement
Human Injury Mechanics Safety Appurtenances Longitudinal Barriers Impact Attenuators Breakaway Hardware	No restrictions. This document is available to the public through the National Technical Information Service, Springfield, VA 22161

19. Security Classif. (of this report)	20. Security Classif. (of this page)	21. No. of Pages	22. Price
Unclassified	Unclassified	170	PC $19.95 / A09

Form DOT F 1700.7 (8-72) Reproduction of completed page authorized

TABLE OF CONTENTS

LIST OF FIGURES

LIST OF FIGURES (continued)

LIST OF TABLES

INTRODUCTION

This report summarizes the analysis procedures and concepts used by the highway research community to design roadside safety appurtenances. The concepts of momentum, kinetic energy and work are presented. Applications to the design of impact attenuators, breakaway hardware, and longitudinal barriers are discussed.

a. Objective

The objective of the report is to present the state of the practice in applying mechanics to the design of roadside safety appurtenances.

The basic approach is to bring together the analysis procedures which have been developed by the highway research community into a single report. The purpose of this effort is to disseminate this existing knowledge to a wide spectrum of the highway community to facilitate the effective application of safety appurtenances.

b. Organization

The report is divided into eleven sections. The first four serve to introduce the fundamental concepts of mechanics and to define a system of units for the report. Sections 4 and 5 discuss the inertial and crush characteristics of vehicles. The subject of human injury is discussed in section 6 with emphasis on human injury criteria. This chapter provides the basis for evaluating the performance of safety appurtenances based on the protection of the occupants of the impacting vehicle. Characteristics of safety appurtenances are next discussed. Included in this section are examples of the values of inertial characteristics of breakaway supports and a discussion of the forces acting on soil-embedded posts of longitudinal barriers. The last three sections

present the design procedures used to design impact attenuators, breakaway hardware, and longitudinal barriers.

c. System of Units

The application of mechanics requires that a system of units of measurement be adopted to quantify physical characteristics. A system of units means a set of units of force, mass, and acceleration in which Newton's Second Law can be written F=MA. This means that a unit of force will produce a unit of acceleration when the force acts on a particle with unit mass.

(1) British Engineering System. In this report the primary system of units is the British Engineering System (BES). In this system, the unit of mass is the slug, the unit of force the pound and the unit of acceleration is one ft/sec/sec. Many times the weight of the vehicle is mistakenly used interchangeably with the mass. The weight of the vehicle is equal to the product of the mass of the vehicle and the acceleration of gravity. Based on the standard value of gravity, 32.174 ft/sec/sec, a body weighing 32.174 pounds on earth has a mass of one slug. For example, an 1,800 pound vehicle has a mass of 55.95 slugs.

Despite the desire to use a single set of units, additional units must be introduced because of everyday usage. Speed is traditionally measured in miles per hour not ft/sec. Acceleration is many times measured in G's, not ft/sec/sec.

(2) Modernized Metric System. A major effort to standardize a system of units for international use has resulted in the International System of Units (SI). SI units are divided into three classes

1. Base units
2. Supplemental units
3. Derived units

Base units are by convention regarded as dimensionally independent. The Base units for the SI system are shown in table 1. and the Supplemental units in table 2. Derived SI units related to mechanics and with application to this report are given in table 3.

The comparison of the BES and SI systems is shown in table 4. Tables to convert from BES units to SI units are given in appendix A.

Table 1. Base SI units.

Quantity	Unit	Symbol
length	meter	m
mass	kilogram	kg
time	second	s
electric current	ampere	A
thermodynamic temperature	kelvin	K
amount of substance	mole	mol
luminous intensity	candela	cd

Table 2. Supplementary SI units.

Quantity	Unit	Symbol
plane angle	radian	rad
solid angle	steradian	sr

Table 3. Selected derived SI units with special names.

Quantity	Unit	Symbol	Formula
frequency	hertz	Hz	1/s
force	newton	N	$kg*m/s^2$
pressure	pascal	Pa	N/m^2
energy	joule	J	N*m
power	watt	W	J/s

Table 4. Comparison of units.

Quantity	BES	SI
force	pounds	newtons
mass	slugs	kilograms
length	feet	meters
time	seconds	seconds
pressure	lbs/ft^2	pascal
energy	ft-lb	joule
power	ft-lb/sec horsepower	watt

d. Notation

The notation for this report is based on :

A. A right hand coordinate system (X,Y,Z) see figure 1.
B. X-Y plane is the horizontal plane
C. Z axis upward
D. Scalar quantities are given in normal type
E. Vector quantities are given in bold type
F. A dot over a variable indicates the time rate of change of the variable (d/dt)
G. Two dots over a variable indicate the second time derivative of the variable.
H. pi=3.14159

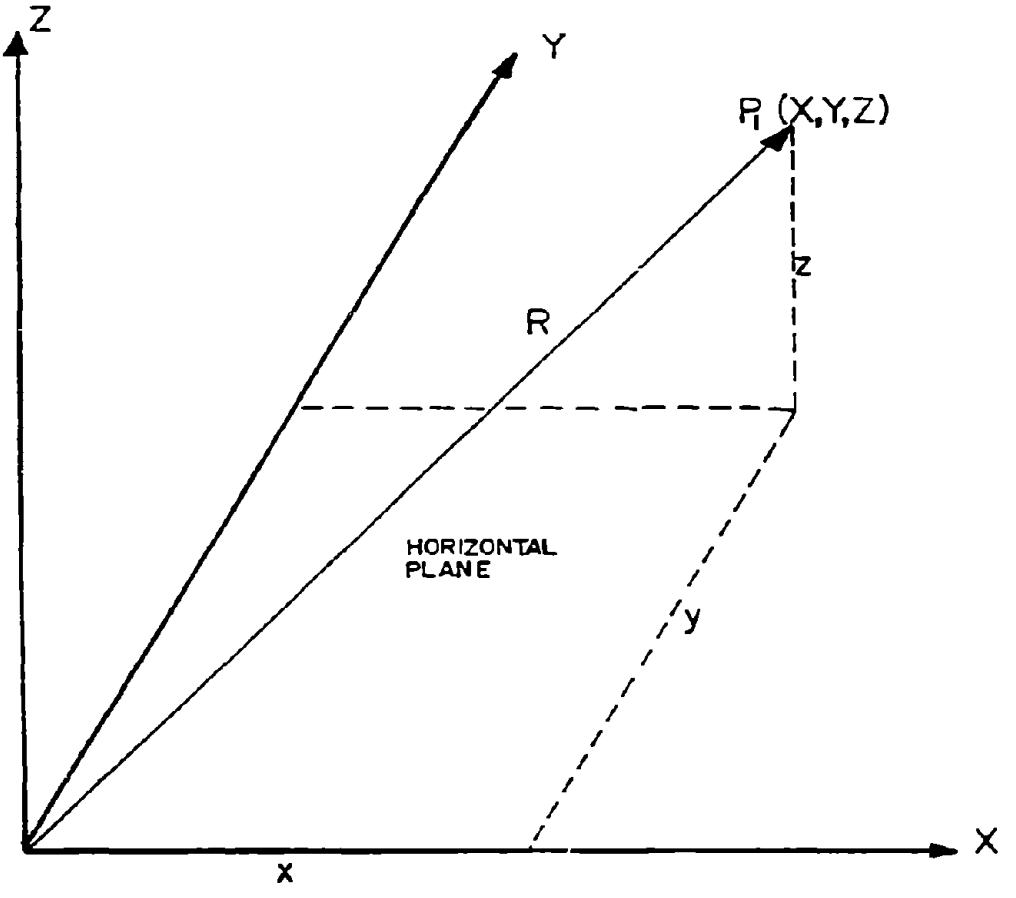

Figure 1. Coordinate system used in report.

1. Fundamentals

Mechanics deals with the motion of material bodies. It has many applications in the design of a safer roadside environment. This section reviews the fundamental concepts of Newtonian Mechanics.

a. Newton's Second Law

The most well known equation of mechanics relates the net force acting on a particle to the product of its acceleration and mass (**F=MA**). The concepts of force and mass are intuitive. However, the concept of acceleration (the time rate of change of velocity) is not so intuitive.

To investigate the meaning of acceleration consider the case of simple linear motion where a mass particle is decelerated at a constant rate A_x. The expressions for the velocity and displacement of the particle are given by:

$$\ddot{X} = -A_x \qquad (1)$$

$$\dot{X} = V_x(t) = V_o - A_x t \qquad (2)$$

$$X = V_o\, t - 0.5\, A_x t^2 + X_o \qquad (3)$$

where

$V(t)$ = speed at time t
$X(t)$ = displacement at time t
V_o = initial speed
X_o = initial displacement
A_x = Deceleration level

These equations may be used to answer the question "what period of time is required to stop the vehicle?" Using equation (2),

we have for T_f (time to stop):

$$T_f = V_o/A_x \qquad (4)$$

A second question is "How far will the vehicle travel in this period of time?" Using equations (3) and (4), we have for the distance traveled:

$$(X_f - X_o) = 0.5\ V_o^2/A_x \qquad (5)$$

One use of these equations is to estimate the forces that must be generated by an impact attenuator to arrest a vehicle. For a vehicle traveling at 60 mi/h to stop in a distance of 23 ft assuming a constant acceleration, the required deceleration is:

$$\begin{aligned} A_x &= (88)^2/(2\ 23) \qquad (6) \\ &= 168.3 \text{ ft/sec/sec} \\ &= 5.23 \text{ G's} \end{aligned}$$

Using Newton's Second Law, the required force is:

$$\begin{aligned} F &= M\ 168.3 \qquad (7) \\ &= W\ 5.23 \end{aligned}$$

where M = Mass of the vehicle
W = Weight of the vehicle

Thus the required force will depend on the weight of the impacting vehicle. For an 1,800 lb vehicle, the force required will be 9,414 lb. For a 4,500 lb vehicle, the force required will be 23,535 lb.

Stiffness of material bodies is often represented by a massless spring. The spring produces a resistive force in

proportion to its deflection. Consider a the case of a vehicle impacting a rigid narrow object. If the impact force acts through the center of mass, the vehicle can be represented as a particle. The crush characteristics of the vehicle are represented as a linear spring of stiffness K, lb/ft. Figure 2 shows the model. The equation of motion is given by:

$$M\ddot{X} + K X = 0 \qquad (8)$$

where K = stiffness of spring (lb/ft)

This second order differential equation has a solution given by:

$$X = B \sin wt + C \cos wt \qquad (9)$$

where C = a constant to be determined from the initial conditions

B = a constant to be determined from the initial conditions

$w = \sqrt{K/M}$ (radians per second)

f = natural frequency = w/(2 pi)

for the initial conditions of $X(0)=0$ and $V(0)=V_o$, the equation becomes:

$$X = (V_o/w) \sin wt \qquad (10)$$

For an 1,800 lb vehicle and a stiffness of 18,000 lb/ft, the natural frequency is given by:

$$f = 2.86 \text{ hertz} \qquad (11)$$

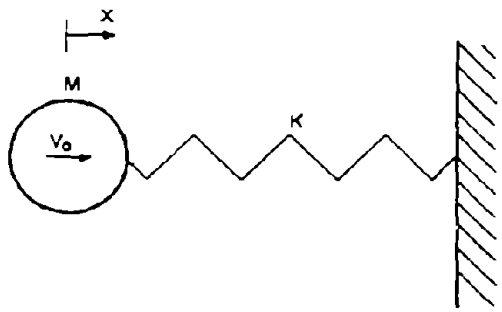

Figure 2. Spring mass system.

The maximum value of the displacement into the pole occurs when sin wt = 1 (t=Ø.ØØ8 sec). For an initial speed of 2Ø mi/h, the maximum displacement is:

$$X_{max} = 1.632 \text{ ft} \qquad (12)$$

b. Rigid Body Mechanics

A rigid body is defined as a collection of particles whose relative distances are constrained to remain absolutely fixed. Such bodies do not exist in nature but are mathematical conceptions which are useful in many applications. A particle can be located by specifying its location (x,y,z). For a rigid body, the orientation must also be specified. The consideration of rotational motions introduces the concept of moments of inertia. Moments of inertia are analogous to mass in translational motion. For a rigid body, six terms are required to fully describe the distribution of mass. The first three are called moments of inertia and are defined by:

$$I_{xx} = \int_V (y^2 + z^2)\, m\, dV \qquad (13)$$

$$I_{yy} = \int_V (x^2 + z^2)\, m\, dV \qquad (14)$$

$$I_{zz} = \int_V (x^2 + y^2)\, m\, dV \qquad (15)$$

where m = Mass density
V = Volume of body

The second three are called products of inertia and are defined by:

$$I_{xy} = \int_V xy\, m\, dV \qquad (16)$$

$$I_{xz} = \int_V xz\, m\, dV \qquad (17)$$

$$I_{yz} = \int_V yz\, m\, dV \qquad (18)$$

In the simplest form, rotational motion about a fixed point in a plane is described by a second order differential equation of the form:

$$P = I_{xx}\, \ddot{\theta} \qquad (19)$$

where P = Moment acting on the rigid body
I_{xx} = Mass moment of inertia about x axis
θ = Rotational acceleration about x axis

This equation is similar to Newton's Second Law with:

Force ---------- Moment
Mass ---------- Mass moment of inertia
Linear acceleration ------- Rotational acceleration

(1) Combined Translation and Rotation. Consider the example of a vehicle impacting a rigid pole as discussed above but now allow the impact force to produce a moment about the vehicle center of gravity. This situation is shown graphically in figure 3. The system has two degrees of freedom. It can translate along the x axis and rotate in the x-y plane. The two equations which describe the dynamics of the system are:

$$M\ddot{X} + K X = K d \theta \qquad (20)$$

$$M R^2 \ddot{\theta} + K d^2 \theta = K d X \qquad (21)$$

where d = Moment arm of impact force
R = Radius of gyration
M = Mass of the vehicle
K = Stiffness of vehicle

The solution to this set of two second order differential equations is given by:

$$X = V\frac{a^2 t}{1+a^2} + V\frac{1.}{w\,(1+a^2)}\sin wt \qquad (22)$$

$$\theta = V\frac{a^2 t}{d\,(1+a^2)} - V\frac{a^2}{d\,w\,(1+a^2)}\sin wt \qquad (23)$$

where $a = d/R$

$w = \sqrt{K/M}\,\sqrt{1+a^2}$

V = Impact speed

The time history of the impact force is shown in figure 4. The force time history for on center impact has also been added to this curve. For times up to 0.050 seconds, there is little difference in the two solutions. However, the offcenter impact does produce a rotation of vehicle while the oncenter impact

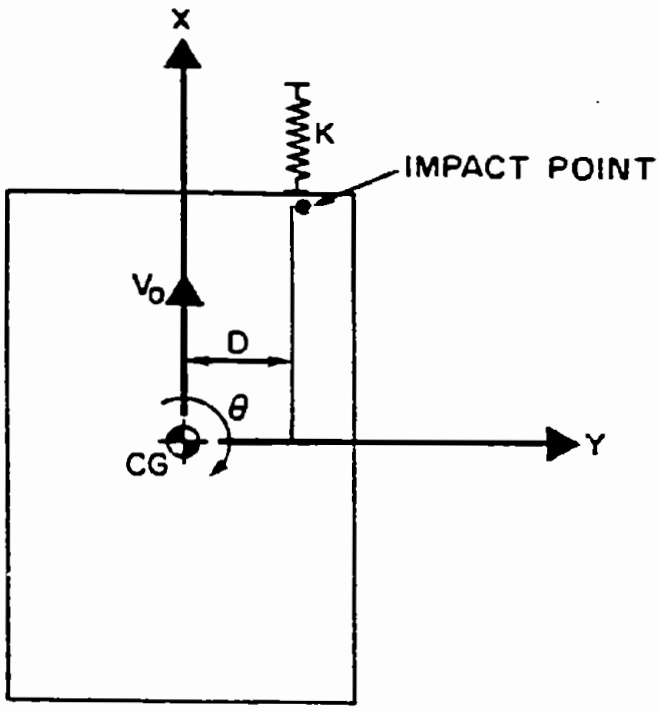

Figure 3. Vehicle/pole impact geometry.

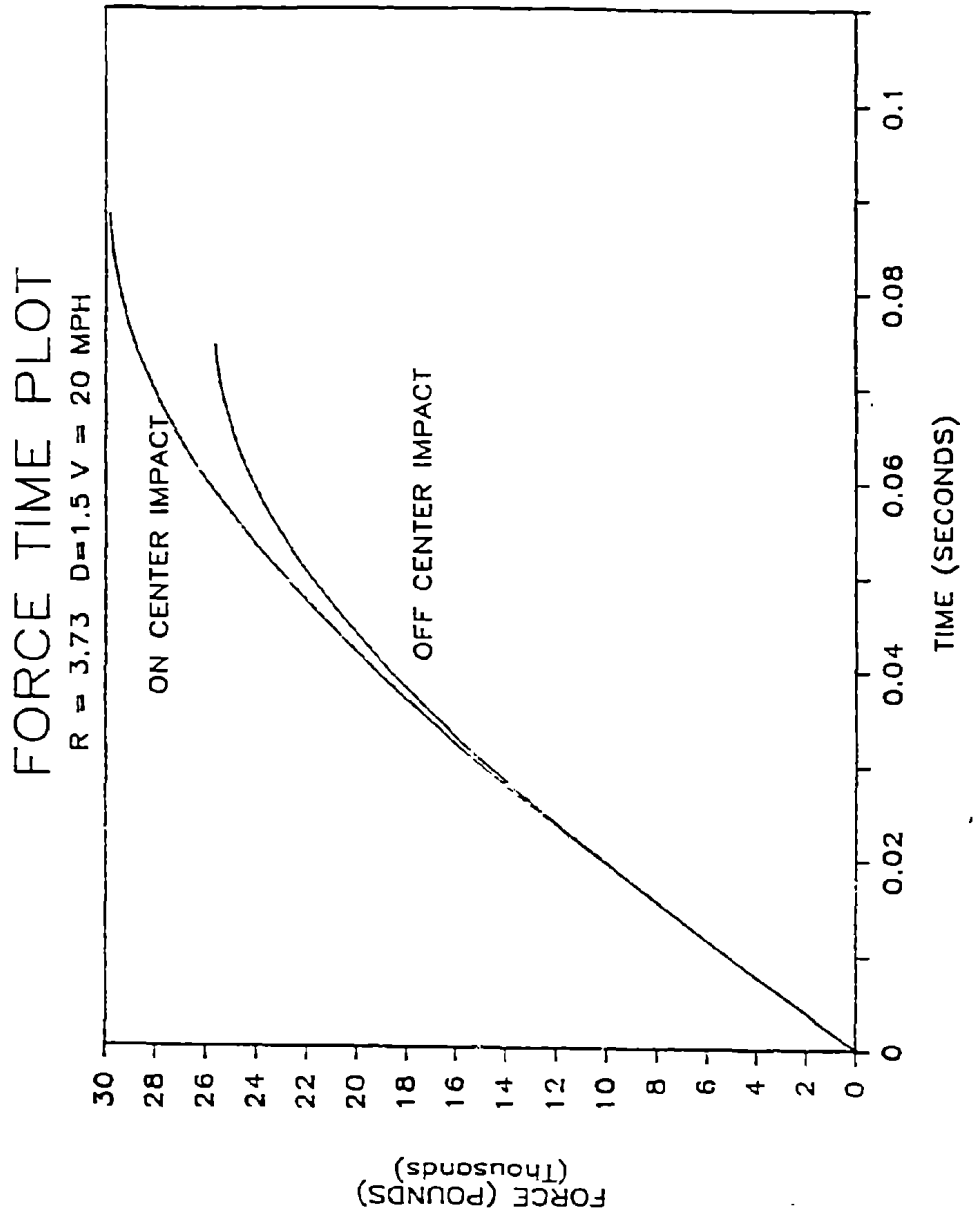

Figure 4. Impact force versus time.

does not produce rotation. The time history of the yaw angle with time is shown in figure 5. Note the the angle is small, on the order of several degrees. Figure 6 shows a plot of yaw rate as a function of time. This figure shows that the yaw rate builds up quickly during the impact reaching a level of over 100 deg/sec.

This example demonstrates that the complexity of the analysis is increased as the degrees of freedom of the model increase. In most instances of simplified analysis approaches, the model is limited to two degrees of freedom.

(2) Radius of Gyration. The concept of the radius of gyration is useful in estimating the value of moments of inertia. The definition of the radius of gyration is given by:

$$M R^2_{xx} = I_{xx} \qquad (24)$$

$$= \int_V (y^2 + z^2)\, m\, dV$$

Since the units of the mass moment of inertia are mass times length times length, the radius of gyration has units of length. The radius of gyration represents the radius from the x axis where the total mass of the body could be placed to provide the same value for the mass moment of inertia. One very useful application of this concept is in estimating the value of the mass moment of inertia. The value of R_{xx} will always be less than the maximum value of $(y^2 + z^2)$. Consider the rectangular prism shown in figure 7. The mass moment of inertia is given by:

$$I_{xx} = M (a^2 + b^2)/3 \qquad (25)$$

and the radius of gyration by:

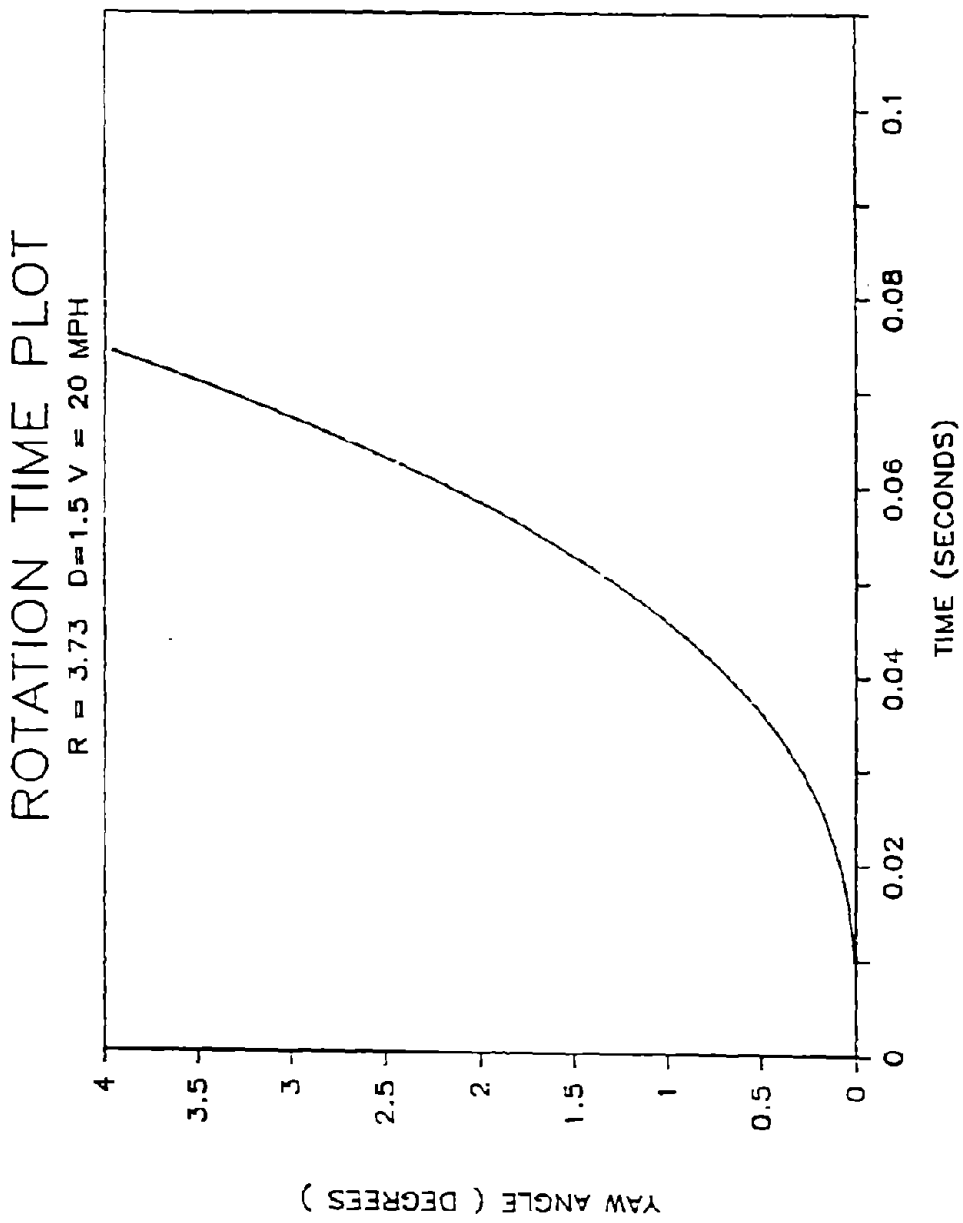

Figure 5. Rotation angle versus time.

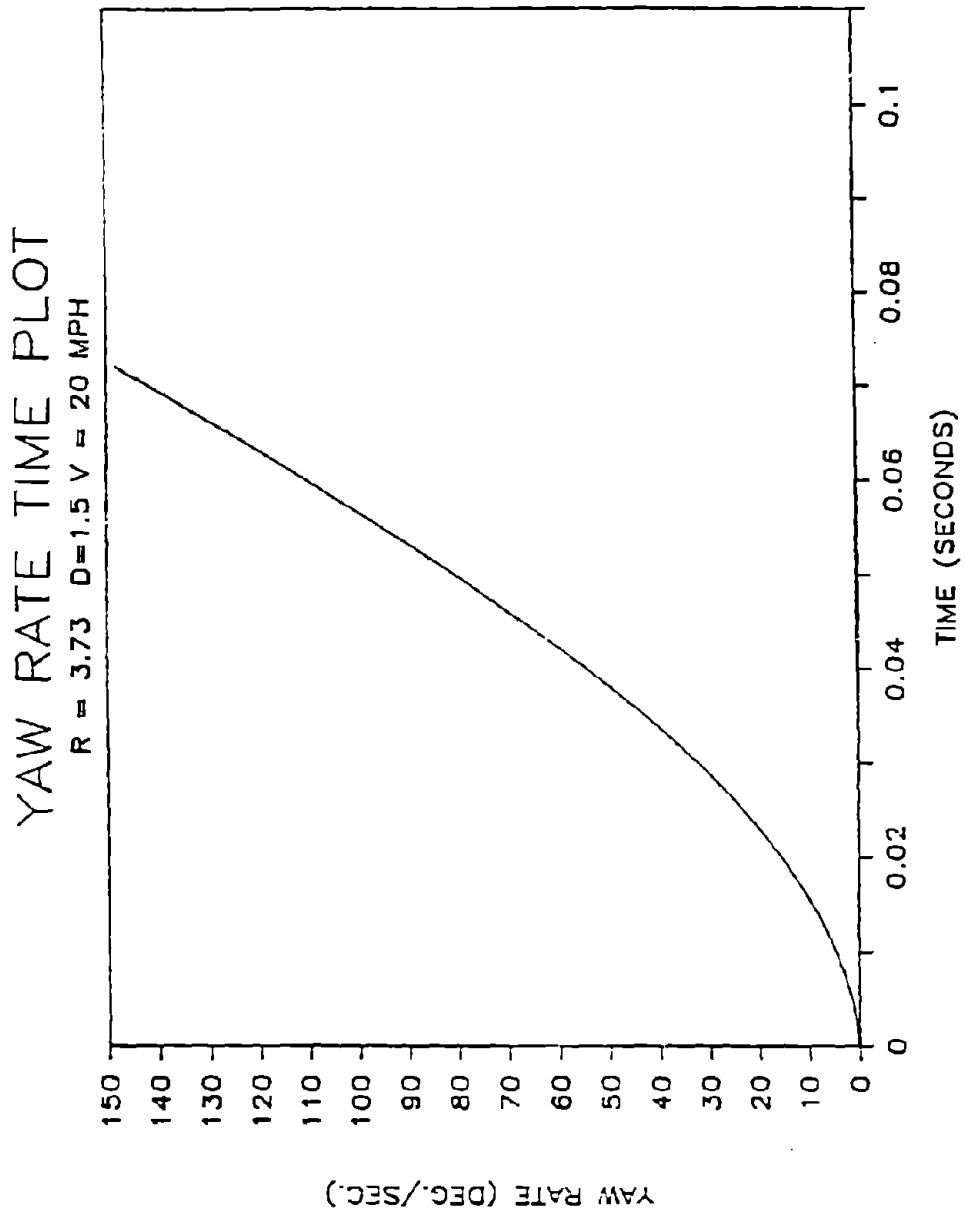

Figure 6. Rotation rate versus time.

$$R_{xx} = 0.577\sqrt{(a^2 + b^2)} = 0.577\ D_{max} \qquad (26)$$

where D_{max} = the maximum value of $(x^2 + z^2)$.

For a right circular cylinder, as shown in figure 8, the value of I_{xx} is:

$$I_{xx} = M\ R^2/2 \qquad (27)$$

and the value of R_{xx} is:

$$R_{xx} = 0.707\ D_{max} = 0.707\ R \qquad (28)$$

where R = radius of cylinder

From the above examples, the process of estimating the mass moment of inertia is based on calculating the maximum distance from the reference axis to a point on the surface of body. The square of this distance times the mass of the body will represent an upper limit on the value of the radius of gyration. A good estimate of the moment of inertia can be made based on a radius of gyration equal to 50 to 70 percent of D_{max}.

c. Friction

Friction forces are required to guide and accelerate the vehicle. The concepts of frictional forces are discussed below.

(1) Coulomb Friction. Coulomb friction is defined as the force distribution at a surface of contact between bodies which prevents or impedes any possible sliding motion between the bodies. Friction between tires and the roadway provide the forces

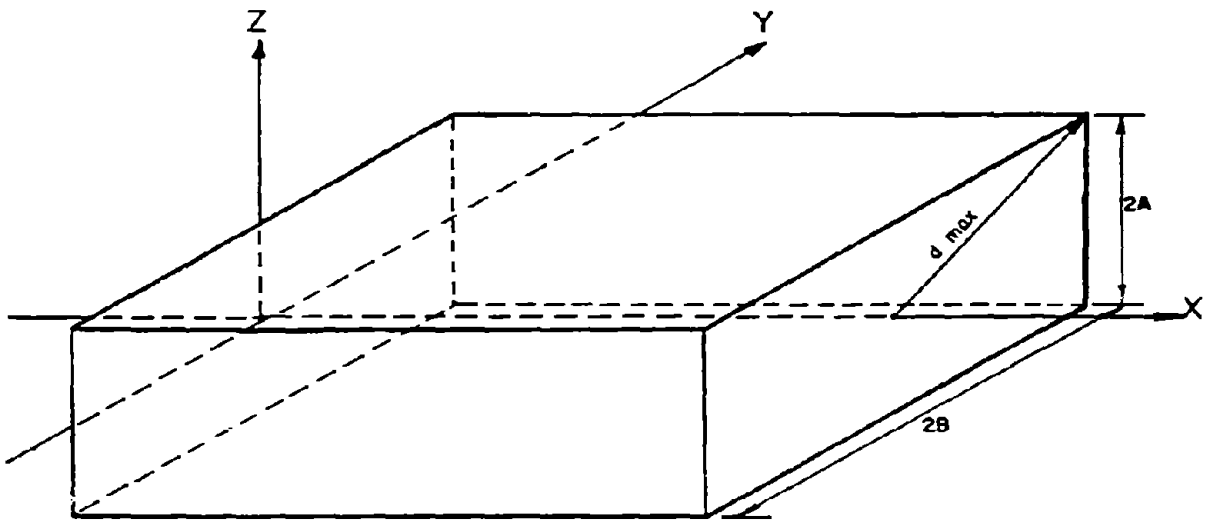

Figure 7. Rectangular prism.

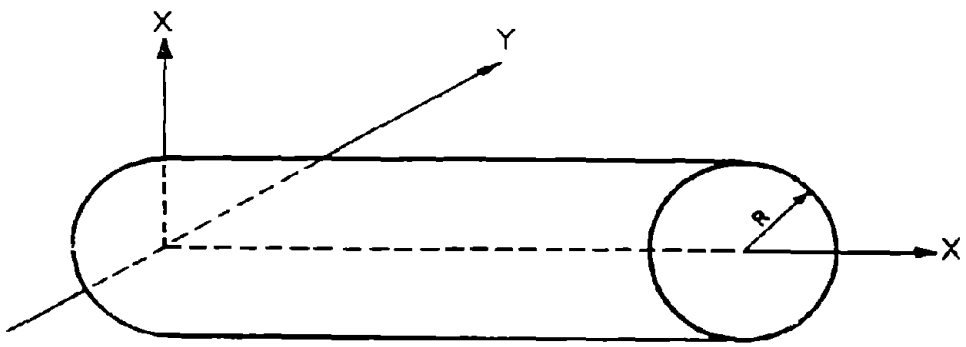

Figure 8. Right circular cylinder.

which decelerate a vehicle. Consider the case of a vehicle traveling at an initial speed, V_o, when the brakes are applied and locked. The question is "how far will the vehicle travel before coming to rest." The friction force is related to the weight of vehicle by:

$$F_f = n\ W \qquad (29)$$

where n = coefficient of friction

Substituting this expression into equation (5), we have:

$$(X_f - X_o) = 0.5\ V_o^2/(n\ g) \qquad (30)$$

where g = acceleration of gravity (32.174 ft/sec/sec)

Figure 9 shows this relationship for various values of n.

Experimental values for the coefficient of friction are shown in figure 10. The values are seen to range from values of nearly one to values approaching zero depending on pavement conditions and tire characteristics. The general feature of these curves is that the coefficient of friction decreases with increased speed.

(2) Tire Guidance Forces. The frictional forces which are used to steer a vehicle are developed between the tires and road. The level of force developed is based on the angle between the plane of the tire and the direction of motion. The angle is called the sideslip angle and is shown in figure 11. The lateral force on the tire increases with sideslip angle as shown in figure 12. At about 12 to 15 degrees of sideslip, the lateral force reaches its maximum value and represents a condition of pure sliding.

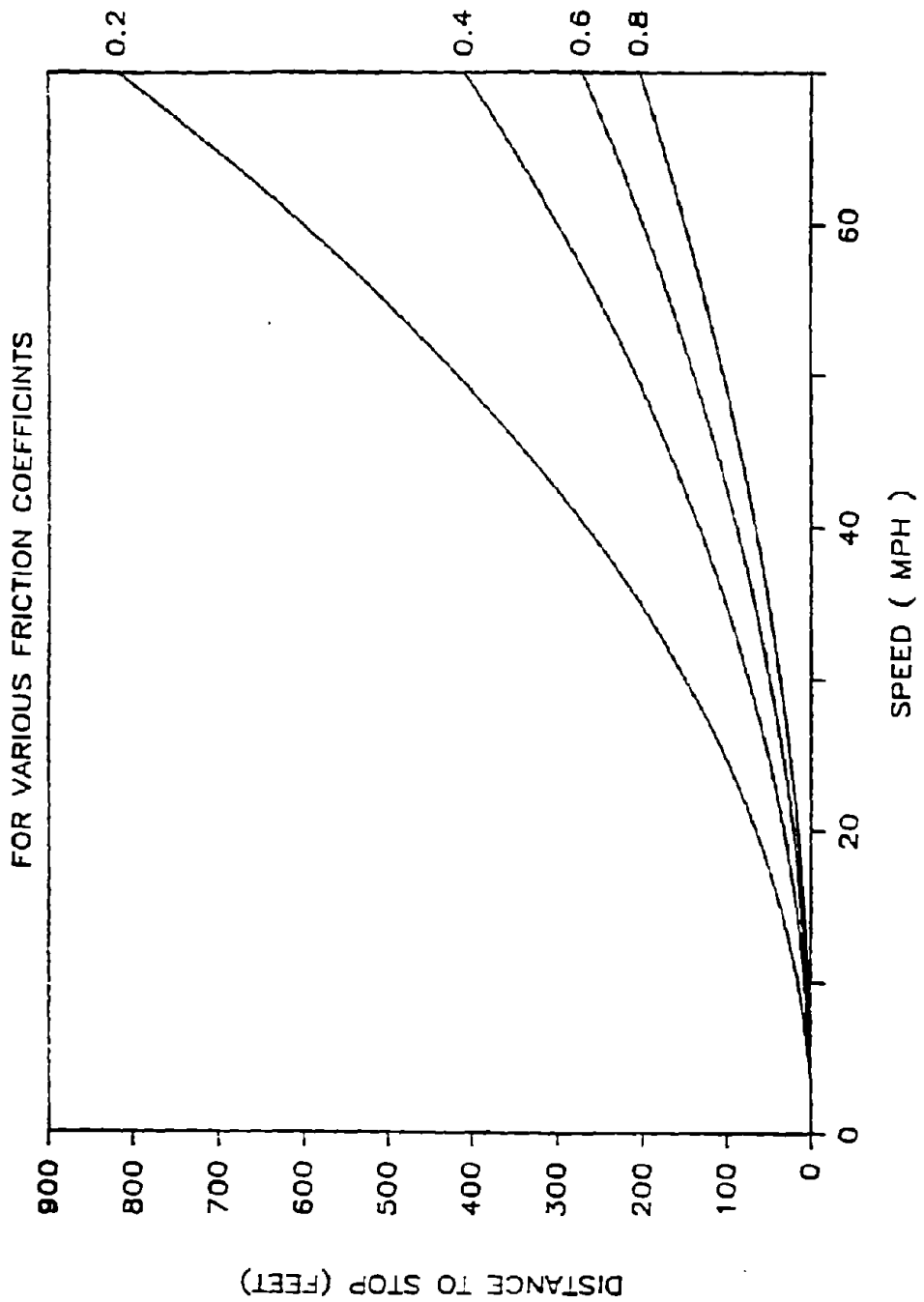

Figure 9. Stopping distance as a function of friction coefficient

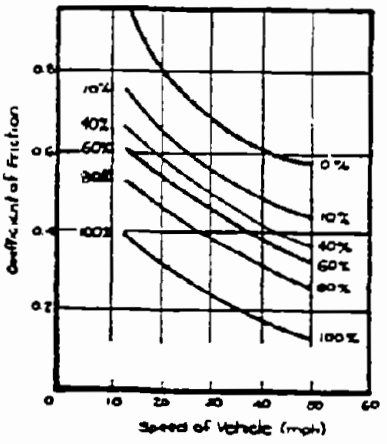

Figure 10. Friction coefficient as a function of speed.

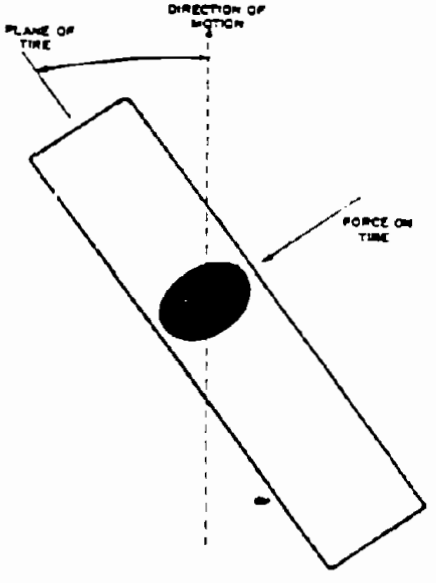

Figure 11. Tire sideslip angle.

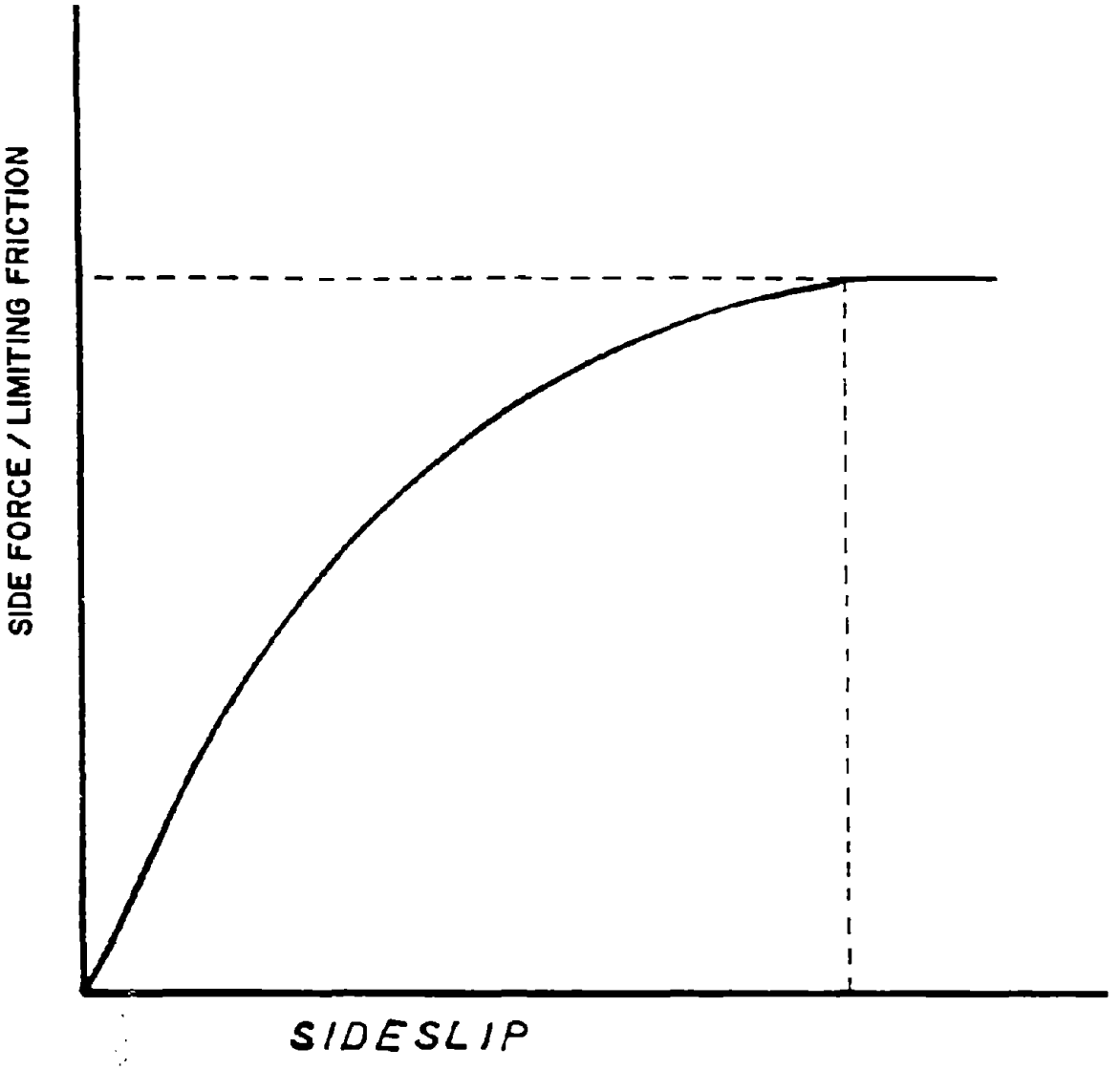

Figure 12. Tire lateral force.

While tire forces are seldom of importance during an impact, they are often important determining the post-impact trajectory of a vehicle.

2. Momentum

Momentum concepts are based on integrating Newton's Second Law with respect to time to provide:

$$\int_{t_1}^{t_2} \mathbf{F}\, dt = M \int_{t_1}^{t_2} \mathbf{A}\, dt \qquad (31)$$
$$= M[V_2 - V_1]$$

The integral on the the left side of the equation is called the impulse of the force F. The term on the right side of the equation is called the momentum change.

a. Linear Momentum

Consider the case of a 1,800 lb vehicle traveling at a speed of 60 mi/h. Its initial momentum is:

$$M\,V = (1800/32.17)\ 88 \qquad (32)$$
$$= 4{,}919 \text{ lb-sec } \{ \text{ x-direction } \}$$

If the vehicle hits a breakaway device providing an impact force as shown in figure 13, the impulse can be calculated as the area under the curve, 500 lb-sec. The momentum of the vehicle after the impact is given by:

$$M\,V_2 = M\,V_1 - \text{impulse} \qquad (33)$$
$$= 4{,}919 - 500 = 4{,}419$$

The velocity change of the vehicle is thus 8.94 ft/sec.

Consider the case of a vehicle impacting a longitudinal barrier at an angle θ as shown in figure 14. The component of momentum perpendicular to the barrier is given by ($M\,V_o \sin\theta$). If

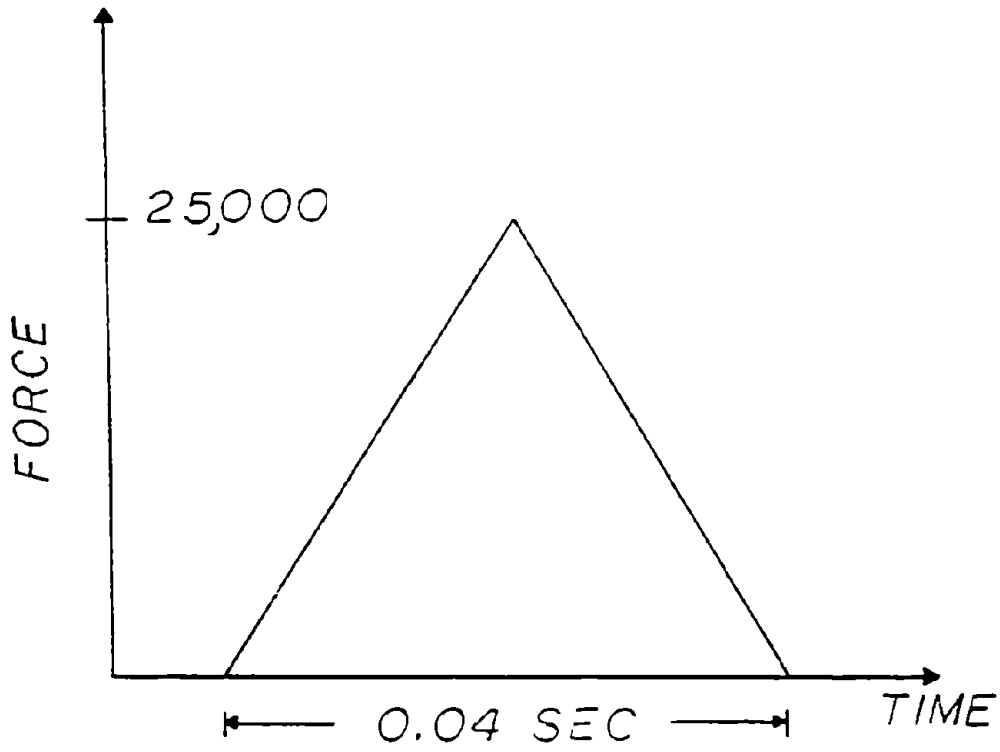

Figure 13. Force time history.

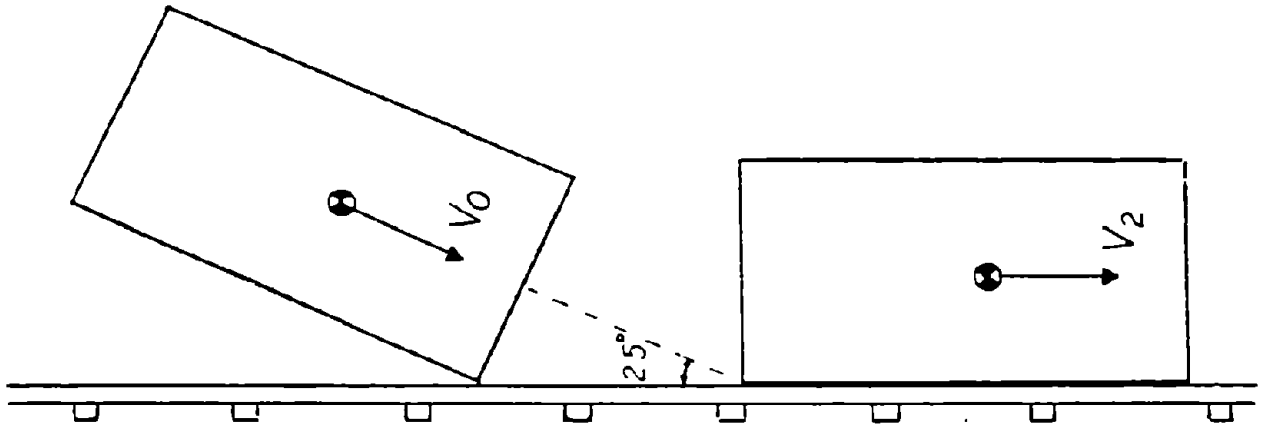

Figure 14. Vehicle impact with longitudinal barrier.

the vehicle is turned during the impact and travels parallel to the barrier, the component of momentum perpendicular to the barrier is zero. The component of the impulse perpendicular to the barrier is given by:

$$\int_{0}^{T} F_n \, dt = M \, V_o \sin \theta \qquad (34)$$

where F_n = force normal to barrier

While the impulse is known, the duration of the impact and the time distribution of the normal force are unknown. The example illustrates that the momentum approach can not be used to determine the peak impact force or the duration of the impact.

In many cases, the value of the maximum force occurring during the impact is of major interest. While momentum considerations will not provide this value, an estimate of its value can be obtained if the duration of impact and shape of the force-time can be made. A half sine wave shape is often used to represent the shape of impact force time history. Based on this assumption, F_n has the form:

$$F_n = F_{max} \sin [pi \ (t/T)] \qquad (35)$$

where F_{max} = maximum level of force during impact
T = duration of impact

Integrating this expression and equating to the momentum change we have:

$$F_{max} \ (2/pi) \ T = M \, V_o \sin \theta \qquad (36)$$

For example if a 4,500 lb vehicle impacts a longitudinal barrier at an angle of 25 degrees and an impact speed of 60 mi/h, the estimated maximum force is:

$$F_{max} = 8,172/T \qquad (37)$$

If the impact duration is .3 seconds, the estimated force is 27,239 lb. Note that the vehicle would travel 24 ft based on the initial impact speed of 60 mi/h before becoming parallel to the barrier.

b. Angular Momentum

Angular momentum or moment of momentum is analogous to linear momentum. In its most simple form, the expression for angular momentum can be derived by integrating (19):

$$P = I \ddot{\theta} \qquad (38)$$

$$P = I [\dot{\theta}_2 - \dot{\theta}_1]$$

where $\dot{\theta}$ = Rotation rate

c. Combined Linear and Angular Momentum

Some application require that the concepts of linear and angular momentum be used simultaneously. Consider the case of a 25 ft steel pole as shown in figure 15. The impact force produces both linear and angular momentum. The equations for the linear and angular momentum are given by:

$$\int P \, dt = I \dot{\theta}_2 \qquad (39)$$

$$\int F \, dt = M V_2 \qquad (40)$$

where θ_2 = the angular rate after application of impulse
V_2 = velocity of the pole at center of gravity

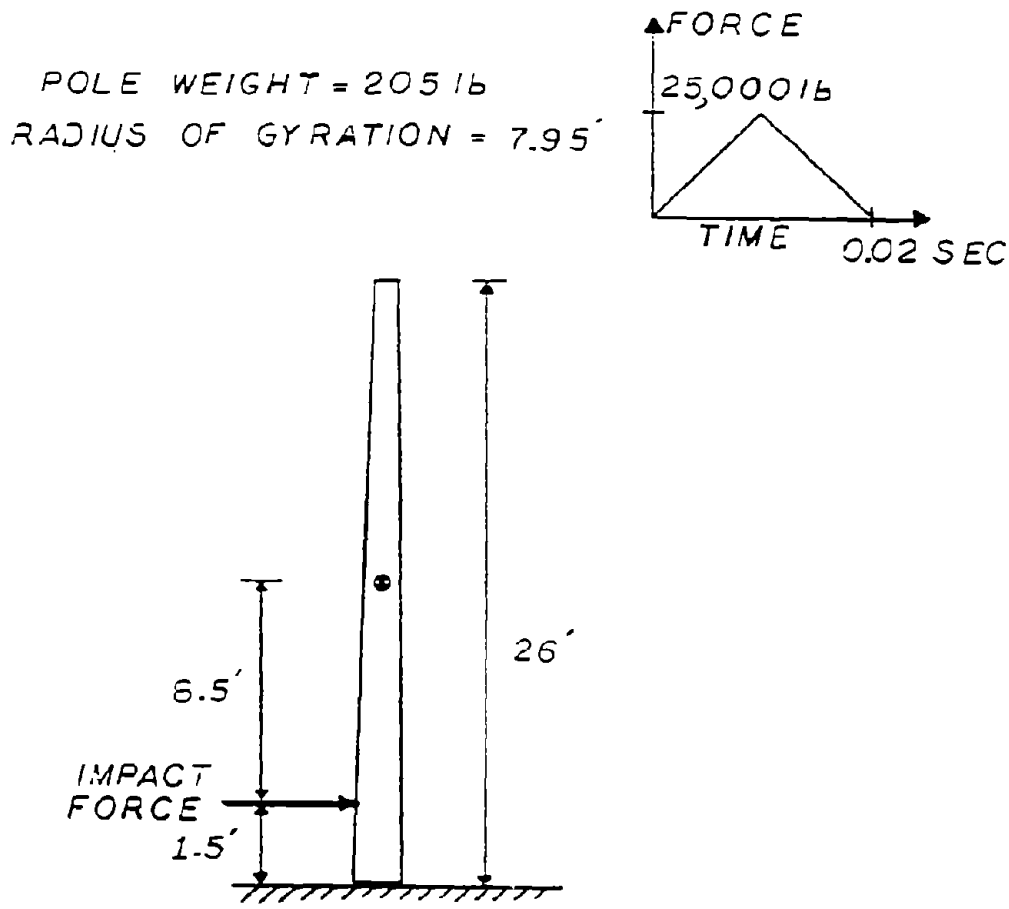

Figure 15. Luminaire support impacted by vehicle.

The impulse is 250 lb-sec. The resulting expression for the translational and rotational speed are:

$$V_2 = 250/(6.37) \qquad (41)$$
$$= 39.23 \text{ ft/sec}$$

$$\dot{\theta}_2 = (250)(8.5)/[(6.37)(7.95)^2] \qquad (42)$$
$$= 5.28 \text{ radians/sec}$$

The speed of the pole at the point of application of the force is given by:

$$V_a = 39.23 + 5.28\ (8.5) \qquad (43)$$
$$= 84.11 \text{ ft/sec}$$

An important use of this approach is to calculate the impulse required to push the pole away from an impacting vehicle. If the force is generated by a vehicle initially traveling at a speed V_o, the impulse generated will produce a velocity at the impact point which is at least as great as V_o. In order for the pole to separate from the vehicle the velocity must be greater than the vehicle. For the purpose of this example, we will assume that the velocity of the pole at point a will be e V_o. The expression for V_a is given by:

$$V_a = V_2 + 8.5\ \dot{\theta}_2 = e\ V_o \qquad (44)$$

$$eV_o = (1/M) \int_0^T F\ dt + (D/(M\ R^2)) \int_0^T F\ dt$$

$$eV_o = \frac{R^2 + D^2}{M\ R^2} \int_0^T F\ dt$$

The resulting expression for the impulse is:

$$\int_{\emptyset}^{T} F\,dt = \frac{R^2}{R^2 + D^2}\; e\; M\; V_o \qquad (45)$$

For this example, the impulse required to push the pole away from the vehicle based on a 60 mi/h speed and e = 1.1 would be:

$$\text{Impulse} = \frac{(7.95)^2\ (1.1)\ (6.37)\ (88)}{(7.95)^2 + (8.5)^2} \qquad (46)$$

$$= 287 \text{ lb-sec}$$

At a speed of only 20 mi/h, the required impulse would be:

$$\text{Impulse} = \frac{(7.95)^2\ (1.1)\ (6.37)\ (29.33)}{(7.95)^2 + (8.5)^2} \qquad (47)$$

$$= 95.9 \text{ lb-sec}$$

3. Energy/Work

The concepts of kinetic energy and work are based on integration of Newton's Second Law with respect to distance. The formulation is given by:

$$\mathbf{F} = M\mathbf{A} \qquad (48)$$

$$\int_{x_1}^{x_2} \mathbf{F} \cdot d\mathbf{x} = M \int_{x_1}^{x_2} (d\mathbf{V}/dt) \cdot d\mathbf{x}$$

$$= M \int_{t_1}^{t_2} d/dt \, (\mathbf{V} \cdot \mathbf{V}) \, dt$$

$$= .5 \, M \, [\, V_2^2 - V_1^2 \,]$$

This is the case for general three dimensional motion. For the case of one dimensional motion, the expression becomes:

$$\int_{x_1}^{x_2} F \, dx = 0.5 \, M \, [V_2^2 - V_1^2] \qquad (49)$$

The kinetic energy is defined by the expression $0.5 \, M \, V^2$.

a. Linear Motion

The above formulation has many applications when a vehicle can be considered a particle. Consider the case of a vehicle stopping with locked brakes. The energy formulation provides:

$$\int_{x_1}^{x_2} -m\ W\ dX = 0.5\ M\ V_o^2 \qquad (50)$$

$$\int_{x_1}^{x_2} -m\ W\ (x_2 - x_1) = 0.5\ M\ V_o^2$$

$$(x_2 - x_1) = V_o^2/(2\ m\ g)$$

This is the same expression that was derived in section 1 based on direct integration of Newton's Second Law.

Consider the case of a vehicle impacting a rigid pole. The vehicle is idealized as a particle and the crush of the vehicle characterized by a linear sp.ing of stiffness K, lb/ft. Applying the energy/work equation, we have:

$$\int_{0}^{X} -K\ X\ dX = 0.5\ M\ [V_2^2 - V_1^2] \qquad (51)$$

$$= 0.5\ K\ X^2$$

If the vehicle comes to a stop (i.e. if $V_2=0$), this expression becomes:

$$0.5\ K\ X_{max}^2 = 0.5\ M\ V_1^2 \qquad (52)$$

$$X^2_{max} = (M/K)\ V_1^2$$

b. Angular Motion

Kinetic energy for rotational motion in a plane has similar

expression to that for translational kinetic energy. This expression is given by:

$$(KE)_{rotation} = 0.5\ I\ \theta^2 \qquad (53)$$

For the case of general 3-dimensional motion of a rigid body, the expression for the kinetic energy is given by:

$$KE = 0.5[\ I_{xx}\ w^2_x + I_{yy}\ w^2_y + I_{zz}\ w^2_z] - [\ w_x w_y\ I_{xy} + w_x w_z\ I_{xz} + w_y w_z\ I_{yz}\ ] \qquad (54)$$

where w_x = x-component of rotation vector
w_y = y-component of rotation vector
w_z = z-component of rotation vector

In most cases which can be addressed by simplified analysis, the rotation is limited to one component and this expression is greatly simplified.

c. Potential Energy

Potential energy is associated with gravitational force. Potential energy is defined by:

$$PE = M\ g\ z \qquad (55)$$

where M = Mass of a particle
g = constant acceleration of gravity
z = Vertical distance above reference horizontal plane

If a particle is raised by an external force a distance of 14 feet, the work done by the external force is :

$$\text{Work Done} = M\ g\ 14 \qquad (56)$$

This amount of energy is stored as potential energy. If the particle is released, it will fall under the acceleration of gravity. When it reaches the reference horizontal plane, the potential energy will be zero. The potential energy will be converted to kinetic energy:

$$M\ g\ 14 = 0.5\ M\ V^2 \qquad (57)$$

$$V = 30.0 \text{ ft/sec}$$

d. Conservation of Energy

Conservation of energy is an important concept in the application of mechanics to roadside safety. The conservation of energy principle can be expressed as:

$$\text{Work Done} = \text{Change in } (PE + KE) \qquad (58)$$

As an example of the use of conversion of energy, consider the example of section 2 where a vehicle impacts a luminaire support. The post impact speed of the vehicle and the rotational and translational speeds of the pole are calculated based on momentum considerations. Based on conservation of energy, the work done during the impact is given by:

$$\text{Work Done} = 0.5\ M_v\ V_o^2 - 0.5\ M_v\ (V_o - DV)^2 + 0.5\ M_p\ \dot{X}_p^2 + 0.5\ I_p\ \dot{\theta}_p^2 \qquad (59)$$

Using the expressions derived in section 2 for DV, X_p and θ_p, this expression becomes:

$$\text{Work Done} = 0.5 M_v V_o^2 \{ 2eSr - e^2[S^2 r^2 + Sr] \} \qquad (60)$$

where $$S = \frac{R^2}{R^2 + D^2} = \text{Speed Ratio}$$

$$r = \frac{M_p}{M_v} = \text{Mass Ratio}$$

The variable, e, represents the ratio of the speed at the impact point to the initial speed of the vehicle. For a given pole/vehicle configuration, the work done is a function of e. If the impact is elastic, no work will be done in crushing the vehicle. Values of e corresponding to elastic impact are shown in figure 16. For values less than the value shown in figure 16, work is done by crushing the vehicle.

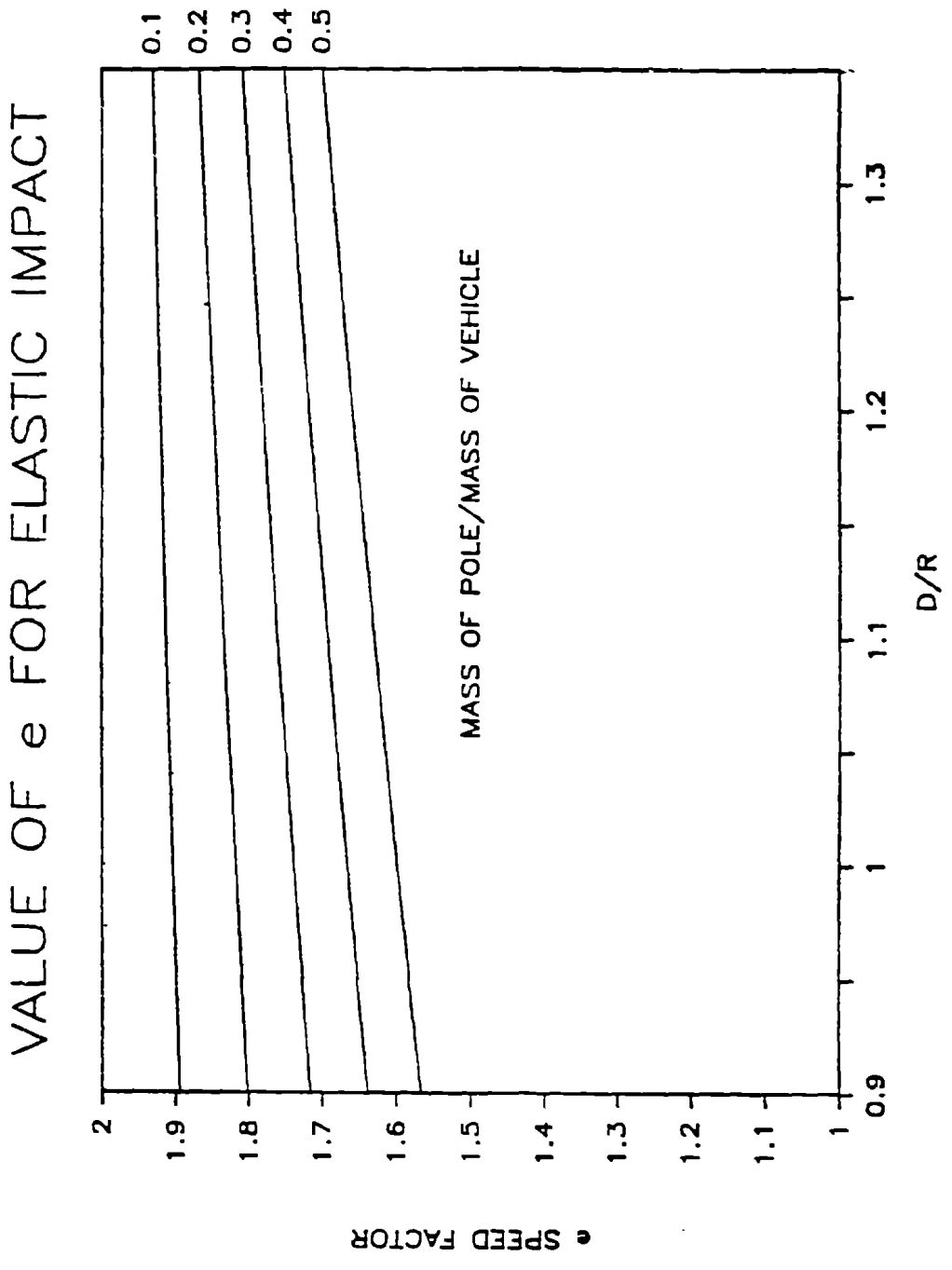

Figure 16. Values of e for elastic impacts.

4. Highway Vehicle Characteristics

The dimensions, weight and weight distribution of highway vehicles are major factors which influence the impact performance of roadside safety appurtenances. The vehicles using the roadway provide a wide range of weights. If motorcycles and micro-minisized vehicles are excluded, this weight range is between 1,800 lb and 80,000 lb.

a. Weight

Highway vehicles can be divided into four categories:

* Passenger cars
* Light trucks
* Heavy single unit trucks
* Combination trucks

The weight ranges for these categories are are not precisely defined but can be generally estimated. Passenger vehicles are the most prevalent vehicles using the highway. Passenger vehicles weigh between 1,800 and 4,500 lb. The 4,500 lb passenger vehicle is disappearing and being replaced by full-sized sedans weighing less than 4,000 lb. The light trucks category includes pick-up trucks and vans and provides a weight range of 3,000 to 10,000 lb. The heavy single unit category includes buses and provides a weight range of 6,000 to 40,000 lb. The combination trucks provide the widest range with values between 20,000 and 80,000 lb.

Table 5 provides typical values for key vehicle characteristics. These values are considered representative of the largest vehicle in the weight category, however a wide range of value can be expected for some variables especially for the heavy trucks and combination trucks.

Table 5. Vehicle characteristics.

(all measurements in feet)

	Cars	Light Trucks	Heavy Trucks	Combination Trucks
Overall length	19.0	22.0	35.0	-
Wheel Base	10.0	12.0	17.0	-
Wheel Track	6.5	6.5	7.5	8.0
Vertical CG	2.0	3.0	68.0	78.0
Long. CG	6.5	10.0	20.0	-
Width	6.5	7.0	8.0	8.0
Radius of Gyration				
Pitch	4.8	-	-	-
Yaw	4.8	-	-	-
Roll	1.9	2.2	3.5	3.8

Information on the weight and dimensions of a given vehicle are usually available from the manufacturer. The weight of a particular configuration can be determined by sequentially placing a load cell under each wheel of the vehicle. This information can be used to determine the longitudinal position of the center of gravity. The measurement of the vertical center of gravity and the mass moments of inertia are more difficult to determine.

b. Vertical Center of Gravity

The vertical center of gravity can be measured by the device shown in figure 17. The device consists of a frame and pivot axis. The vehicle is positioned on the frame with its center of gravity directly above the pivot axis when the frame is in the horizontal position. The pivot axis is selected to go through the center of gravity of the frame. With the frame in the horizontal position, the system is balanced. When the frame is rotated, the system in no longer in balance since the center of gravity of the vehicle now produces a moment about the pivot axis. This moment can be measured and equated to the product of (W z sin θ). Given the moment, the vehicle weight, and the angle of rotation, the distance z can be calculated.

c. Mass Moments Of Inertia

Mass moments of inertia for passenger cars can be directly measured using a special test fixture such as the Inertial Measurement Device (IMD) located at FOIL facility. This device consist of a frame, a pivot axis and two pretensioned springs as shown in figure 18. The pivot axis is constrained to pass through the center of gravity of the frame. To measure the mass moment of inertia of a vehicle, the vehicle is positioned on the frame with its center of gravity directly above the pivot axis when the frame is in the horizontal position. The frame is than rotated and the period of oscillation is measured. The equation describing the motion of the vehicle and frame is given by:

$$I\ddot{\theta} = (T-K\ L\ \theta)L - (T+K\ L\ \theta)L + W\ Z\ \sin\theta \qquad (\ 61\ )$$

where I = Mass moment of inertia of vehicle/frame system
T = Pretension in the springs
K = spring stiffness

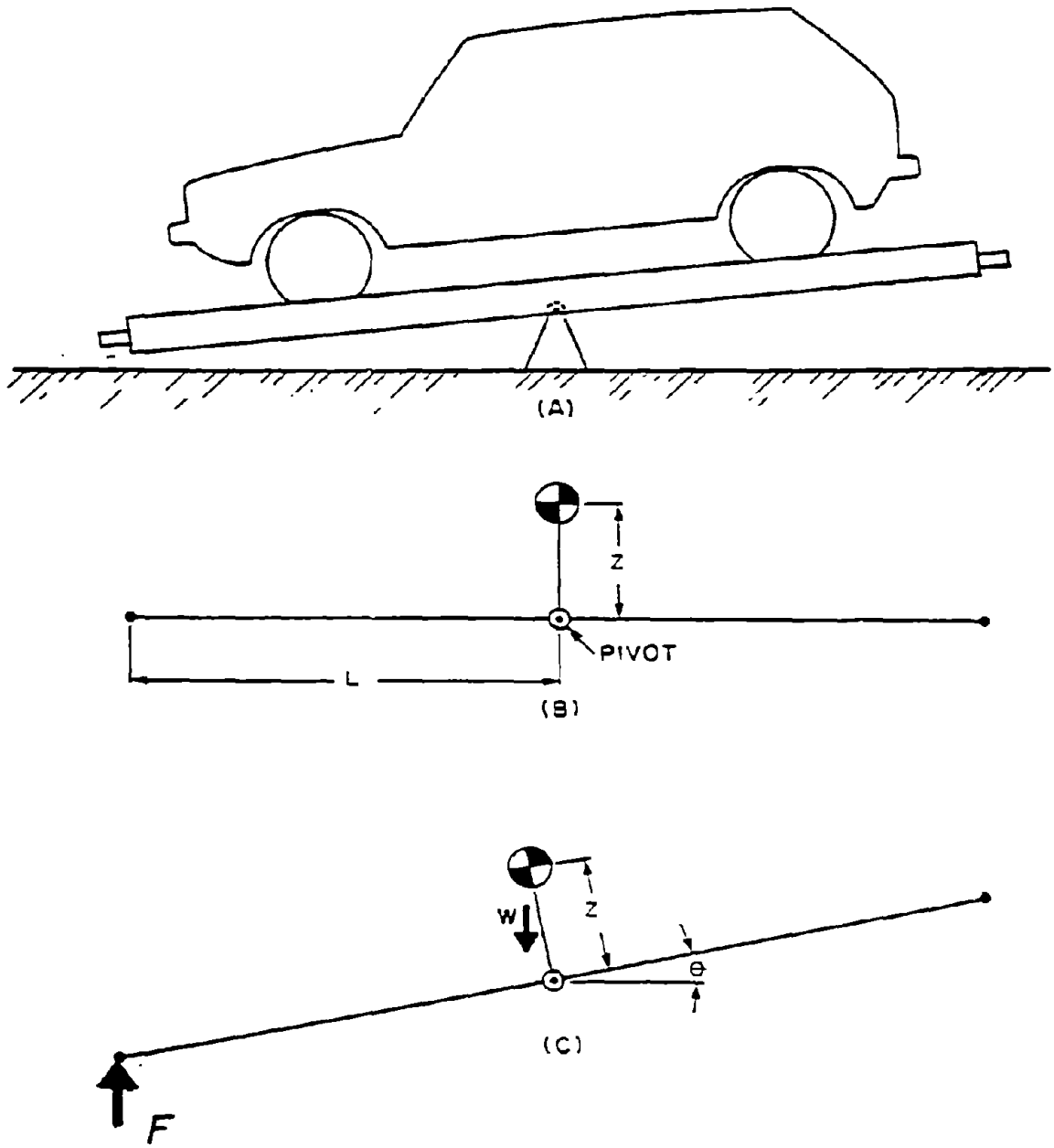

Figure 17. Device for measuring vertical C.G.

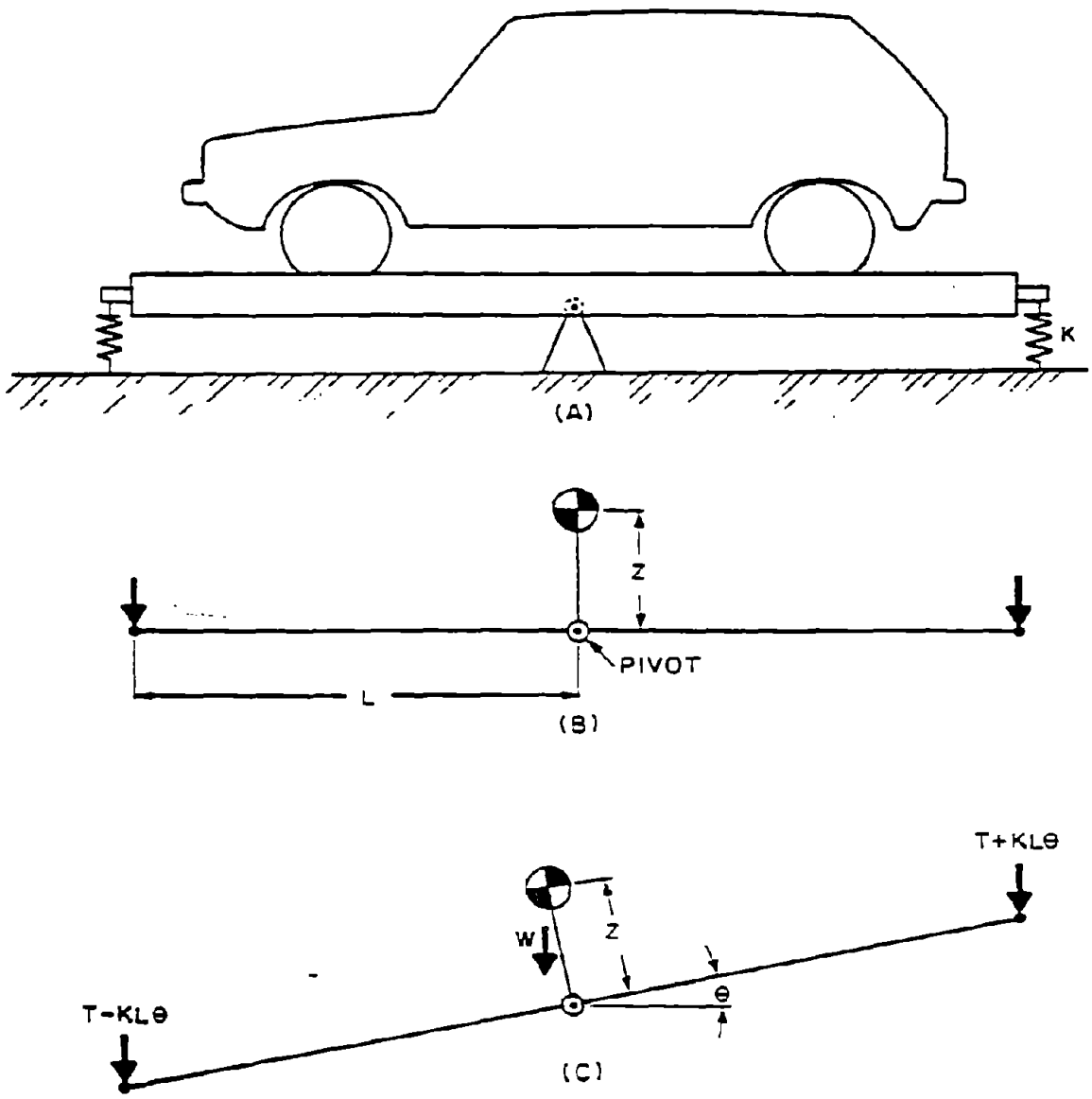

Figure 18. Device for measuring mass moment of inertia.

L = Distance from pivot point to spring
W = Weight of vehicle
Z = Height of vehicle CG above axis
θ = Angle of rotation

For small angles, the sine of the angle is approximately equal to the angle measured in radians. Using this approximation, the equation becomes:

$$I\ddot{\theta} + (2 K L^2 - W Z)\theta = 0 \qquad (62)$$

The solution to this equation predicts simple harmonic motion with a period given by:

$$T = 2\pi \sqrt{\frac{I}{(2 K L^2 - W Z)}} \qquad (63)$$

The value of I can be calculated based on known values for the vehicle weight, vehicle vertical center of gravity, spring rates and location and the measured value of the period of oscillation. The measured I represents the total moment of inertia of the vehicle/frame system. Based on a knowledge of the mass moment of inertia of the frame, the mass moment of inertia of the vehicle about its CG can be calculated.

While this approach is quite simple, the results are quite sensitive to the measurement of the vehicle weight, vehicle center of gravity location, spring rates and the period of oscillation. Use of the system at the FOIL facility have indicated that with careful measurement and test procedures, mass moment of inertia values can be determined to within 3 percent.

An alternate approach to direct measurement is to estimate the moment of inertia based on past measurements. General Motors has published a paper entitled " Typical Vehicle Parameters for Dynamics Studies Revised for the 1980's" which uses such an

approach. This report uses a regression analysis approach to relate the mass moments of inertia in roll,pitch,and yaw to the the total weight of the vehicle. The data base for the regression analysis is based on 17 vehicles including both domestic and foreign production vehicles. The range of vehicle characteristics included:

Body Style	Two Passenger Sports Car - Station Wagon
Curb Weight	1,265 lb - 3,875 lb
Wheel Base	6.6 ft - 9.7 ft

The paper provides regression equations for both the mass moment of inertia of the total mass of the vehicle and the sprung mass based on the total weight of the vehicle. The data from this report has been modified in format to provide estimates of the radius of gyration versus total vehicle weight. The purpose of modifying the format is the radius of gyration approach provides a better understanding of the physical significance of the data.

The sprung mass of the vehicle represent about 85 percent of the total vehicle weight. Figure 19 shows the percentage of sprung and unsprung weight as a function of the total weight of the vehicle based on a regression analysis.

Figure 20 shows the radius of gyration for the sprung mass and the total mass as a function of the total mass of the vehicle for the yaw mode. The radius of gyration for the total mass is about 10 percent higher than the radius of gyration of the sprung mass. For vehicles in the weight range of 1,800 to 4,500 lb, the radius of gyration for the yaw mode is 3-ft to 4.8-ft. Figure 21 shows the radius of gyration for the pitch mode. The values are quite similar to the yaw mode. The data for the roll mode is shown in figure 22. The radius of gyration is nearly constant over the weight range of 1,800 to 4,500 lb with a value of 1.9-ft.

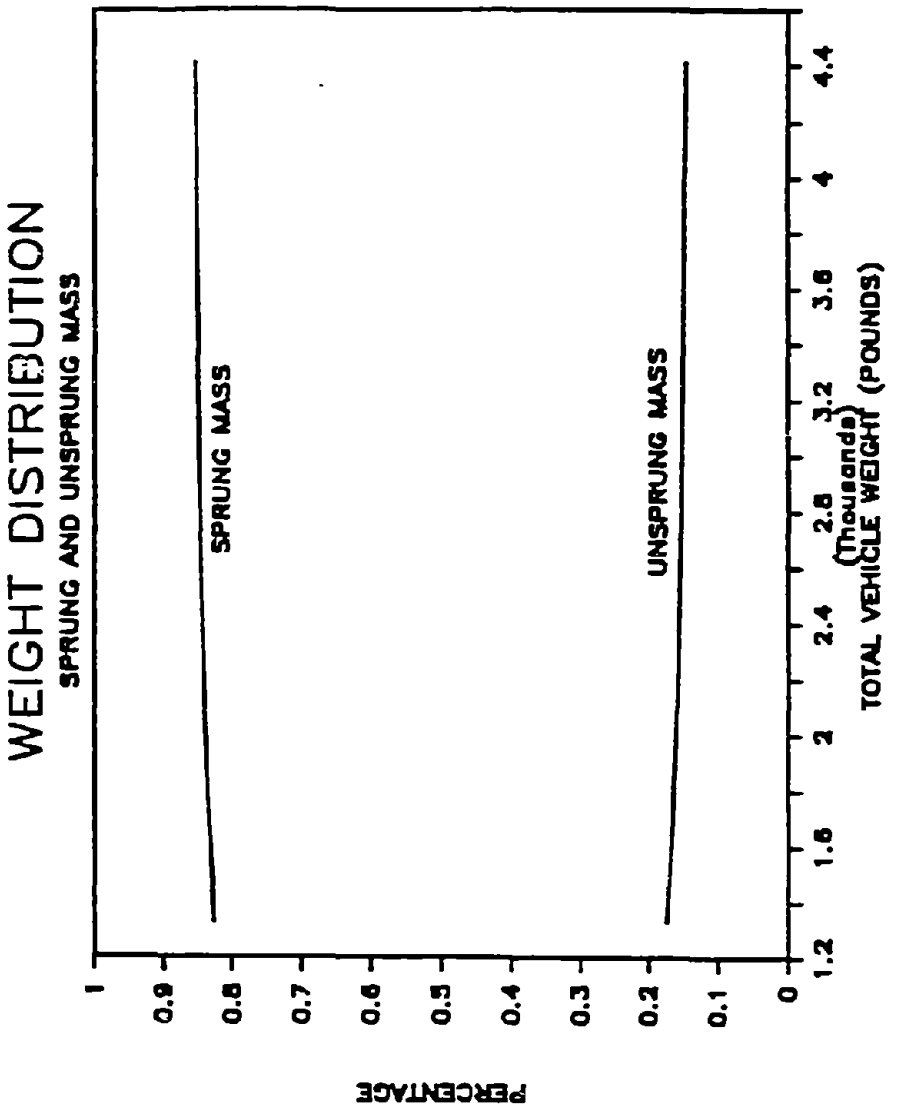

Figure 19. Sprung mass as a function of total weight.

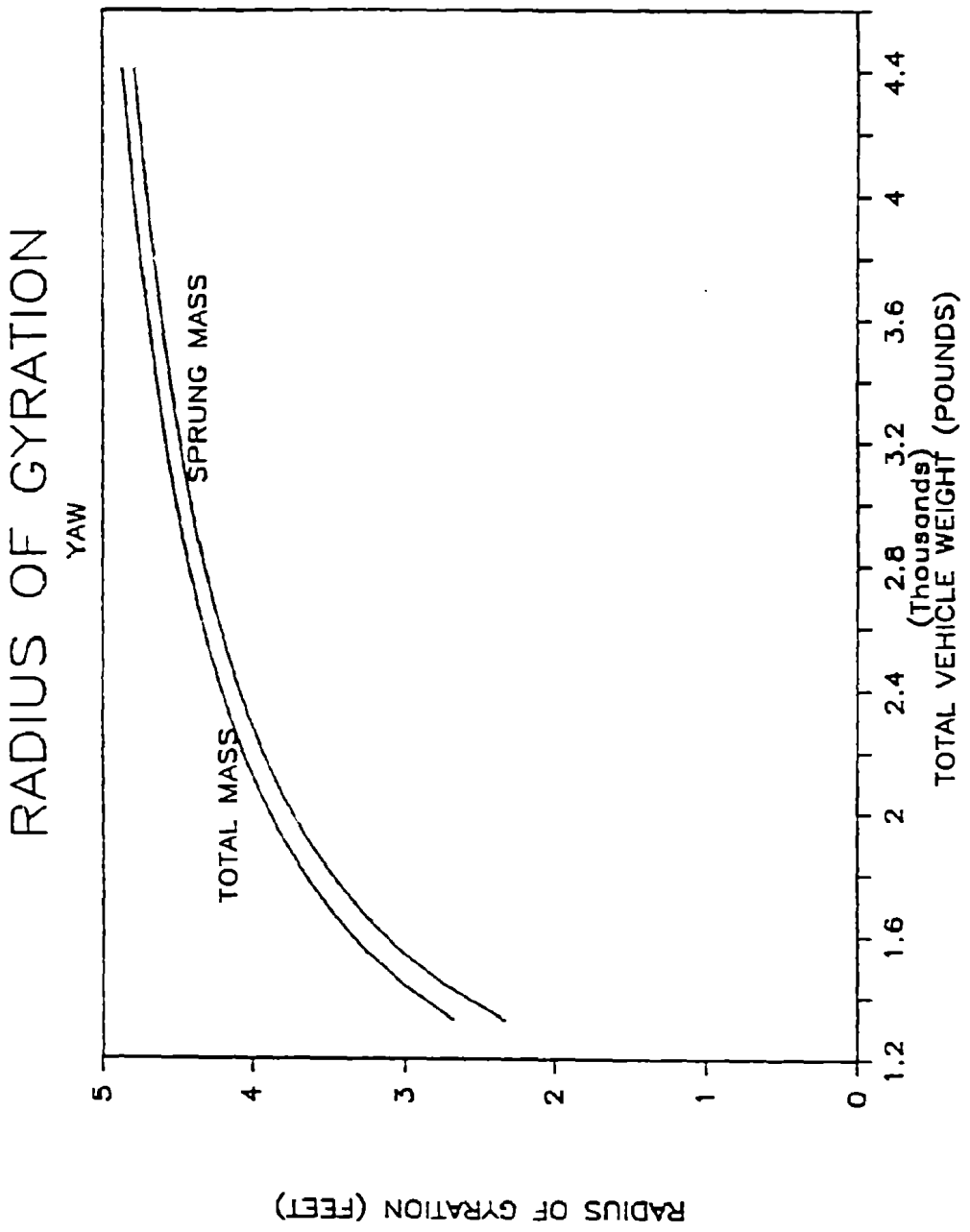

Figure 20. Yaw radius of gyration.

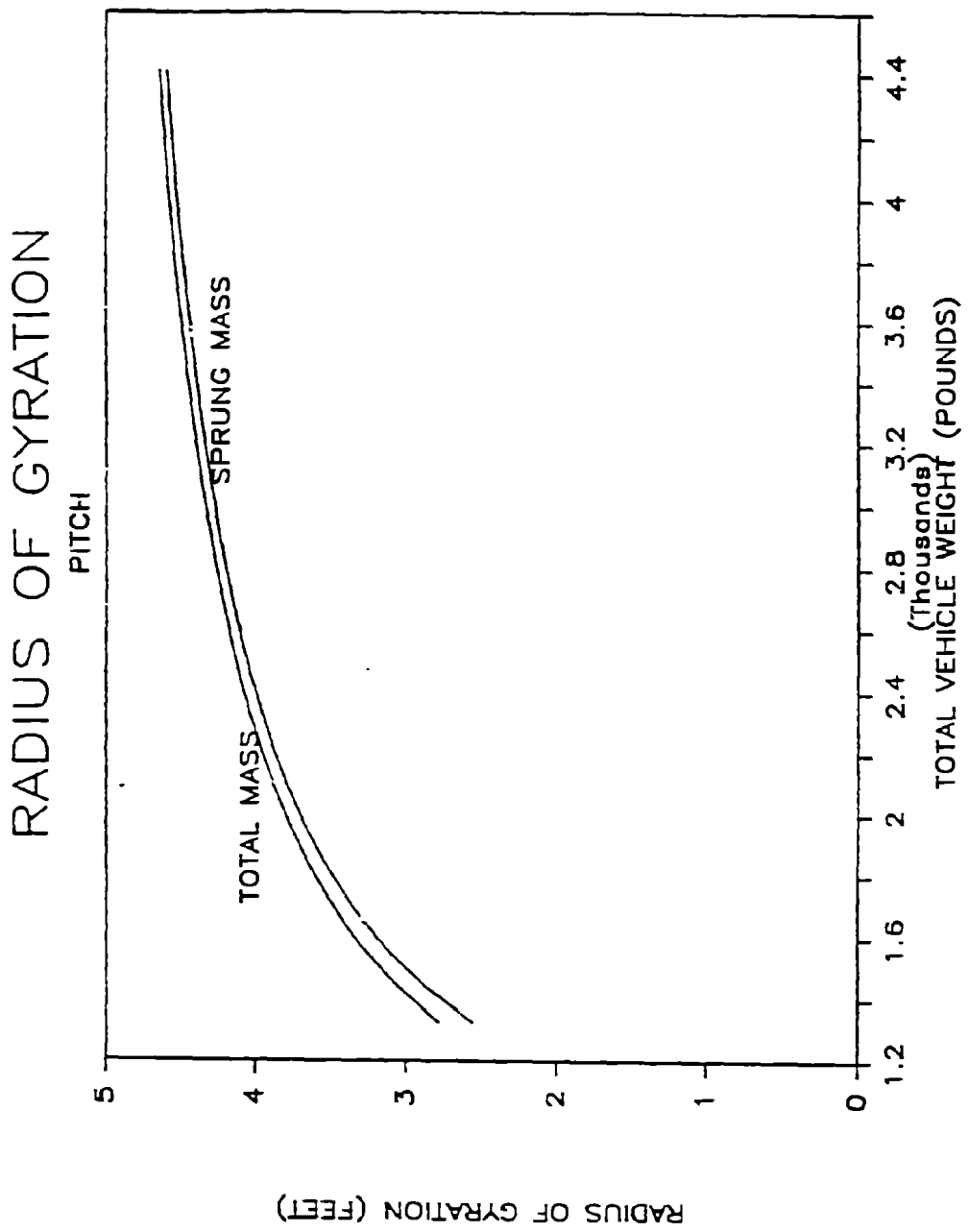

Figure 21. Pitch radius of gyration.

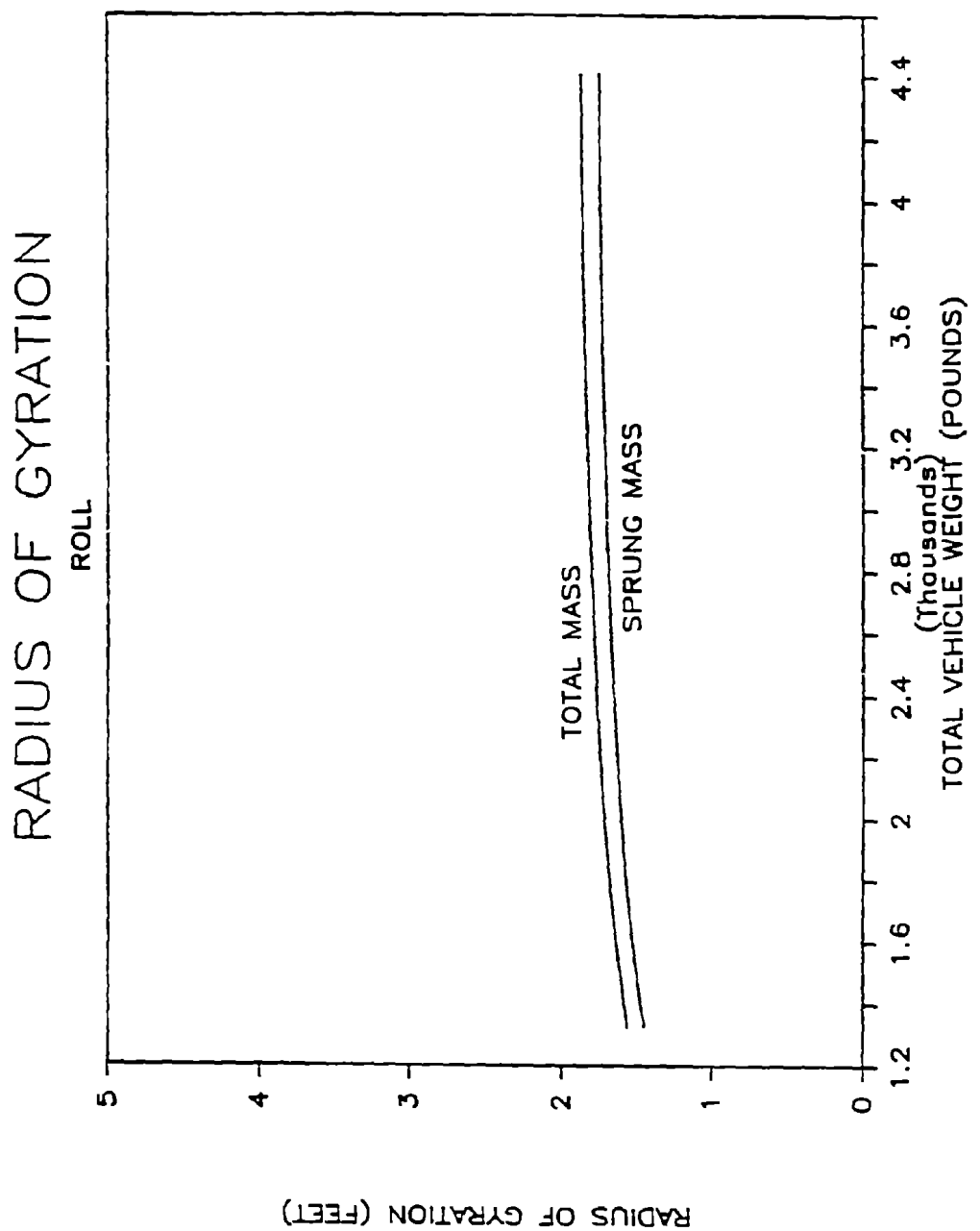

Figure 22. Roll radius of gyration.

5. Vehicle Crush Characteristics

Crush characteristics of vehicles are important factors in the impacts with safety appurtenances. The crush characteristics will depend on the dimensions of the object struck and the impact point. This chapter discusses both the frontal and side crush characteristics of passenger vehicles.

a. Frontal Crush Characteristics

The frontal crush characteristics of vehicles depend on the width of the object struck. Information is available on crush characteristics with narrow objects such as utility poles, luminaire supports and sign supports. Most of this information is based on impacts with a rigid instrumented pole. The instrumented pole provides a detailed time history of the crush forces acting on the vehicle. Information is also available on vehicle impacts with rigid walls.

(1) Rigid Pole Tests. In a rigid pole test, a vehicle impacts a narrow (normally 8 to 10-in in diameter) rigid pole at some point along the front of the vehicle. The impact force time history and the motion of the vehicle center of gravity are recorded. The data is plotted in the form of a force deformation curve to define the crush characteristics of the vehicle. This type of test has typically been conducted at a speed of 20 mi/h. The 20 mi/h test produces displacements on the order of 20 to 25 in. This is the range of interest for studies of breakaway hardware. When the displacement exceeds these levels the engine is directly contacted by the crushed slug of material in front of the pole. Since the engine is very rigid, the impact force can increase rapidly due to the large inertial force required to arrest the engine.

The general characteristic of the force deformation curves

generated from rigid pole tests is an increasing force deformation relationship with a slope of 18,000 lb/ft. Figure 23 shows typical force deformation curves for mini-sized vehicles.

(2) Rigid Wall Tests. Vehicles sold in the United States are required to pass FMVSS 208 "Occupant Crash Protection". The test procedure requires that the vehicle impact a rigid wall at a speed of 30 mi/h. The response of dummies located in the front seating positions of the vehicle are monitored during the impact. The response of the dummies must meet prescribed specifications for the vehicle to pass the test.

In addition to these tests, NHTSA has conducted a series of 35 mi/h tests in a rigid instrumented wall. The instrumented wall test provide an excellent measurement of the impact force time history. The stiffness measured by these tests is defined as the ratio of the peak force occurring during the impact to the dynamic crush which occurs at that point in time. Stiffness values of 45,000 to 90,000 lb/ft are reported from this series of tests.

b. Side Impact Crush Characteristics

Limited data is available on the side crush characteristics of passenger vehicle with narrow objects. Recent tests conducted by Ensco at the FHWA FOIL Facility provide side crush data for three mini-sized vehicles and a full size sedan. The test procedure used a rigid instrumented pole with a three segment face. Each segment was instrumented to provide a detailed time history of the forces acting on it. The bottom segment was designed to measure the component of the impact force associated with the side sill of the vehicle. The center segment was designed to measure the component of the impact force associated with the door. The top segment was designed to measure the component of the impact force associated with the roof structure. The

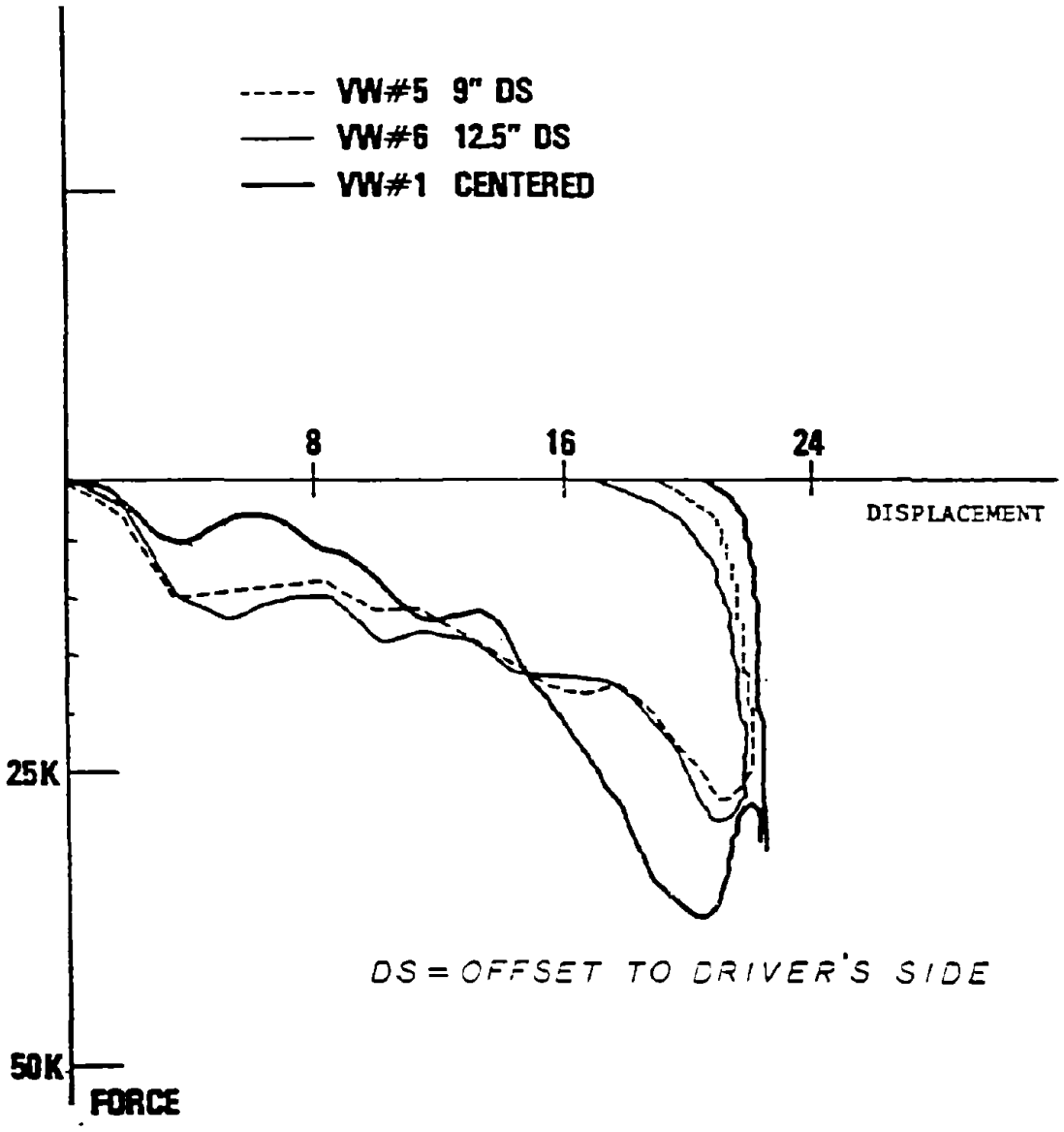

Figure 23. Force-deformation for frontal impact with narrow object.

dimensions of the rigid instrumented pole are given in table 6.

Table 6. Instrumented Rigid Pole.

(all dimension in inches above ground level)

	Lower Edge	Upper Edge	Diameter (in)
Top Segment	1.75	14.00	8.625
Center Segment	14.25	35.75	8.625
Bottom Segment	36.00	47.75	8.625

The test matrix for the test program is shown in table 7. Note the the three mini-sized car tests were conducted at a nominal impact speed of 25 mi/h while the large car test was conducted at a speed of only 10 mi/h. The force deformation data from the tests is shown in figure 24 through figure 27. The general characteristics of the force deformation curves is an increasing force with deformation up to 16-in and then a leveling off of force with increased deformation. The initial stiffness of the curve is 13,500 lb/ft. The maximum force level varies from 15,000 to 17,000 lb

An alternate form of displaying the the data to highlight the importance of each segment is shown in figures 28 to 31. These figures are in the form of a stacked bar graph of force versus time. Each bar represents the average magnitude of the force acting in a 20 millisecond period. The contribution of each segment is shown.

Table 8 shows the total momentum change associated with each test and the peak level of the impact force. The instrumented pole data was used to divide the total momentum change into three components based on the three segments of the pole. This data is also shown in the table. The three small cars provide similar

results. The large car differs in that the door and roof provide most of the momentum change.

Table 7.
Test matrix for side impact test.

Test Number	Vehicle	Nominal Test Speed	Test Weight
Test SI1	Honda Civic	25 mi/h	1806 lb
Test SI2	VW Rabbit	25 mi/h	1835 lb
Test SI3	Dodge Colt	25 mi/h	1800 lb
Test SI8	Dodge St. Regis	10 mi/h	4490 lb

Table 8.
Momentum change distribution.

	Momentum Change (lb-sec)			Total	Peak Force (kips)
	Bottom	Center	Top		
Honda Civic	963 (52%)	668 (36%)	212 (12%)	1843	17.8
VW Rabbit	894 (46%)	857 (44%)	194 (10%)	1945	15.3
Dodge Colt	793 (42%)	920 (49%)	168 (9%)	1881	16.0
Dodge St. Regis	110 (5%)	1431 (68%)	606 (28%)	2147	17.5

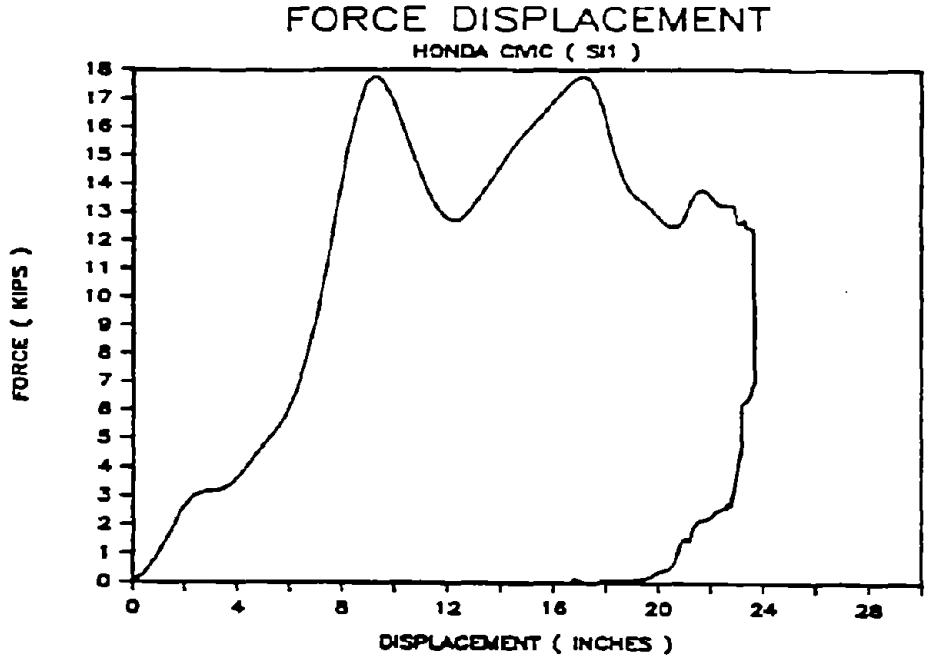

Figure 24. Force Deformation Honda Civic.

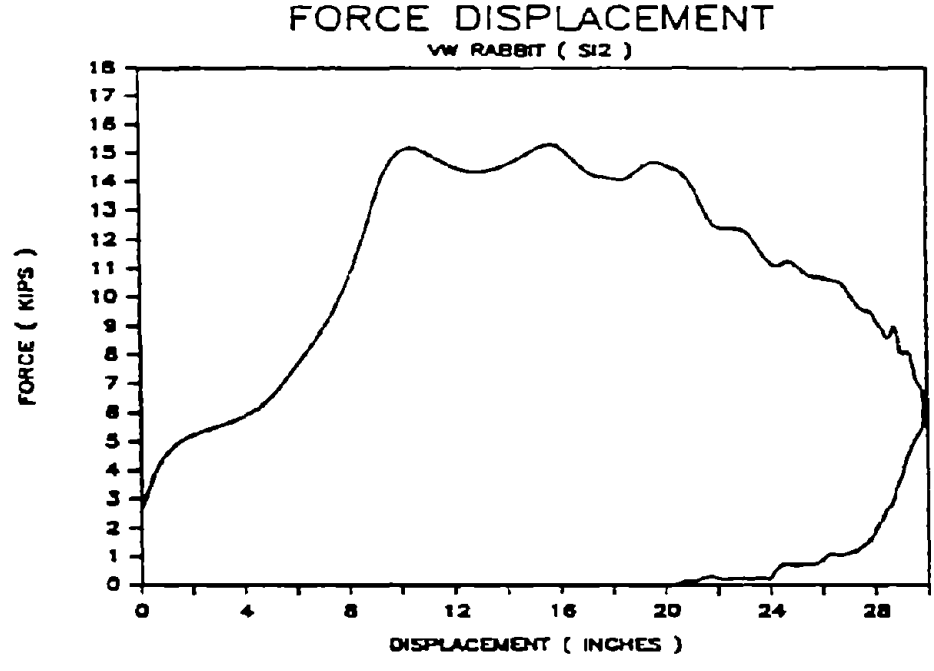

Figure 25. Force Deformation VW Rabbit.

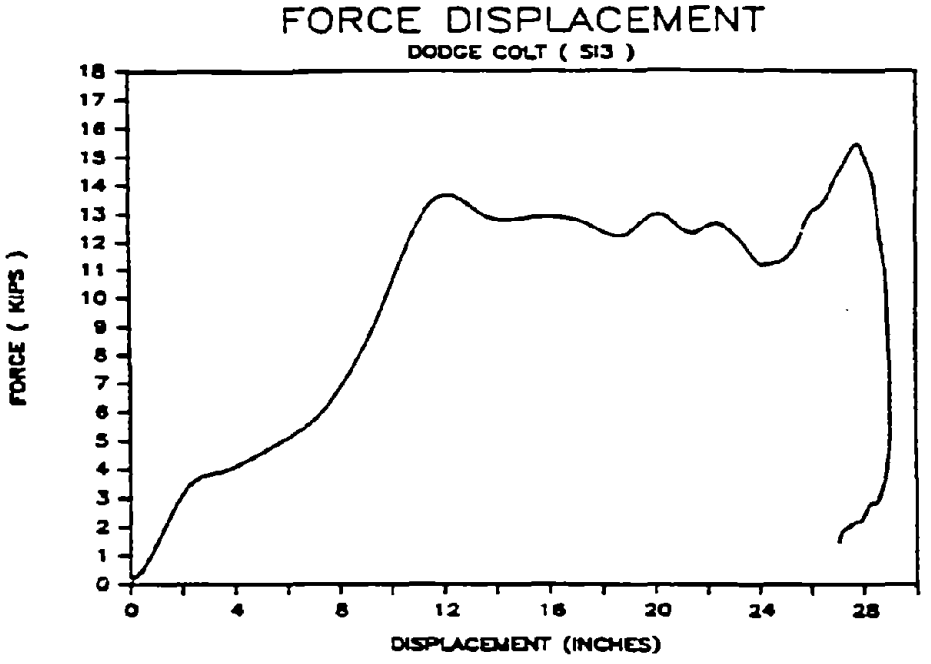

Figure 26. Force Deformation Dodge Colt.

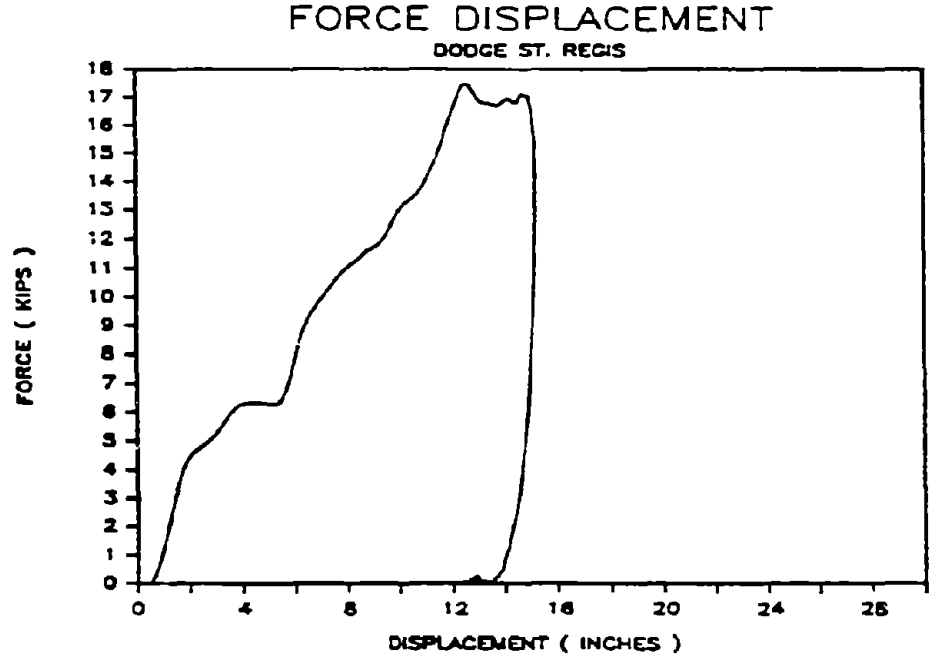

Figure 27. Force Deformation Dodge Saint Regis.

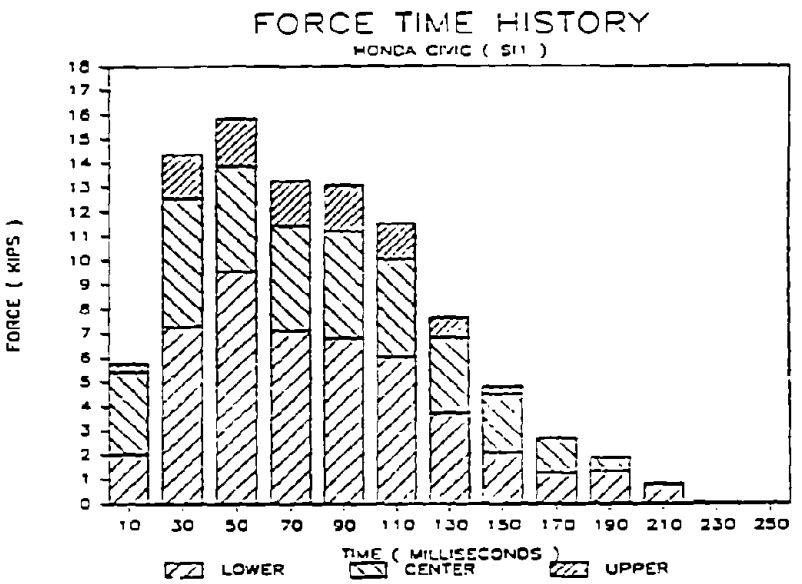

Figure 28. Force Time Honda Civic.

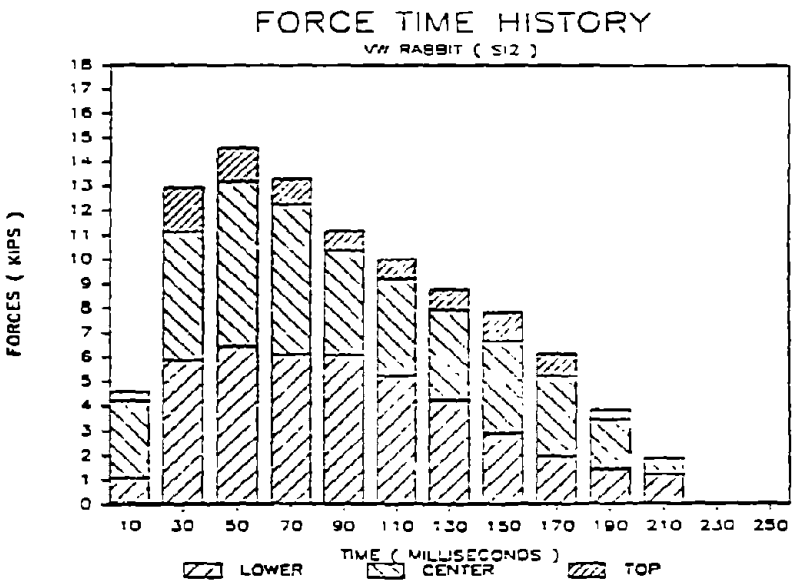

Figure 29. Force Time VW Rabbit.

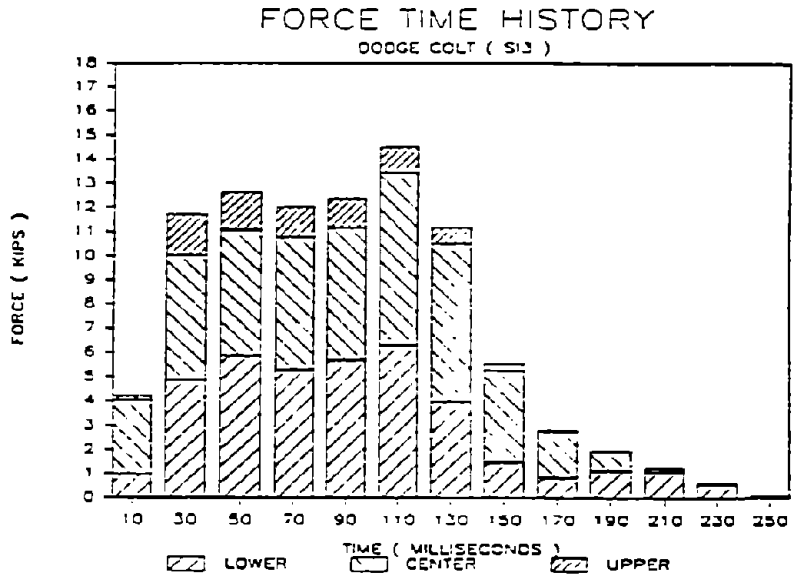

Figure 30. Force Time Dodge Colt.

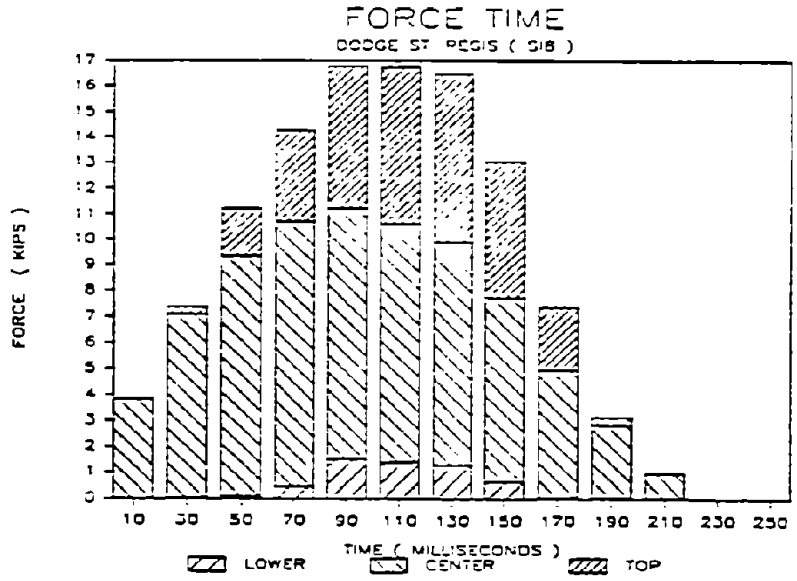

Figure 31. Force Time Dodge Saint Regis.

6. Human Injury Criteria

The purpose of a roadside safety appurtenance is to prevent or mitigate injury to the passengers of an encroaching vehicle. A major question in the design of roadside safety appurtenances is the level of human tolerance to impact conditions. There is no reason to believe that human injury will be a yes/no situation. First there are degrees of injury and second the tolerance to impact conditions will depend on the individual. Factors such as age, weight and physical condition are expected to be important. Given these factors a probabilistic approach to human injury is required. However, in the end the designer is faced with defining physical measurements which describe the severity of an impact and setting design limits on these measurements.

For impacts which do not produce intrusion into the passenger compartment, there are two separate impacts to be considered. First the impact between the vehicle and the object struck. Second, the impact between the passenger and the interior of the vehicle. Both impacts depend on the characteristics of the vehicle. In the first case, the geometry, weight, weight distribution and the crush characteristics are important. In the second case, the interior design of the passenger compartment is certainly important.

Biomedical research has made great strides in addressing the question of human injury due to impact conditions. This research has been conducted internationally. In the United States, NHTSA has conducted and sponsored much of this research. The result has been the development of anthropomorphic dummies (mechanical devices built to shape and weight distributions of humans) to serve as surrogates for passengers. Instrumentation housed in the dummies record the levels of acceleration and force experienced by the dummies during impact. Based on experiments with animals and human cadavers, the relationship between the characteristics of the recorded data and injury has been established. The result

is a series of processing algorithms which define descriptors of impact severity based on the recorded data. Design limits have been established for each of these descriptors.

Human injury criteria for cases where there is intrusion into the passenger compartment are much more complicated. Intrusion into the passenger compartment can occur for very high speed frontal impacts but occurs most frequently under side impact conditions. Much of the present biomedical research is devoted to the development of a side impact dummy.

a. Fixed Barrier Impact Test

As an example of the use of anthropomorphic dummies consider the frontal barrier crash test required of all passenger car by federal standards. The test calls for the vehicle to impact a rigid wall that is perpendicular to the path of travel at a speed of 30 MPH. Dummies are placed at each front designated seating position. Seat belts which require the passenger to fasten them into position are not used during the impact. In order to pass the test, the dummies must be contained within the outer surfaces of the vehicle passenger compartment throughout the test and the descriptors of human injury from the dummies must be below prescribed levels.

To explore the nature of the injury descriptors, the detail of the Part 572 dummy will be reviewed. This dummy is designed to represent the characteristics of the 50 percentile male in the United States. The dummy weighs approximately 165 lb. It is instrumented with 6 accelerometers and two load cells. The instrumentation is located at four locations:

- three uniaxial accelerometers installed in the head cavity
- three uniaxial accelerometers installed in the chest cavity

- load cell in the upper right leg
- load cell in the upper left leg

The locations are shown in figure 32.

Detailed specifications for the data collection and process of the data from these transducers are prescribed. This includes the bandwidth or frequency response for each channel,the digitizing rate for converting the data to digital form and the mathematical formula for the processing algorithms.

Processing of the head injury descriptor is based on computing the resultant acceleration from the three orthogonal accelerometers located in the head cavity from the formula:

$$A_r = \sqrt{A_x + A_y + A_z} \qquad (64)$$

This results in time series A_r over the crash duration. The descriptor for head injury is called the Head Injury Criteria (HIC) and is defined by:

$$HIC = \left[\frac{1}{(t_2 - t_1)} \int_{t_1}^{t_2} A_r \, dt \right]^{2.5} (t_2 - t_1) \qquad (65)$$

where t_1, t_2 = any two times during the impact
A = acceleration level at time t measured in G's

Given values of t_1 and t_2, the HIC is easily calculated. The expression in the square brackets represents the average acceleration during the interval. This level is raised to the 2.5 power and multiplied by the time interval $(t_2 - t_1)$. A HIC of 1000 or less is required for the vehicle to pass the rigid barrier test.

For each pair of times (t_1, t_2), a HIC value can be calculated. The processing algorithm requires that all possible

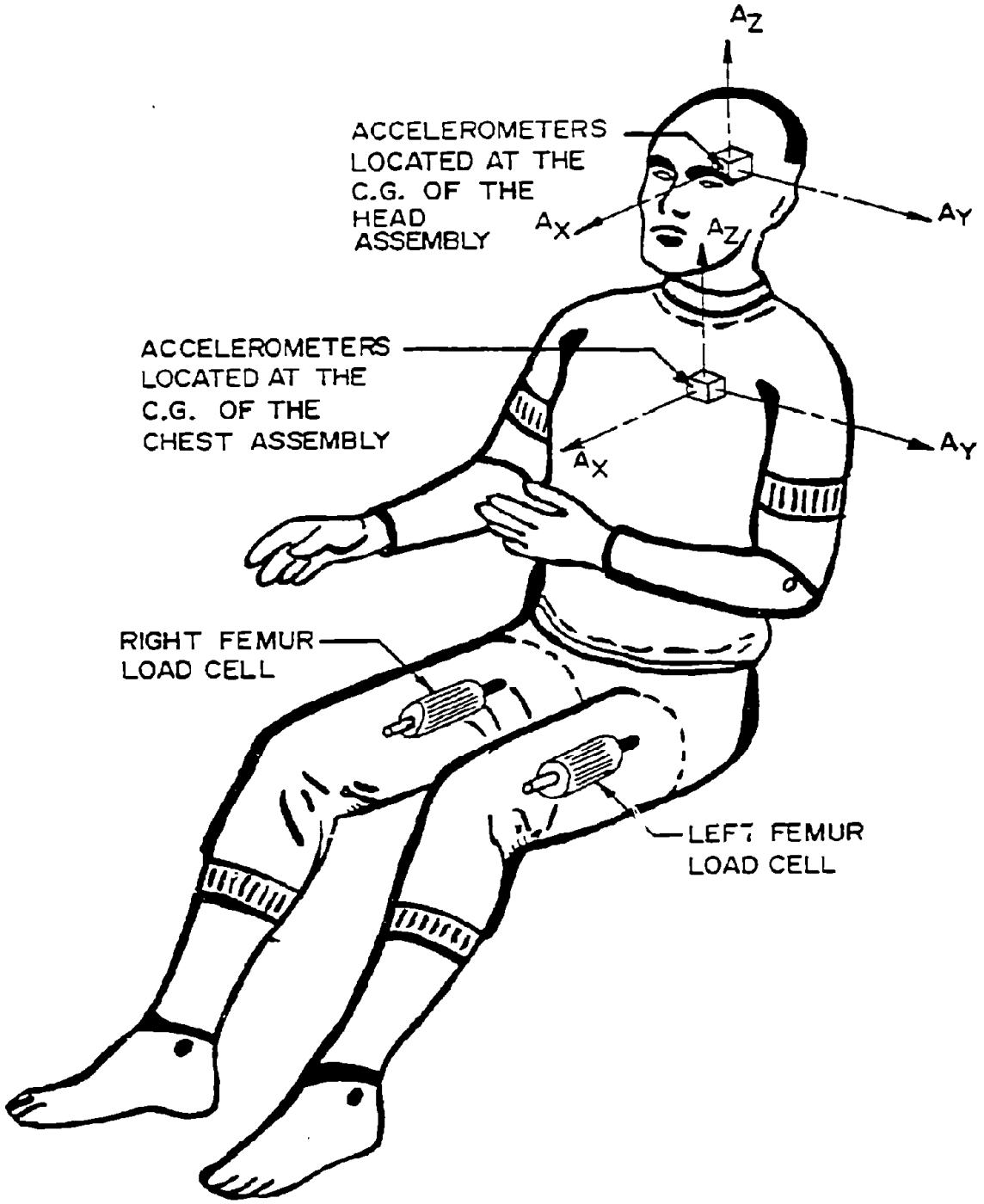

Figure 32. Instrumentation for Part 572 test dummy.

-pairs be used and the maximum HIC value be selected. Thus the complexity is not in the calculation itself but in the number of times the calculation must be calculated.

The formula for the HIC number does not provide much insight into the level of impact that is represented by a HIC of 1000. To gain insight into the level of impact corresponding to a HIC of 1000, the HIC formula can be put in the form

$$HIC = [DV(t_1,t_2)/DT]^{2.5}\ [1/g]^{2.5}\ DT \qquad (66)$$

$$= [DV(t_1,t_2)]^{2.5}/[\ (g)^{2.5}\ (DT)^{1.5}]$$

where $DV(t_1,t_2)$ = velocity change in interval (t_2-t_1)
$DT = (t_2-t_1)$ time duration
g = acceleration of gravity

This equation is plotted in figure 33 for HIC values of 1000, 500 and 250. The plot shows that the velocity change allowable for a given HIC level increases with increased time duration (t_2-t_1). The time duration can be increased by providing more give in the object struck. A HIC of 1000 corresponds to a velocity change of 32.2 ft/sec and a time duration of 10 milliseconds. Test data for frontal impacts indicate that time durations of 7 to 50 milliseconds can be expected.

The HIC algorithm selects the values of t_1 and t_2 based on a search of all combinations of t_1 and t_2. To develop insight into this selection process consider an acceleration pulse with the shape of half cosine wave as shown in figure 34. For a given value of the duration (t_2-t_1), the maximum value of the average acceleration occurs when the time interval is centered about the peak of the acceleration trace. This implies that $-t_1=t_2$. Using this approach the HIC is only a function of a single parameter b as defined by:

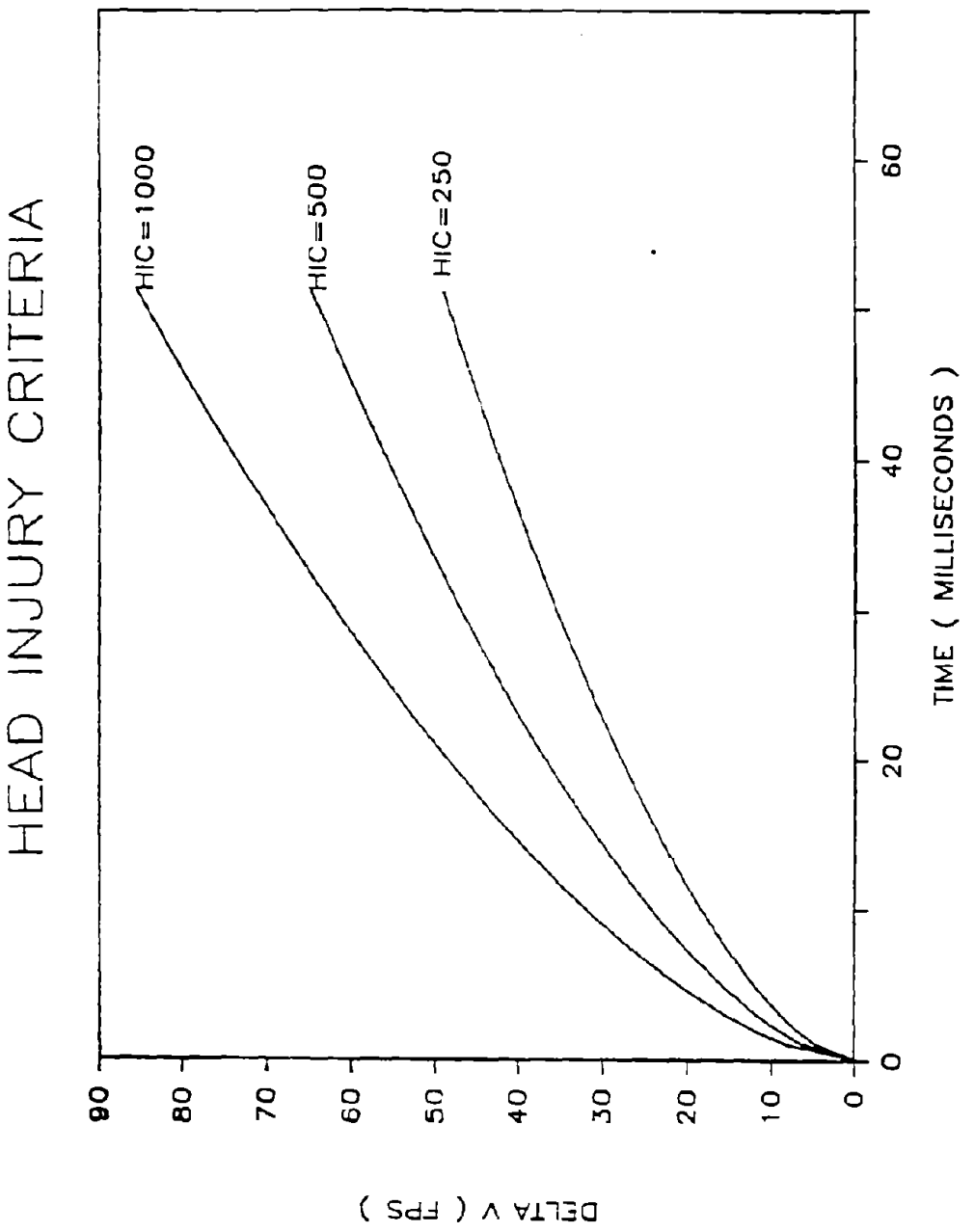

Figure 33. HIC number as a function of delta V and time duration.

$$HIC = \left[\frac{A_m}{bT} \int_{-bT/2}^{bT/2} \cos(\pi t/T)\, dt \right]^{2.5} bT \qquad (67)$$

$$HIC = [A_{max}]^{2.5}\, T\, [\, (2/\pi)\, \sin(\pi b/2)\,]^{2.5}/(b^{1.5})$$

$$HIC = [A_{max}]^{2.5}\, T\, F(b)$$

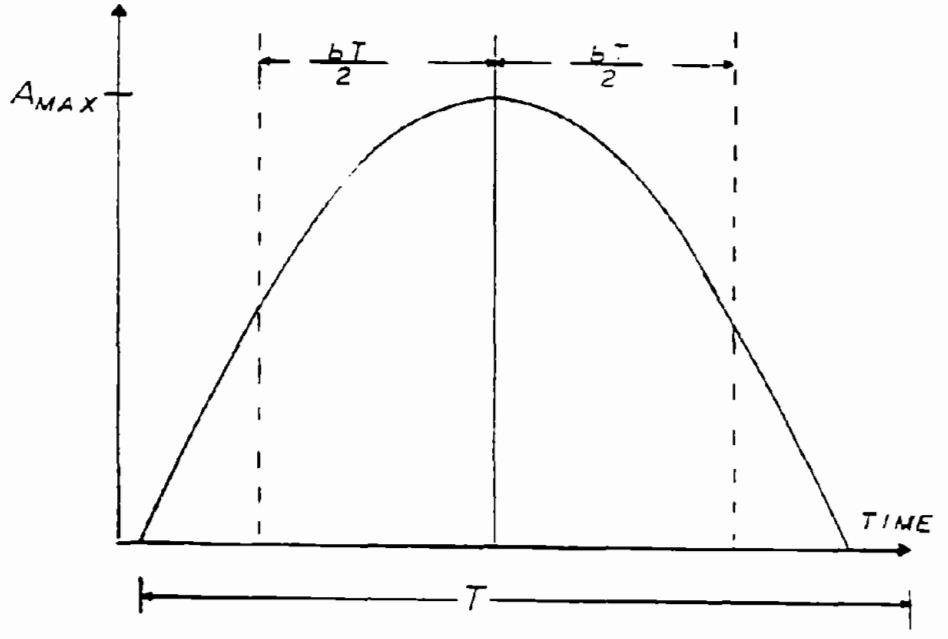

Figure 34. Sine wave pulse shape.

A plot of F(b) versus the parameter b is shown in figure 35. The peak value occurs at b=Ø.65 and has a value of .41. The HIC value can thus be estimated for head decelerations that resemble a cosine wave shape by the equation:

$$HIC = [\ A_{max}\ ]^{2.5}\ T\ (Ø.41) \qquad (\ 68\ )$$

where T is the duration of the cosine pulse

The equation for the HIC number will depend on the wave shape of the deceleration pulse. However the cosine wave shape appears reasonable based on limited data. The velocity change associated with the HIC is not the total velocity change resulting from the impact but only a portion of this impact. For the case of the cosine wave shape, the relationship between the delta V associated with HIC and the total delta V is given by:

$$DV(t_1,t_2) = Ø.85 \text{ Total delta V} \qquad (\ 69\ )$$

The accelerometers in the chest cavity are processed by first calculating the resultant acceleration in the same fashion as the head accelerometers. Two descriptors are predicted from the chest resultant acceleration. The first descriptor of chest injury is the maximum chest peak acceleration whose cumulative duration is greater than 3 milliseconds. The limiting value for the maximum chest acceleration is 60 G's. The second descriptor is called the Severity Index and is defined by:

$$SI = \int_{Ø}^{T} A^{2.5}\ dt \qquad (\ 7Ø\ )$$

where A = Resultant chest acceleration measured in G's

The time interval is the duration of the impact. The limiting value is 1ØØØ. This descriptor sums the weighted acceleration

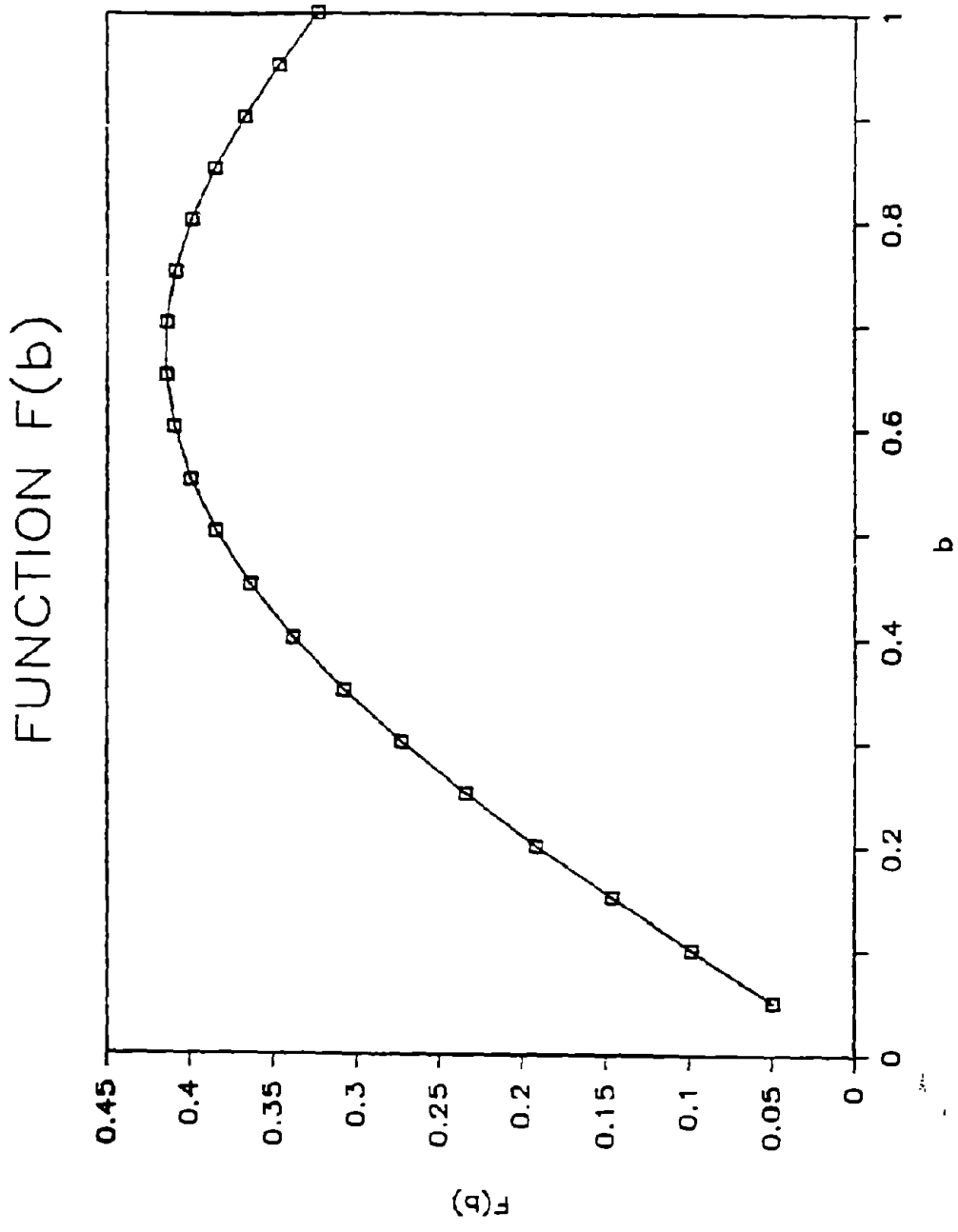

Figure 35. Function F(b) for a half cosine wave pulse.

over the entire impact. If the acceleration history has a half cosine wave shape as shown in figure 34, the integral for SI would become:

$$SI = [A_{max}]^{2.5} \, T \int_{-T/2}^{+T/2} [\, \cos (\text{pi } s/2) \,]^{2.5} \, ds \qquad (71)$$

$$= [A_{max}]^{2.5} \, T \, (0.46)$$

This is similar to the expression for evaluation of the HIC for the case of a half cosine wave shape.

The remaining injury descriptor is the peak force experienced in the upper leg of the dummy. The limiting value is 2,250 lb.

b. NCHRP 230 Approach

The designer of highway safety appurtenances is faced with the task of providing a safe roadside environment for a wide range of vehicles. It would be impractical to attempt to test every safety appurtenance with every vehicle using the roadway. The approach has been to divide the vehicles using the roadway into classes based on vehicle weight. Any vehicle meeting the given weight constraints and being no older than 5 years can be used to represent the weight class in a crash test. To access the performance of an appurtenance, the dynamics of the vehicle are measured and descriptors related to human tolerance derived from these measurements. The concept being that if the dynamics of the vehicle are kept within prescribed limits, the resultant loading on the occupants of the vehicle will be within safe limits.

Another aspect of the problem faced by the designer is the definition of the conditions under which the performance criteria must be met. The approach has been to crash test under reasonable worst case conditions. Usually this means high speed conditions

(60 mi/h) and in the case of barriers, an impact angle of 25 degrees.

The National Highway Research Program Report 230 "Recommended Procedures for the Safety Performance of Highway Appurtenances" is the document used by the Federal Highway Administration to evaluate the performance of safety appurtenances. The safety goals defined by this document are:

A. Smoothly redirect the vehicle away from a Hazard zone

OR

B. Gently stop the vehicle

OR

C. Readily breakaway

The first requirement to meet these goals is that the vehicle remain upright during and after the impact (rollover of the vehicle is not acceptable). The quantification of the goals is based on 4 human injury descriptors derived from the acceleration time histories measured at the vehicle center of gravity. Two descriptors are associated with the longitudinal direction and two with the lateral direction. The two descriptors address distinct and sequential phases of the impact between the occupant and the interior of the vehicle. The first descriptor is the relative speed with which the occupant impacts the interior of the vehicle. The second descriptor is the maximum deceleration experienced by the vehicle after the impact between the occupant and the interior of the vehicle.

The algorithm for estimating the relative speed between the occupant and the interior of the vehicle is based on an approach known as the flail space approach. The approach assumes that during the initial phase of the impact between the vehicle and the safety appurtenance, the occupant moves as a free body at the

impact speed. As the vehicle decelerates in response to the impact force generated, the initial distance (flail distance) between the occupant and the vehicle interior decrease. The relative velocity between the occupant and the vehicle increase during this period. The expression for the relative speed between occupant and vehicle is given by:

$$V_i = V_o - [\, V_o - \int_{\emptyset}^{t} a(t^*)\, dt^* \,] \qquad (72)$$

$$= - \int_{\emptyset}^{t} a(t^*)\, dt^*$$

where $a(t^*)$ = time history of acceleration

The expression for the distance between the the occupant and vehicle is the time integral of the relative speed:

$$D(t) = D_o - \int_{o}^{t} V_i(t^*)\, dt^* \qquad (73)$$

where D_o = initial distance between occupant and vehicle

When $D(t)=\emptyset$, the occupant will impact the interior of the vehicle.

The processing algorithm for estimating the relative speed of impact separates the longitudinal and lateral directions and treats each separately. The appropriate time history is first integrated with respect to time to produce a relative speed time history. This time history is than integrated to provide the relative displacement time history. From this time history, the time at which the relative displacement is equal to zero is recorded. The value of relative speed corresponding to this time is the value called the delta V for the test. The flail distance for the longitudinal direction is nominally taken as 2 feet. The

flail distance for the lateral direction is normally taken as 1 ft.

Based principally on dummy head impacts into windshields, a limiting value of delta V for the longitudinal direction was set at 40 ft/ sec. The implication being that the HIC value would be high for such impacts indicating severe but not fatal injury. While a similar argument might be made for side impacts, accident data suggested that a lower limiting value was appropriate for side impacts. A delta V of 30 FPS was selected for the lateral limiting value.

To provide insight into the nature of the flail space approach, consider an impact which produces a constant deceleration. The speed and displacement of the vehicle are given by:

$$V_v(t) = V_o - g\ t \qquad (74)$$

$$D_v(t) = V_o\ t - .5\ g\ t^2 \qquad (75)$$

where g = deceleration level (feet/second/second)
V_o = Impact speed (feet/second)

Since the occupant is assumed to be free of external forces during the initial phases of the impact, the occupant will travel at the impact speed during this phase. The speed and displacement of the occupant are given by:

$$V_{oc}(t) = V_o \qquad (76)$$

$$D_{oc}(t) = V_o\ t \qquad (77)$$

Impact between the occupant and the vehicle will occur when the initial displacement between occupant and vehicle interior, D_o, is equal to $(D_{oc} - D_v)$ or

$$D_o = 0.5\ g\ t^2 \qquad (78)$$

The time when the occupant reaches the interior of the vehicle is given by:

$$T_i = \sqrt{2\ D_o/g} \qquad (79)$$

Figure 36 is a plot of deceleration level versus time to impact for 4 values of D_o (1, 1.5, 2, and 2.5 ft). This plot indicates that the occupant/vehicle impact occurs 0.075 and 0.150 seconds for a wide range of deceleration levels and flail distances. The impact speed is given by:

$$V_i = 2\ g\ T_i \qquad (80)$$

A plot of impact speed versus deceleration level is shown in figure 37. For a flail distance 2-ft, an impact speed of 40 ft/sec is predicted for an acceleration level of 12 G's. For a 1-ft flail distance, an impact speed of 30 ft/sec is predicted for 14 G's.

The second descriptor of human injury is associated with the ride down phase of the impact. This phase occurs after the initial occupant/vehicle impact and continues to the end of the vehicle/appurtenance impact. The assumption during this phase of the impact is that the occupant remains in contact with the impact surface and then directly experiences the vehicle acceleration. A limiting value of 20 G's was selected for this acceleration for both the longitudinal and lateral directions. Again the value is compared to severe but not life-threatening conditions.

The algorithm for determining the value of ride down acceleration specifies that the accelerometer signal be filtered with an SAE j211b class 180 filter and then processed with a 10

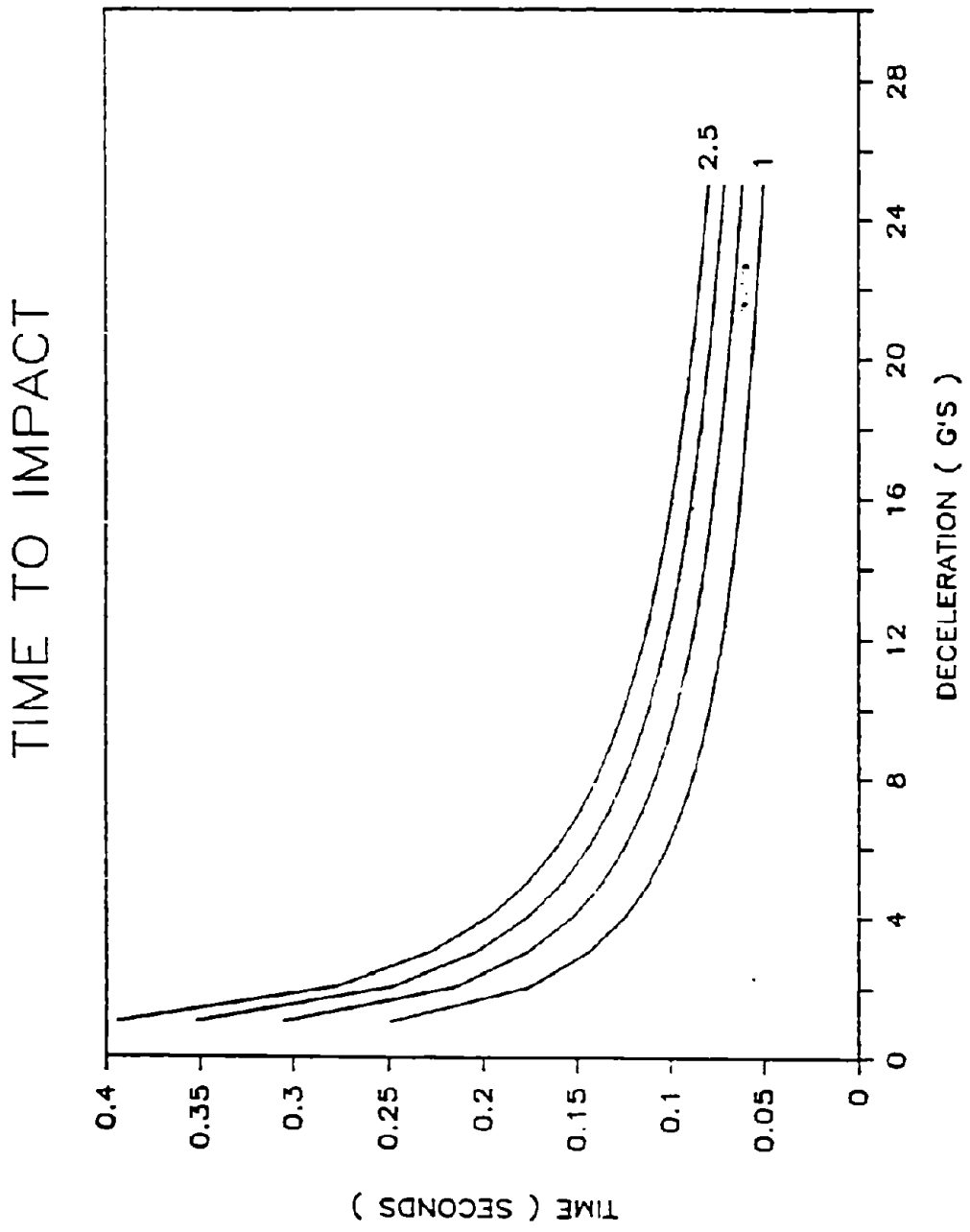

Figure 36. Time to impact versus deceleration level.

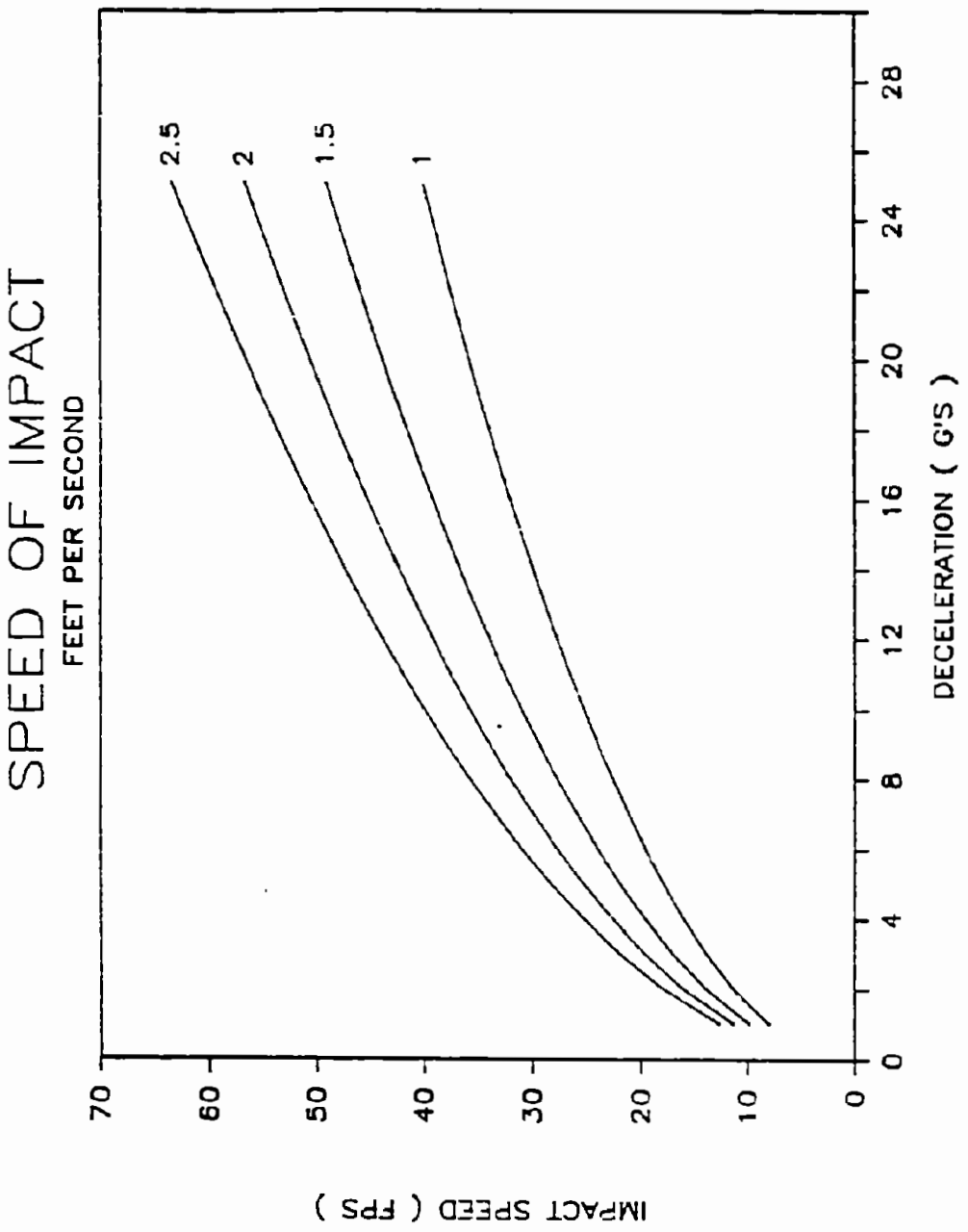

Figure 37. Occupant delta V as a function of deceleration level.

millisecond averaging filter. This filter specification is very important since the peak acceleration can be highly dependent on the filtering process. A class 180 filter produces little or no attenuation of frequencies up to 180 hertz (cycles per second). At a frequency of 300 hertz, the attenuation is only 30 percent. The 10 millisecond averaging filter produces larger attenuation in this frequency range. To explore the filtering characteristics of the averaging filter consider a sine wave of frequency f and amplitude A_{max}. The output of an averaging filter is given by:

$$\text{output}(t) = (1/T)\int_{t-T/2}^{t+T/2} A_{max} \cos (2 \pi f) t \, dt \qquad (81)$$

$$= A_{max} \cos (2 \pi f) t \; [\, \sin (\pi f T) / (\pi f T) \,]$$

where T = the averaging window duration

The term in the square brackets defines the filtering characteristics of the averaging filter. A plot of filtering characteristics for a 10-millisecond and 50-millisecond window are shown in figure 38. The longer the averaging window the more filtering of the signal. Filters are usually described in terms of the 3db point (i.e. the point at which the ratio of output to input is .707). If this approach was applied to the averaging process, a 10-millisecond averaging filter would be a 44-hertz filter while a 50 millisecond filter would be a 8-hertz filter.

NCHRP 230 states that the limiting values for the human injury descriptors be considered threshold limits and that test results should fall well below these limits to promote safer performing appurtenances. The question of how much lower than the limiting value, the values should be is considered a policy decision. In making this policy decision, NCHRP 230 recommends

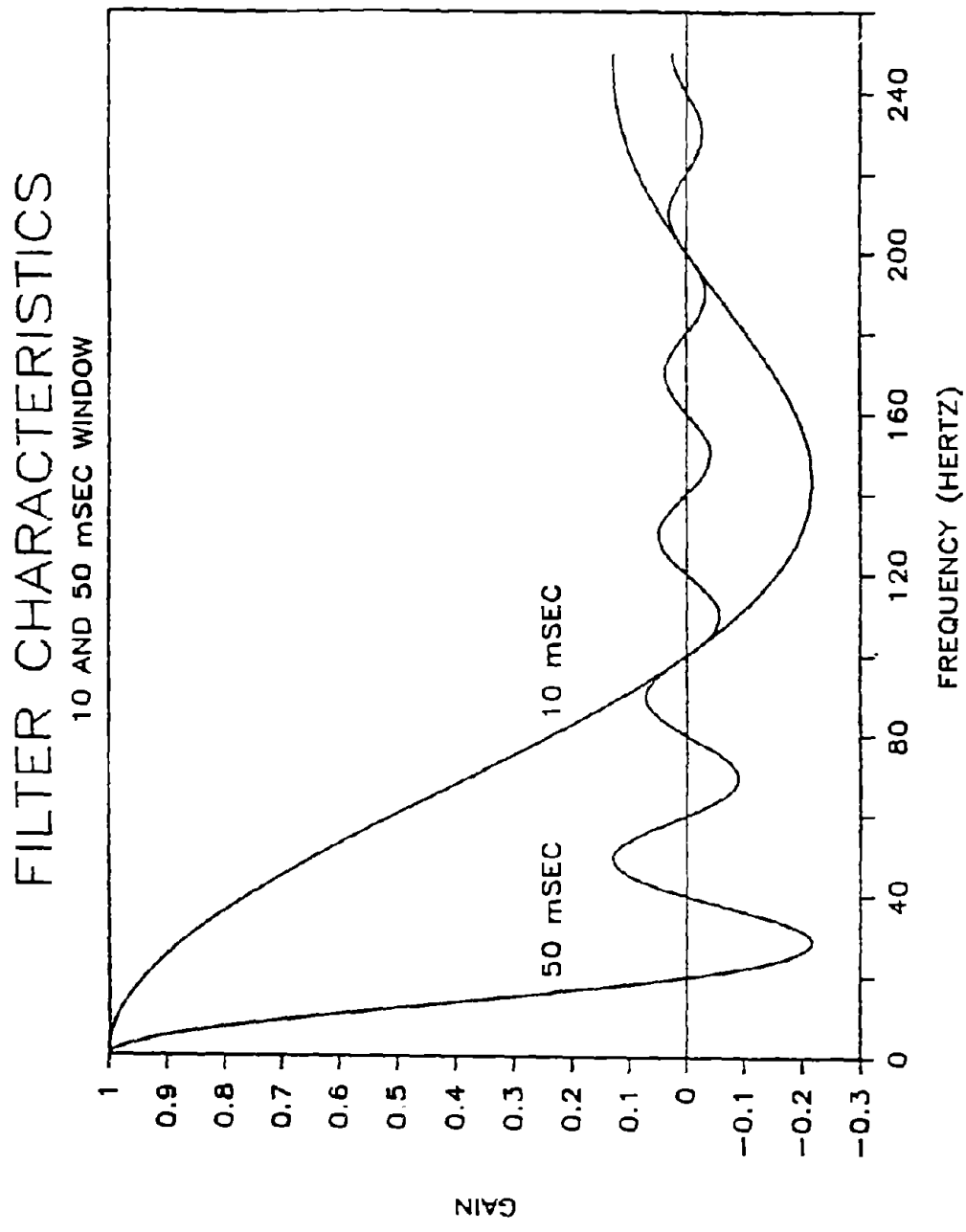

Figure 38. Filter characteristics of 50-millisecond and 10-millisecond averaging windows.

that cost effectiveness and "art-of-the-possible" be considered. The document, however, provides recommended design values for four appurtenance types. These values are given in table 9 for the longitudinal direction and in table 10 for the lateral direction.

Table 9. NCHRP 230 recommended occupant risk values longitudinal direction.

Appurtenance Type	Delta V	Ridedown Acceleration
Breakaway/Yielding Supports		
* Signs and Luminaire	15	15
* Timber Utility Poles	30	15
Vehicle Deceleration Devices	30	30
Redirectional Barriers	30	15

Table 10.NCHRP230recommended occupant risk values for lateral direction.

Appurtenance Type	Delta V	Ridedown Acceleration
Redirectional Barriers	20	15

c. Comparison of Occupant Injury Criteria

A number of test programs conducted by FHWA in the last several years involved crash testing where both dummies and NCHRP 230 criteria were used to evaluate performance. This presents the opportunity to compare these criteria. The example used in this section is based on a series of tests conducted by ENSCO,Inc. on impact attenuators. All the data used is for head-on arresting types of tests.

(1) Comparison of Nominal and Measured Flail Distance. In NCHRP 230, the flail space approach is introduced and a flail distance of 2-ft recommended as typical for the longitudinal direction. In the test program the actual flail distance (the distance from the head of the dummy to the windshield) was measured. Two delta V were calculated for each test, one for a flail distance of 2-ft and one for a flail distance of the measured value. This data is shown in figure 39. A linear regression analysis was performed to determine the relationship between the two resulting values of delta V. The relationship resulting is:

$$\text{Delta } V_a = 0.96 \text{ Delta } V_n - .54 \qquad (82)$$

where Delta V_a is based on the measured flail distance
Delta V_n is based on nominal flail distance, 2 feet

The correlation coefficient was very high (0.959) indicating a strong relationship. This tends to indicate that the nominal flail distance of 2 ft is a good choice.

(2) Comparison of HIC and Delta V_n. HIC values and Delta V_n are plotted in figure 40. for unrestrained dummies in the driver position. The linear regression analysis for this data

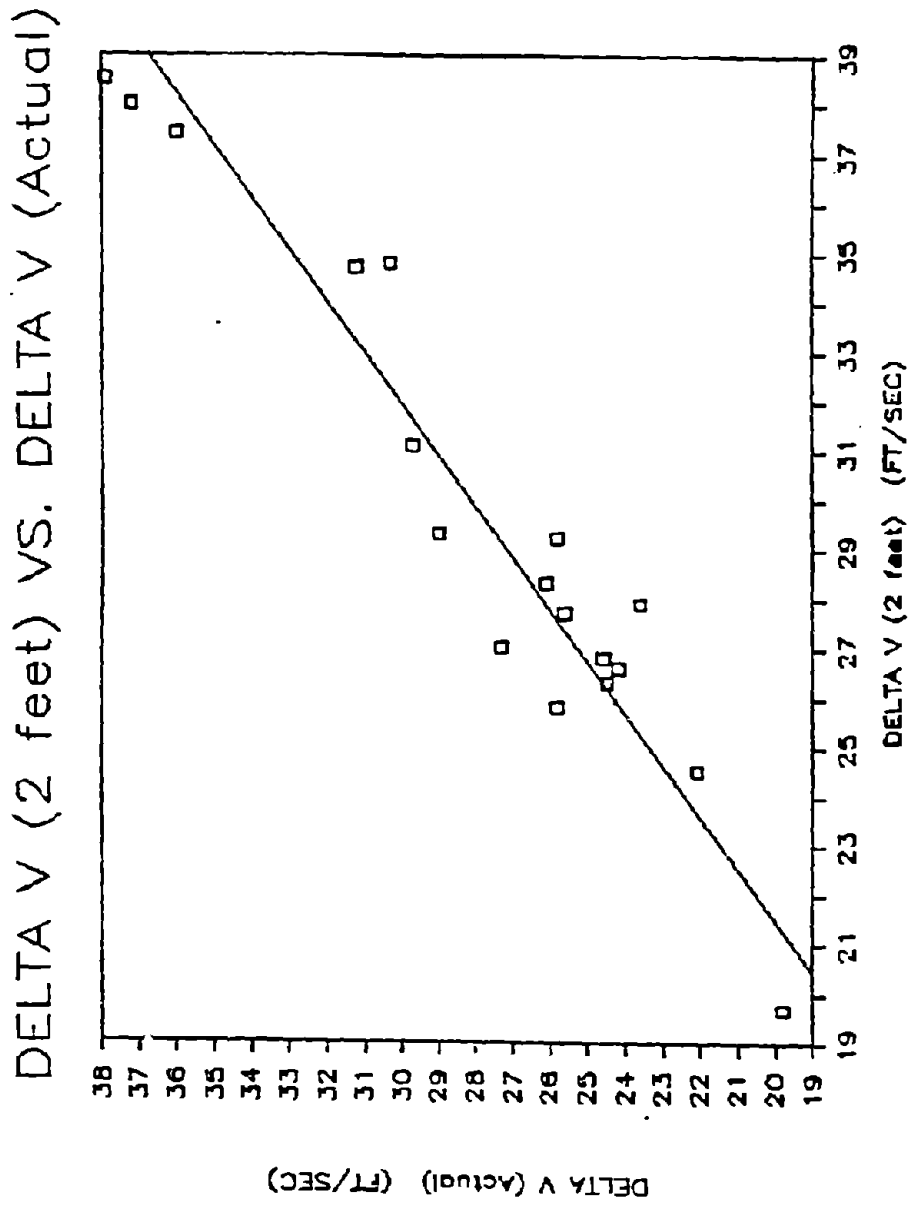

Figure 39. Correlation of delta V for actual and nominal flail distances.

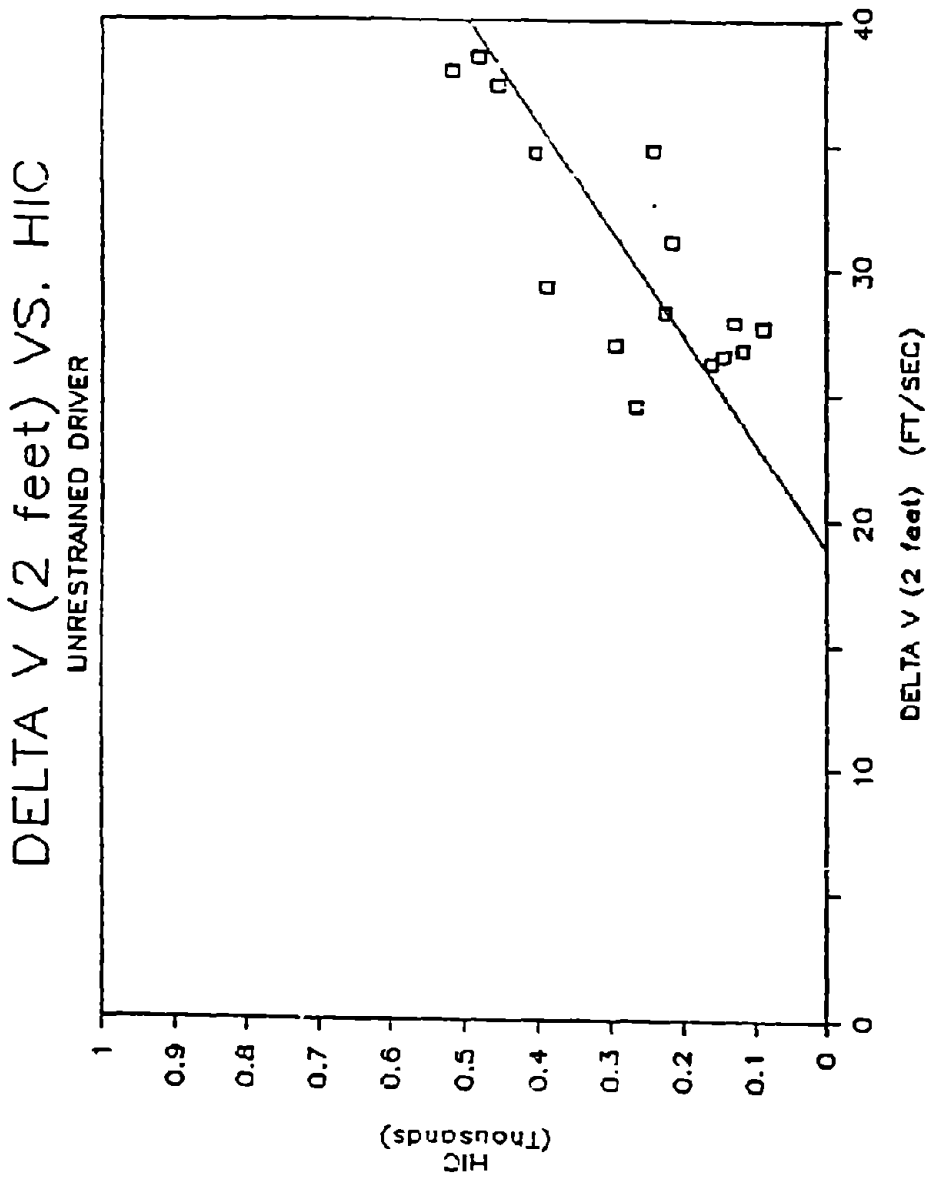

Figure 40. HIC correlation with delta V.

set provides the equation:

$$HIC = 23.56 \text{ delta } V_n - 445.68 \qquad (83)$$

The correlation coefficient is 0.791 indicating a good correlation between HIC and delta V_n. The delta V_n range for the data set was between 24 and 39 ft/sec.

(3) Comparison of Chest Severity Index and delta V_n. Figure 41 shows the data for the values of CSI and delta V_n. The regression analysis provides the equation:

$$CSI = 10.14 \text{ delta } V_n - 75.47 \qquad (84)$$

The correlation coefficient is 0.478 which while not as high as previous values still indicates a reasonable relationship.

(4) Comparison of Maximum Chest Deceleration and Delta V_n. The data for this comparison is shown in figure 42. The resulting regression equation is given by:

$$C_{max} = 0.85 \text{ delta } V_n + 8.15 \qquad (85)$$

The correlation coefficient is 0.479 indicating a reasonable relationship between the variables.

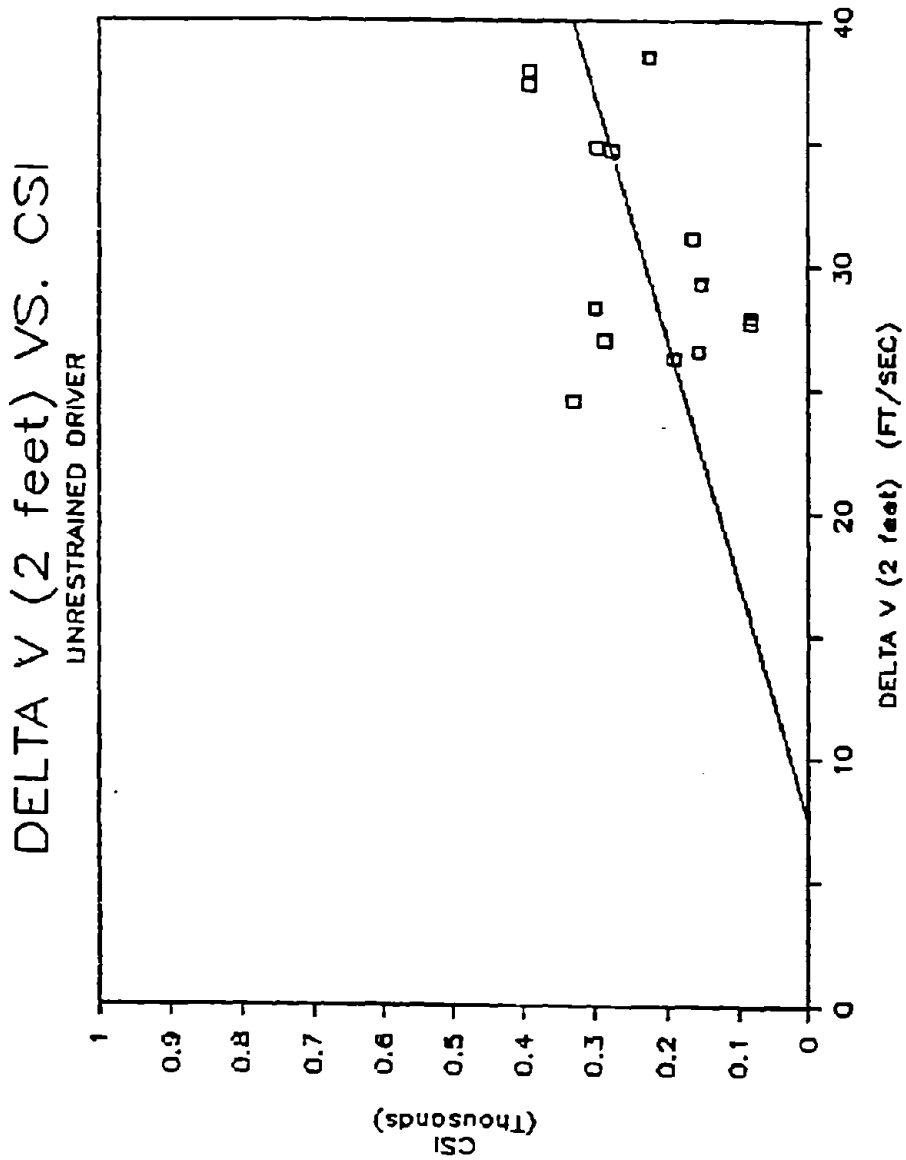

Figure 41. CSI correlation with delta V.

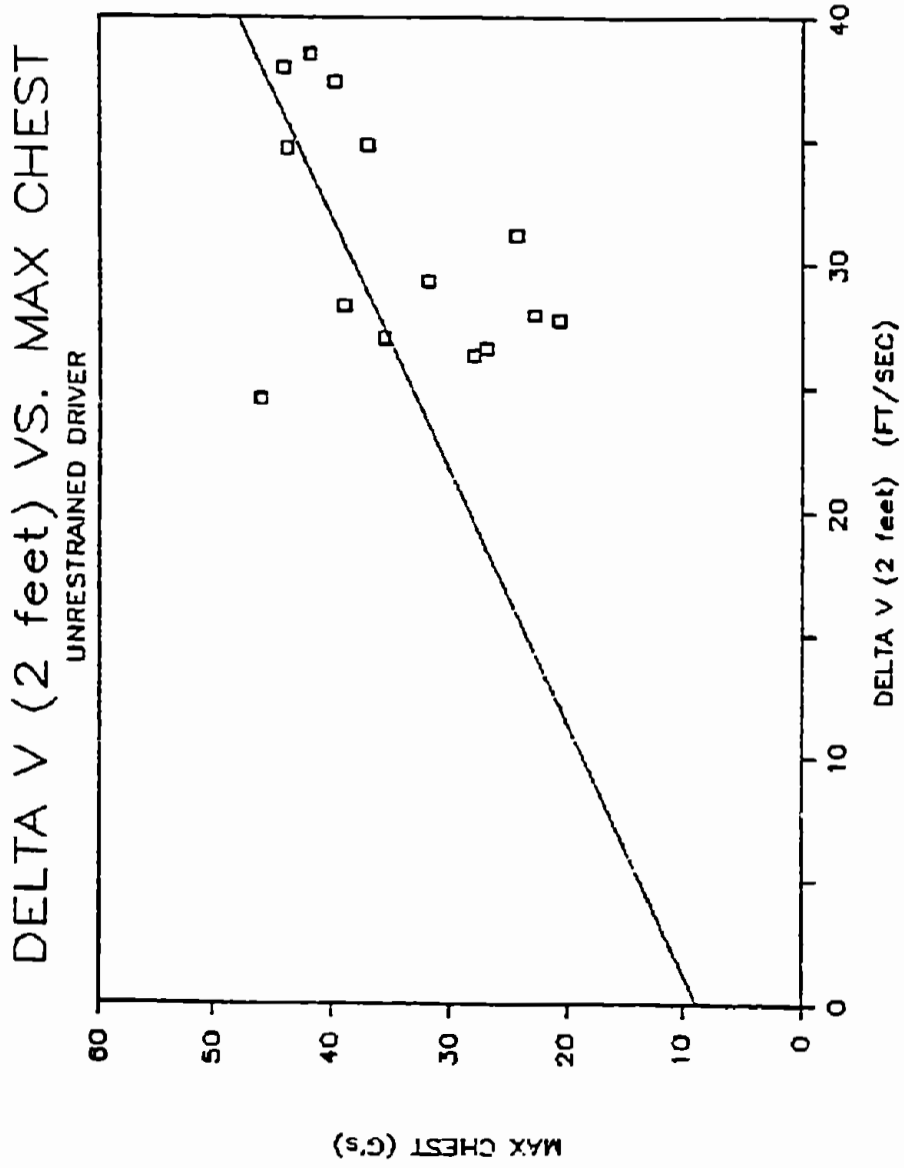

Figure 42. Maximum chest acceleration with delta V.

7. Characteristics of Safety Appurtenances

This chapter addresses the inertial characteristics of breakaway supports and the stiffness characteristics of guardrail posts. In both cases the analysis procedures presented are quite simple but provide insight and quantification of important characteristics.

a. Inertial Characteristics of Breakaway Supports

The dimensions, weight and weight distribution of breakaway hardware can play an important role in the dynamics of impact and the post impact trajectory of the device. After breakaway, the impacting vehicle must push the support out of its way. This results in a momentum change to the vehicle. At high speed, impact forces significantly higher than the breakaway force can be produced.

In section 2, the momentum change required to push the support away from the vehicle was related to the mass of the support, the radius of gyration and the distance from the impact point to the CG of the support. In this section, these characteristics will be quantified.

Luminaire supports are usually hollow taper shafts ranging in height from 20 to 40-ft. Typical values for the dimensions of aluminum and steel pole are given in table 11.

Table 11. Luminaire support dimensions.
(all dimensions in inches)

	Steel	Aluminum
Taper	0.14	0.10
Wall Thickness	0.1196	0.188
Base Diameter	0.15 L + 3.35	0.158 L + 3.684

The taper is defined as the change in outer diameter measured in inches per ft of length along the support. A typical 40-ft aluminum pole might have a base diameter of 10-in and and a top diameter of 6-in. A 40-ft steel pole might have a base diameter of 9.35-in and a top diameter of 3.75-in. Figure 43 describes the luminaire/mast arm/pole model. Based on the geometry defined in table 11 and the data provided in figure 43, the total weight of the support was calculated. The results are shown in figure 44 for steel poles and in figure 45 for aluminum poles. Pole length varies from 20 to 40-ft. In each figure, three mastarm/luminaire weights are shown. Weights approaching 500 lb are predicted for 40-ft steel poles with the heavy mastarm/luminaire configuration. For the 40-ft aluminum pole with the 120 lb mastarm/luminaire configuration, the weight approaches 350 lb.

The speed ratio for steel pole and aluminum pole configurations are shown in figures 46 and figure 47 respectively. The speed ratio is defined as the expression:

$$\text{Speed Ratio} = \frac{R^2}{R^2 + D_o^2} \qquad (86)$$

R = Radius of gyration of the pole

D_o = moment arm of impact force about pole CG

It relates the ratio of translational speed of the pole to the speed at the impact point. In most cases, the value of the speed ratio is between 0.3 and 0.5.

In section 2, the momentum change associated with pushing the pole away from the vehicle after breakaway was defined by

$$\int F\,dt = \frac{R^2}{R^2 + D_o^2}\, e\, M_p\, V_o \qquad (87)$$

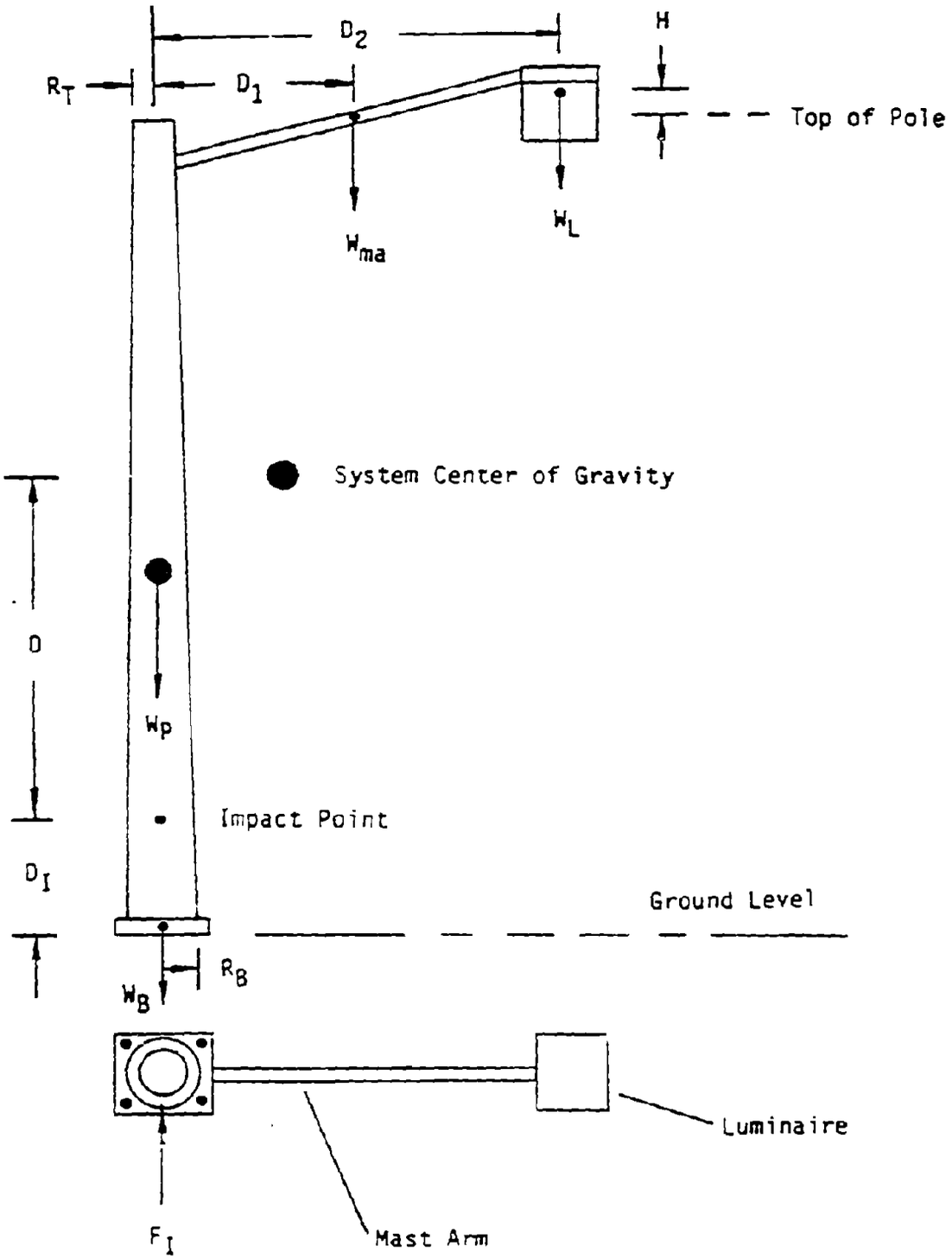

Figure 43. Luminaire/mast arm/pole model.

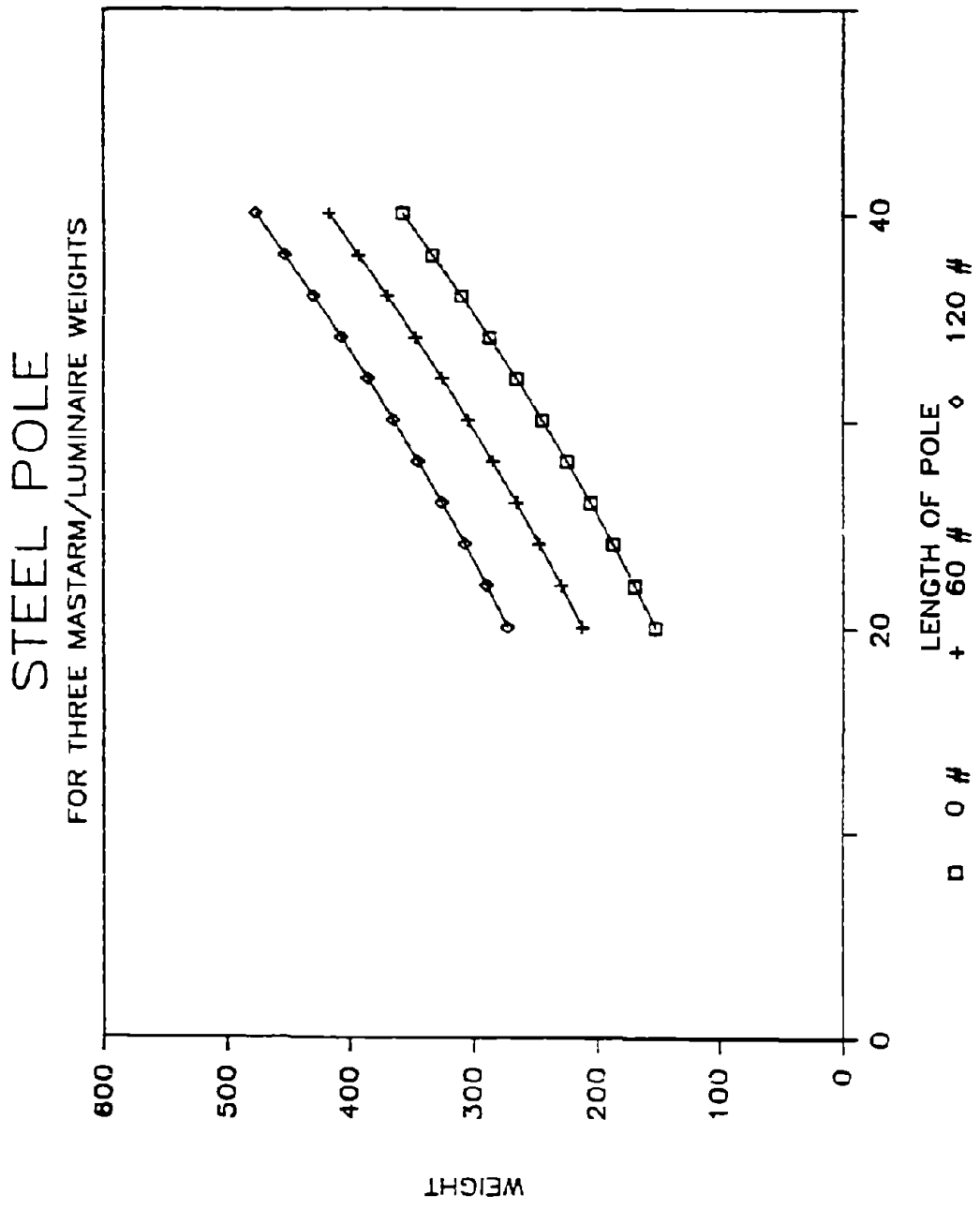

Figure 44. Weight of steel luminaire configuratıcns.

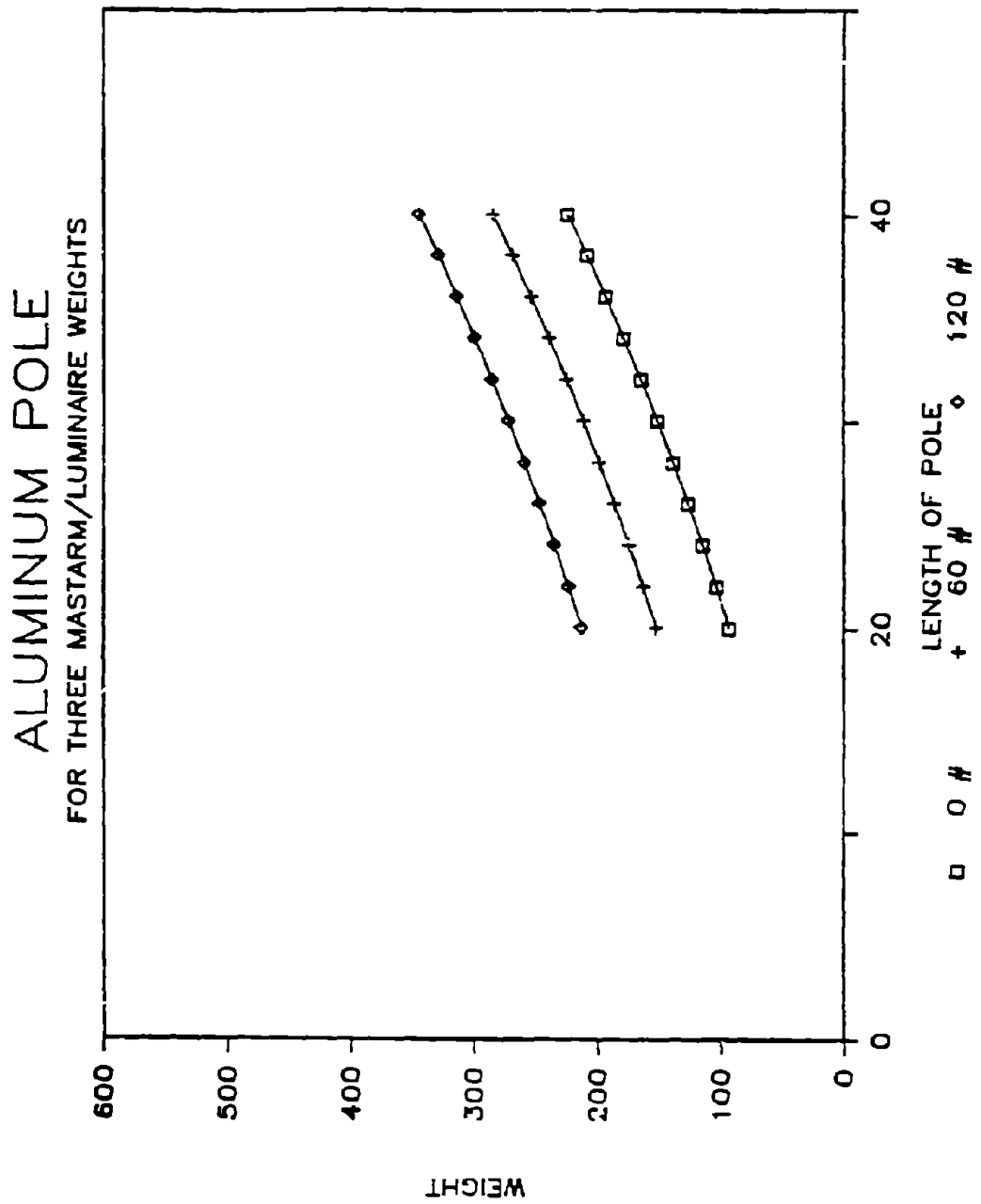

Figure 45. Weight of aluminum luminaire configurations.

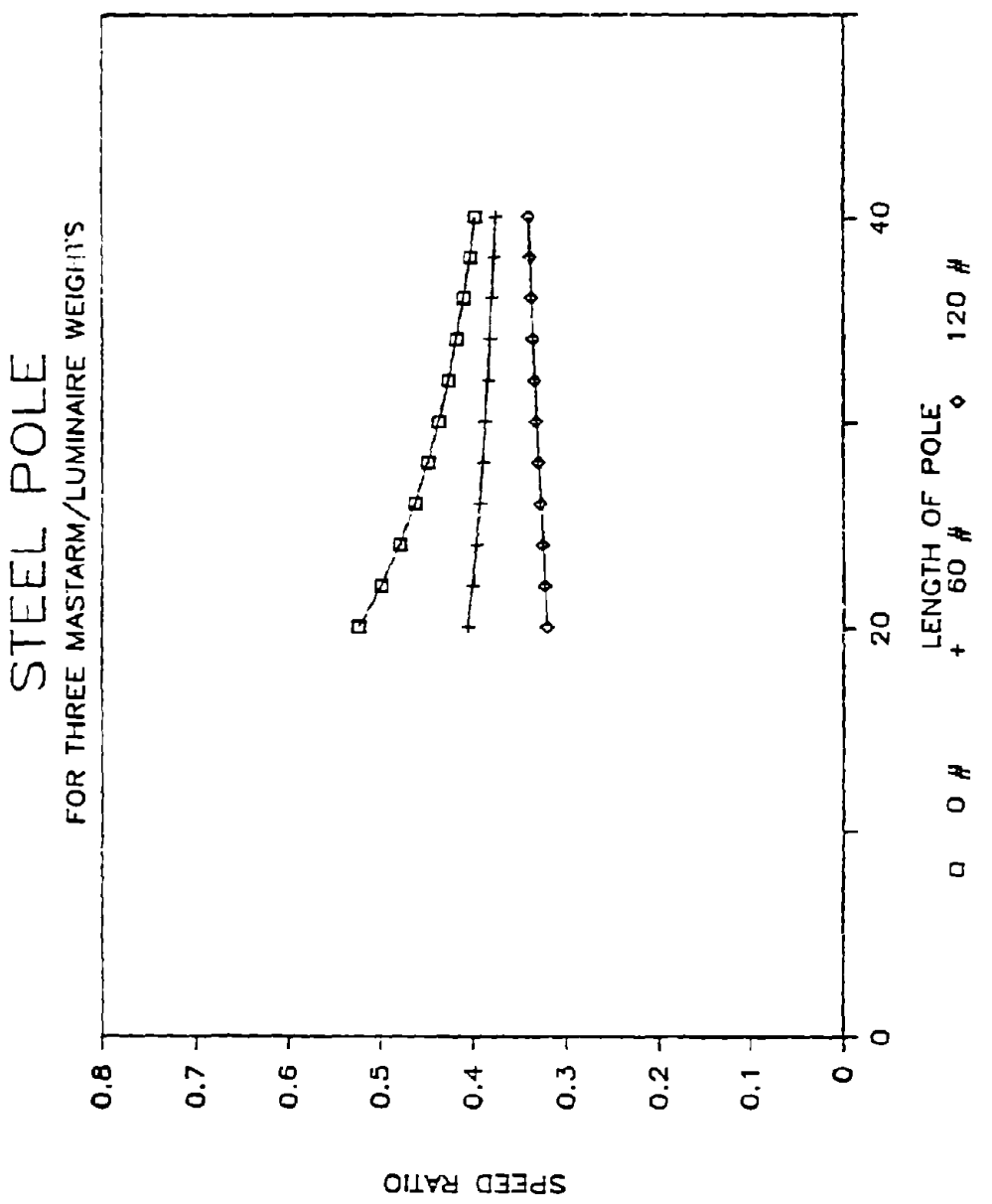

Figure 46. Speed ratio for steel luminaire configurations.

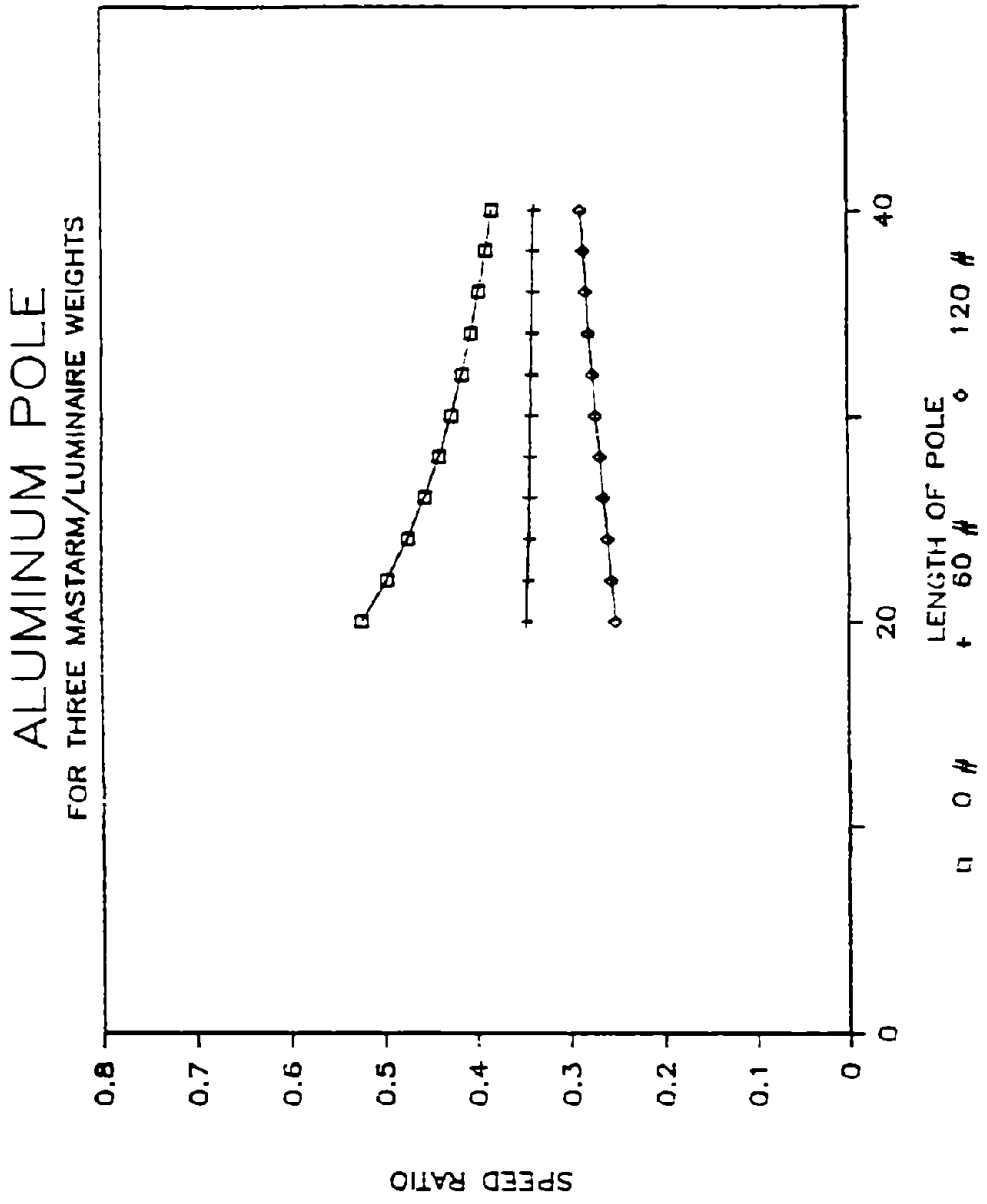

Figure 47. Speed ratio for aluminum luminaire configurations.

This expression indicates that product of the mass and the speed ratio are important in determining the momentum change. Figures 48 and 49 show this product for steel and aluminum poles. Note that the product of speed ratio and the mass shows much less variation with mastarm/luminaire weight changes than do mass or speed ratio curves individually.

The trajectory followed by the pole after the separation from the impacting vehicle can be calculated based on the equations:

$$V_x = V_i \; e \; [R^2/(R^2 + D_o^2)] \qquad (88)$$

$$V_y = g \; t \qquad (89)$$

$$RR = V_i \; e \; [D_\emptyset/(R^2 + D_o^2)] \qquad (90)$$

where RR = rotation rate of pole

g = 32.17 ft/sec/sec

In these expressions, the factor e represents the ratio of the speed of the pole, at the impact point, to the impact speed of the vehicle (at the time of separation). Typically this parameter has a value of 1.1 to 1.3.

These equations can be integrated to provide the displacement of the center of gravity in the x and z directions and the rotation of the pole. The equations for displacement are given by:

$$X_p = V_x \; t \qquad (91)$$

$$Z_p = \emptyset.5 \; g \; t^2 \qquad (92)$$

$$A = RR \; t \qquad (93)$$

Figure 50 shows the trajectory of the pole for a 55 mi/h impact. In this figure, the dimensions of the car are based on a mini-

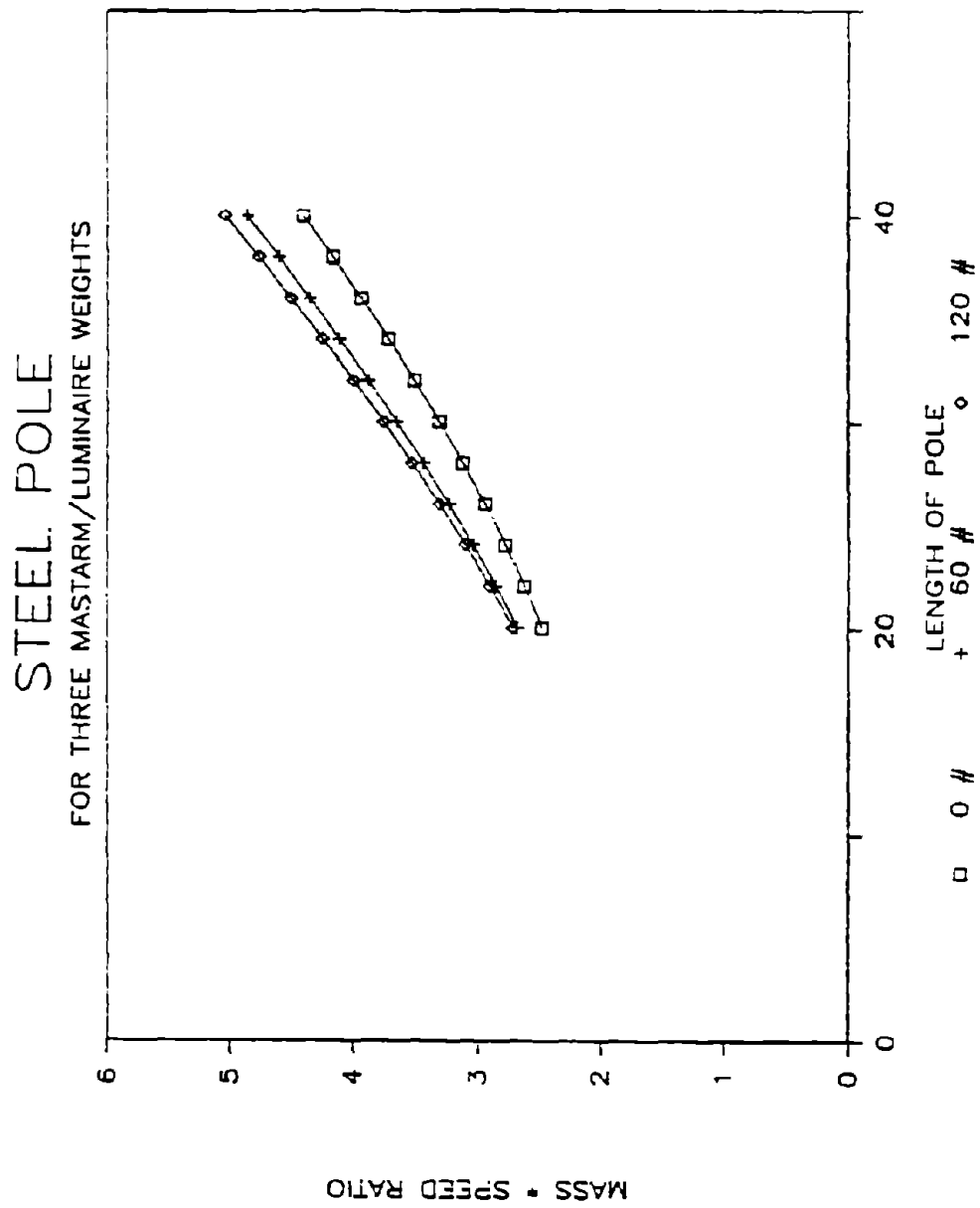

Figure 48. Product Of mass and speed ratio for steel luminaire configurations.

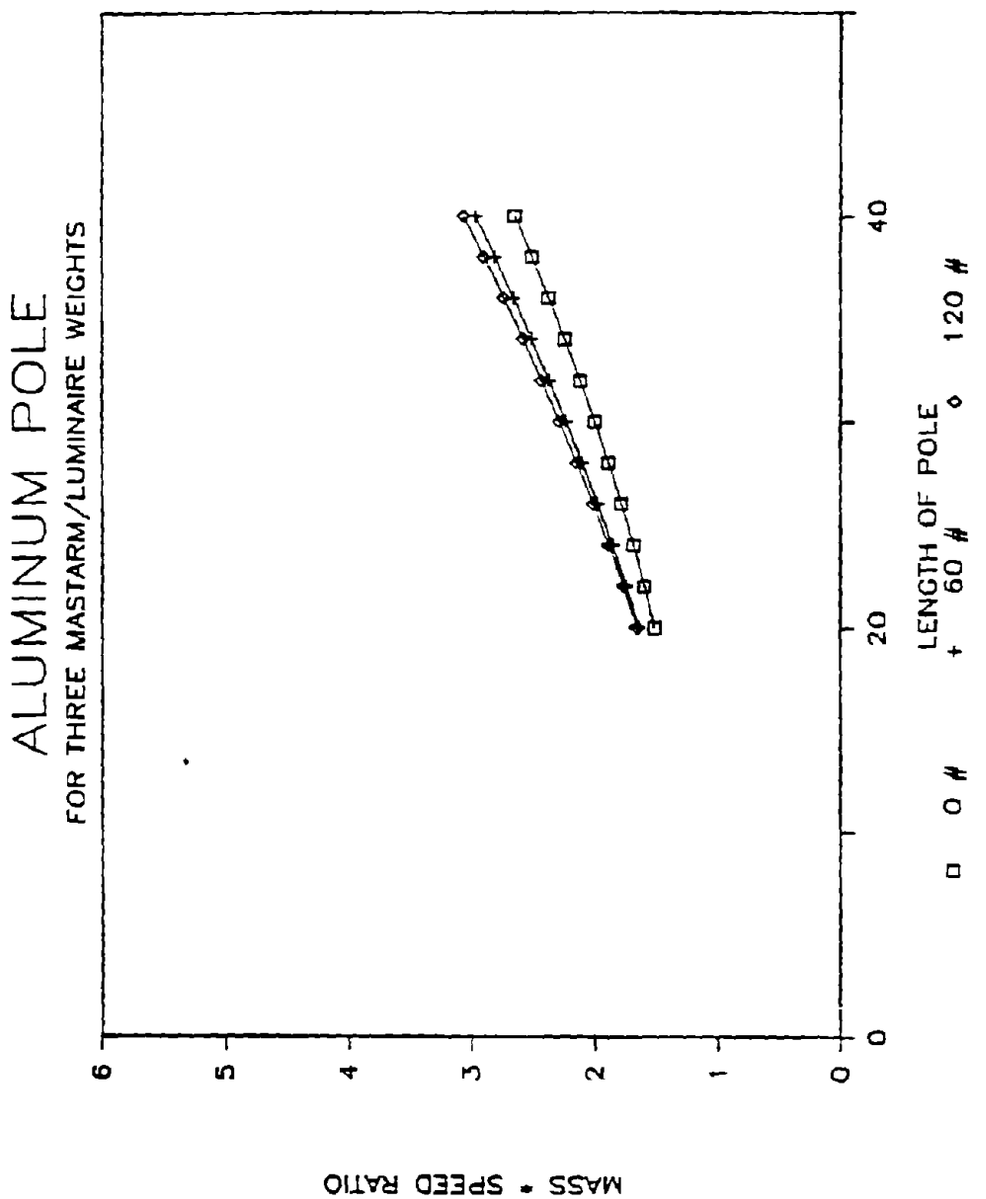

Figure 49. Product of mass and speed ratio for aluminum luminaire configurations.

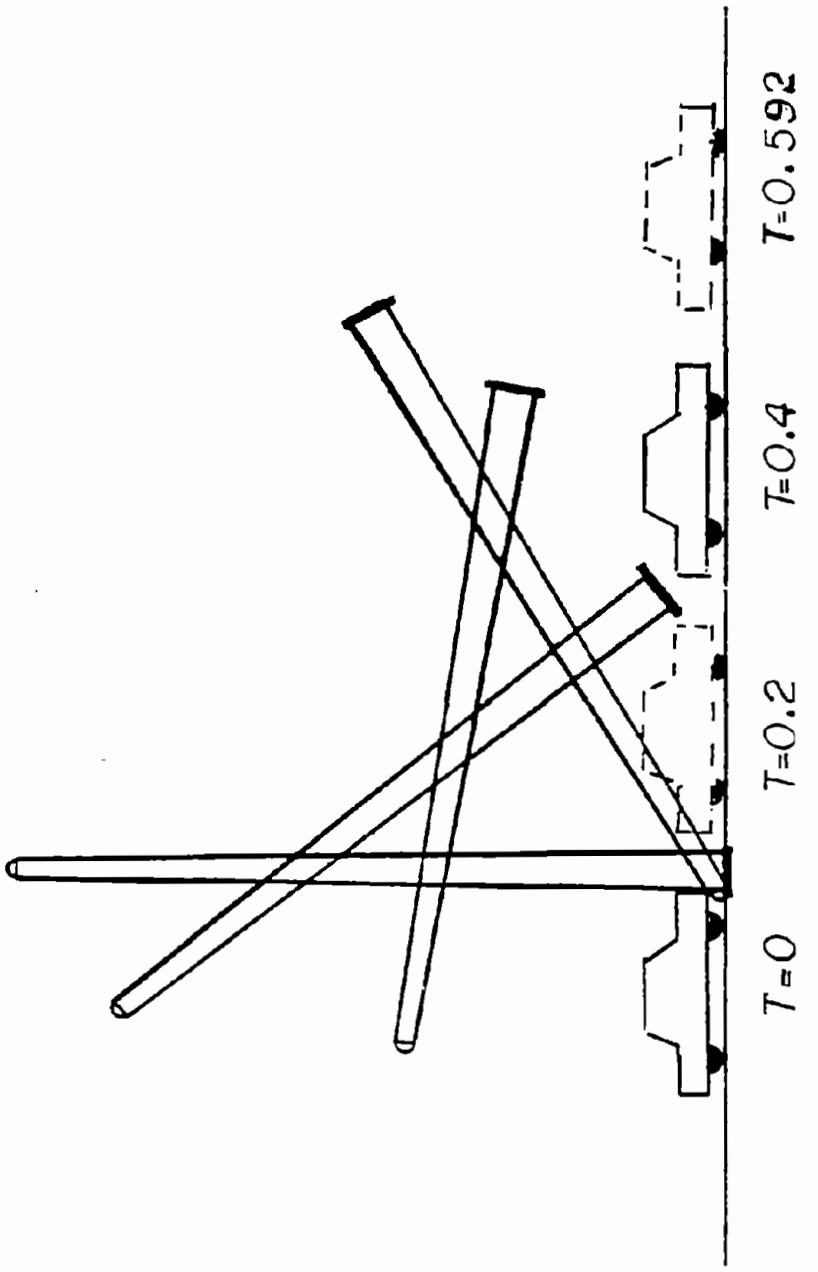

Figure 50. Trajectory plot for high speed scenario.

sized vehicle. The pole represents a 40-ft aluminum support. The pole rotates through a 120 degree angle with the top of the pole striking the ground approximately at the foundation. The time between breakaway and the top of the pole striking the ground is approximately 0.6 sec.

Figure 51 shows a similar scenario but now the speed is lowered to 20 mi/h. In this case the bottom of the pole hits the ground soon after the impact leading to a secondary impact between the car and the pole. This impact is not expected to be severe since the relative impact speed is low. However the pole will usually fall on the car as a result of this type of impact. Tests indicate that the roof structure is strong enough to absorb this impact without significant crushing of roof and resulting intrusion into the passenger compartment.

A situation which must be avoided is the case of a short breakaway device where the pole rotates to a nearly horizontal position with the top of the pole hitting the windshield. This can result in direct intrusion into the passenger compartment.

b. Guardrail Posts

Guardrail posts transmit forces generated during impact to the soil. The magnitude and distribution of the soil forces along the embedded length of the posts are of major importance in the design of guardrail systems. The analysis procedure provided in this section describes the distribution and magnitude of the soil forces acting on the post.

The model is based on the assumption that the post can be considered rigid. The rotation and translation on the post are thus a result of the movement of the soil. The soil "stiffness" in the lateral direction provides the soil forces which resist the applied force.

The concept of soil "stiffness" is similar to the stiffness of a spring. For a spring, the stiffness is given by:

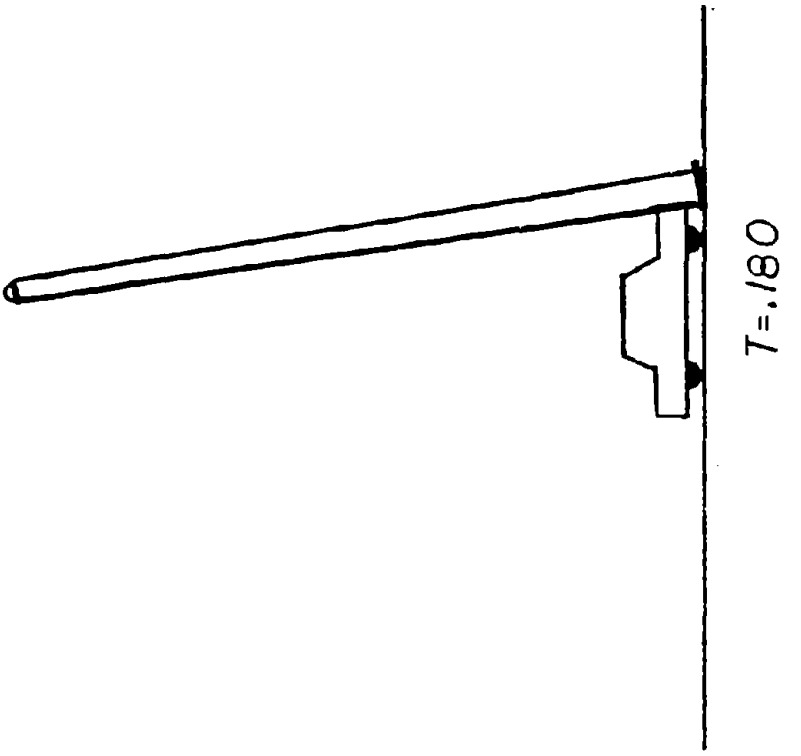

Figure 51. Trajectory plot for low speed scenario.

$$F = K X \qquad (94)$$

where F is the applied force
K is the spring constant
X is the displacement

For the soil model the force is replaced by the the pressure. The equation becomes:

$$P = S X \qquad (95)$$

where P is the soil pressure (lb/ft^2)
S is the soil stiffness constant (lb/ft^3)
X is the soil displacement (ft)

For the case of guardrail posts which are embedded in the ground in distance of several feet, the soil lateral stiffness is expected to increase with depth. For the model the soil lateral stiffness is taken as a linear function of depth. The equation for the soil pressure becomes:

$$P(z) = S' z X(z) \qquad (96)$$

where the soil lateral stiffness at depth z is given by $S' z$. Consider the model shown in figure 52. The post is embedded to a depth L. The applied load, F, is applied at a height, H, above ground level. Since the post is considered rigid, the motion of the post can be be expressed as the translation of the post at ground level and a rotation R. The expression for the displacement at any point along the post is given by:

$$X(z) = X_{top} - R z \qquad (97)$$

for small angles.
The force generated on an incremental slice, dz, of the post is

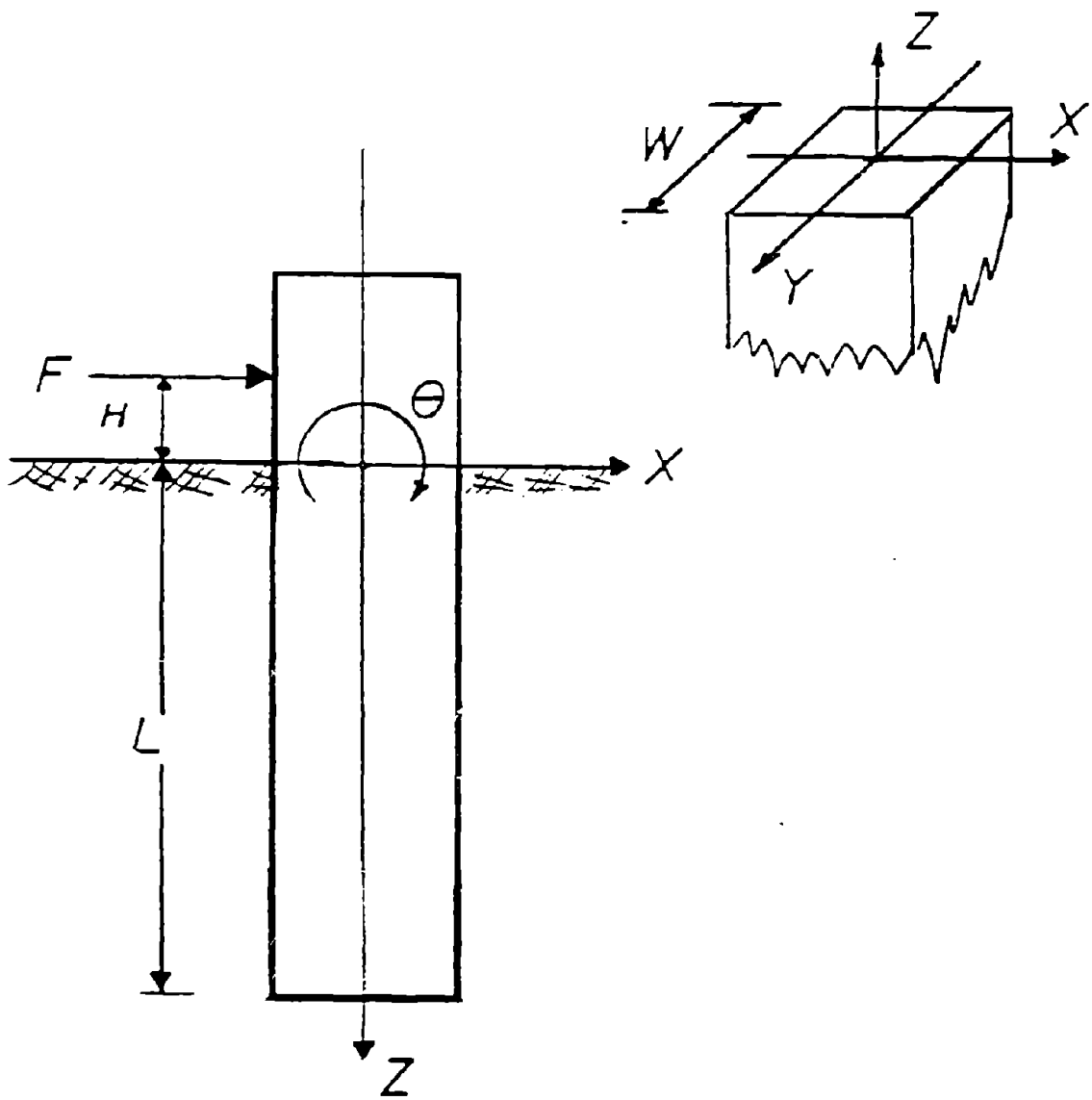

Figure 52. Model for soil/post interaction.

given by:

$$dF = -S(z)\ X(z)\ w\ dz \qquad (98)$$

where w = width of the post.

S(z) = lateral soil stiffness at depth z = S' z

X(z) = displacement of post at depth z

For the post to be in equilibrium, the net force and moment on the post must be equal to zero. This provides the following two equations:

$$F = \int_{0}^{L} S'\ z\ X(z)\ w\ dz \qquad (99)$$

$$F\ H = \int_{0}^{L} z\ S'\ z\ X(z)\ w\ dz \qquad (100)$$

Using the expression for the post displacement, these equations become:

$$F = w\ S' \int_{0}^{L} z\ X_{top}\ dz\ - w\ S' \int_{0}^{L} R\ z^2\ dz \qquad (101)$$

$$F\ H = -w\ S' \int_{0}^{L} z^2\ X_{top}\ dz\ + w\ S' \int_{0}^{L} R\ z^3\ dz \qquad (102)$$

When integrated, these equations provide the expressions for X_{top} and R given by:

$$X_{top} = [F/(w\ S'\ L^2)]\ [\ 18 + 24\ (H/L)] \qquad (103)$$

$$R = [F/(w\ S'\ L^3]\ [\ 24 + 36\ (H/L)] \qquad (104)$$

The displacement of the post at ground level is shown to decrease by a factor of 4 if the embedment length is doubled. The rotation is seen to decrease by a factor of 8 if the embedment length is doubled.

The first useful application of these equations is to find the center of rotation of the post. This will be the point where the displacement is equal to zero. The expression for the displacement is given by:

$$X(z) = [F/(w\ S'\ L^2)] \left[(18 + 24(H/L)) - (z/L)\ (24 + 36(H/L)) \right] \quad (105)$$

Setting this expression to zero, we have the expression for the center of rotation:

$$(z/L) = [\ (18 + 24(H/L))/(24 + 36(H/L))] \quad (106)$$

Figure 53 shows a plot of (z/L) for a range of values of (H/L). The plot shows that the post rotates about a point located at approximately 70 per cent of the embedment length and is independent of the applied load.

The second application is to locate the point of maximum bending moment. This application is important for post which fail due to bending. The bending moment at any point along the embedment length is given by:

$$M(z) = +F(H+z) + \int_0^z (Z-z)\ S'\ Z\ X(Z)\ dZ \quad (107)$$

Performing the integration, this expression becomes:

$$M(z) = +FH \left[1 + (z/L)(L/H) - 3(z/L)^3(L/H) - 4(z/L)^3 + 2(z/L)^4(L/H) + 3(z/L)^4 \right] \quad (108)$$

This equation shows that the moment distribution along the post is proportional to the applied moment at ground level and a function of (L/H). Typical values for embedment length are 3 to 4.5 ft and a typical value of H is 1.5 ft. Figure 54 shows the moment distribution for values of (L/H)=2 and (L/H)=4. The

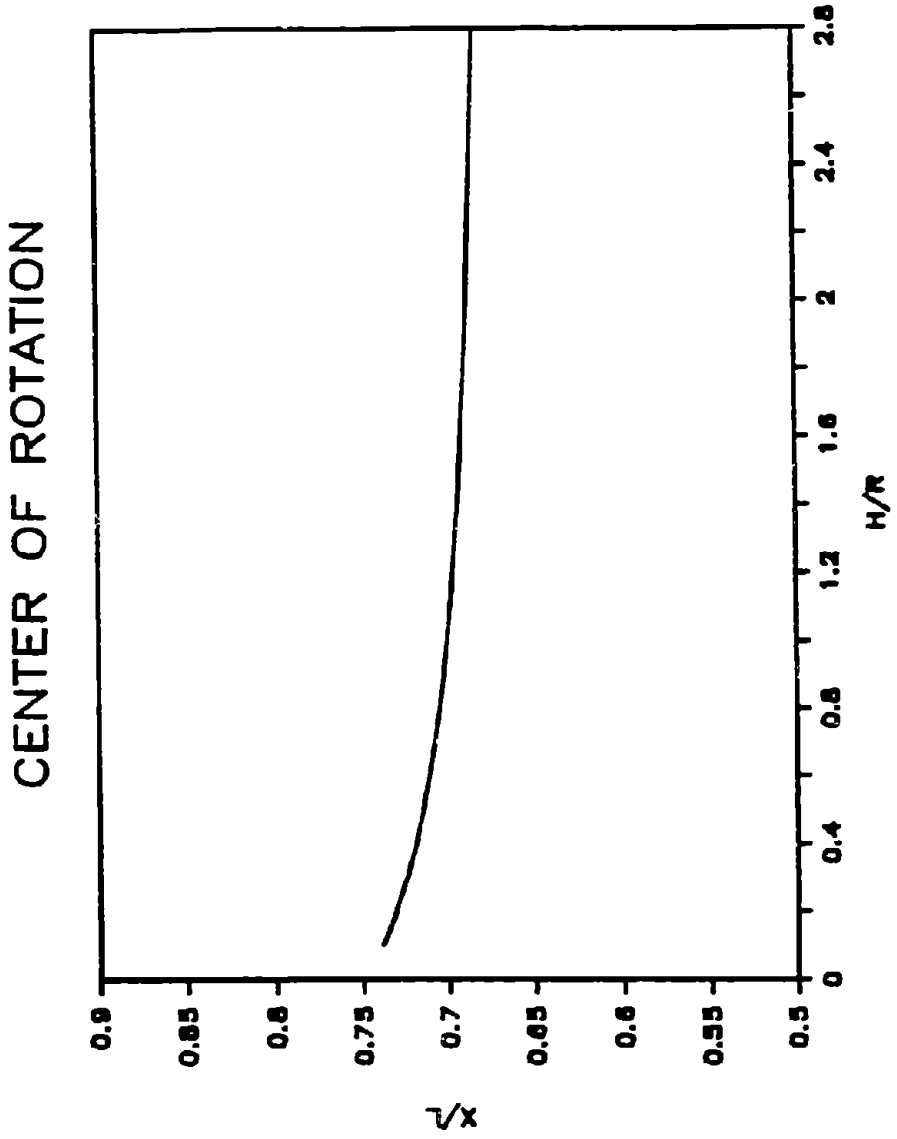

Figure 53. Center of rotation for guardrail posts.

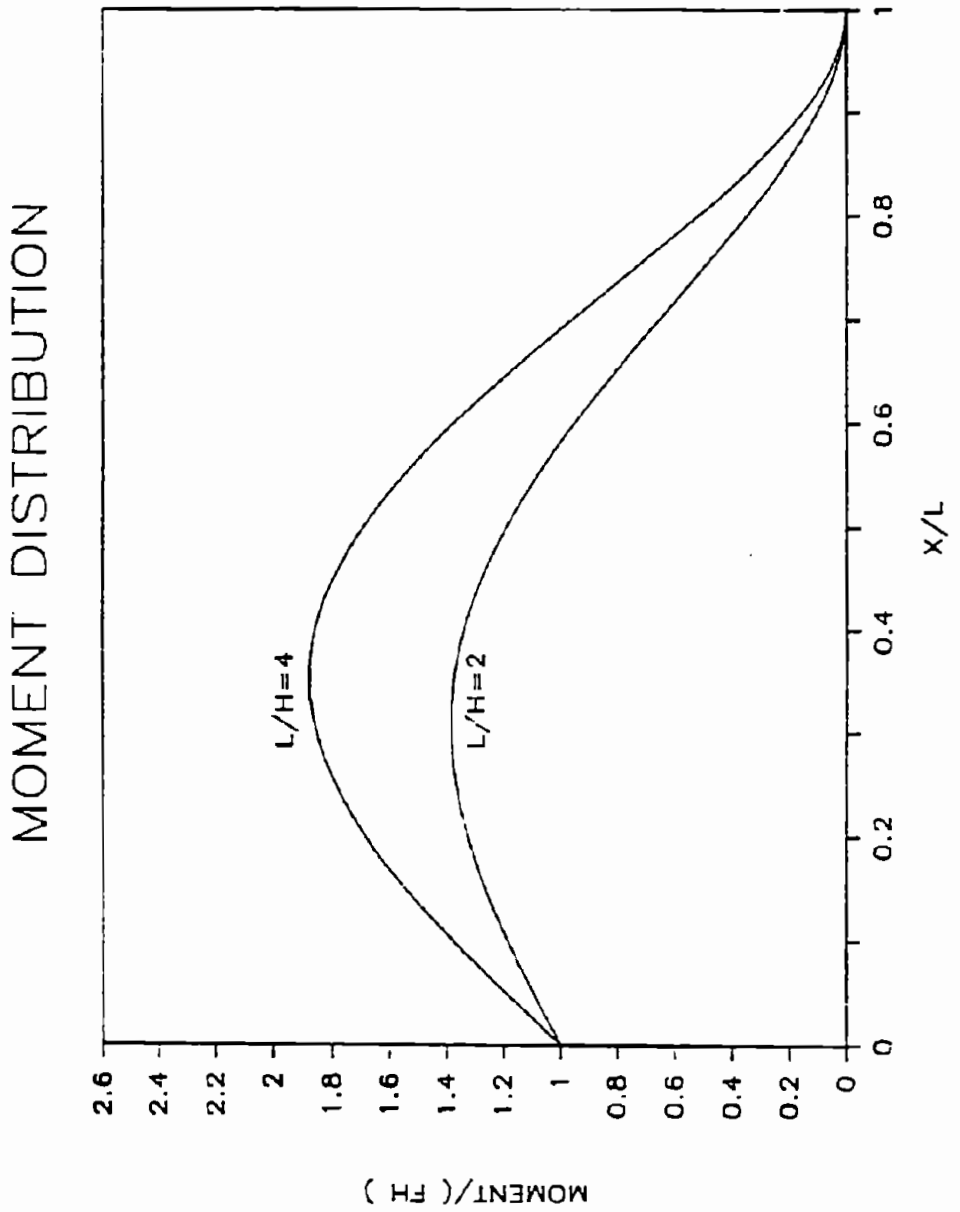

Figure 54. Moment distribution for guardrail posts.

maximum moment occurs around (z/L)=.3 and has a value of 1.8 for a long post and a value of 1.4 for a short post.

The expression for the moment distribution can be used to derive the expression for the shear distribution based on the relationship:

$$dM/dz = SHEAR \qquad (109)$$

The expression for the shear along the embedded length of the post is given by:

$$Shear = +F\ [\ 1- 9(z/L)^2- 12(z/L)^2(H/L) +12(z/L)^3(H/L)+ 8(z/L)^3] \qquad (110)$$

This expression is plotted in Figure 55 for (H/L) = to 2 and 4. The maximum shear occurs at (z/L) approximately equal to 0.75 and has a value of 1.25 for the long post and 1.53 for the short post.
The loading on the post expressed in lb/ft can be determined from the relationship:

$$Loading = dS(z)/dz \qquad (111)$$

The loading is given by the expression:

$$Loading = +(F/L)\ [\ -18(z/L)- 24(z/L)(H/L) + 36(z/L)^2(H/L)+24(z/L)^2] \qquad (112)$$

Figure 56 shows the loading on the post. The loading on the post is maximum at the bottom of the post and has a value of approximately 10(P/L). For a post of width w, the soil pressure at the bottom of the post is approximately

$$P_{max} = (10\ P)/(w\ L) \qquad (113)$$

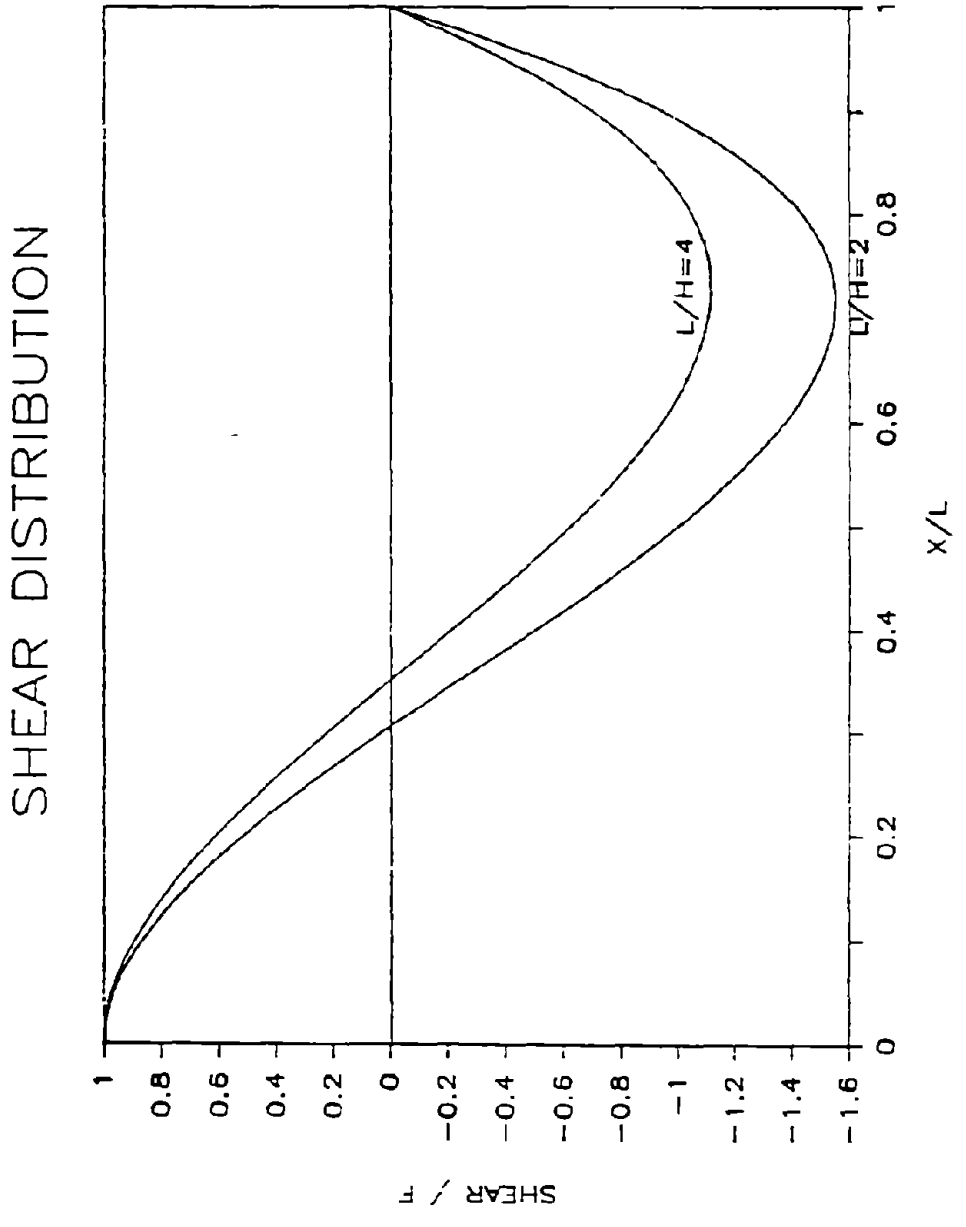

Figure 55. Shear distribution for guardrail posts.

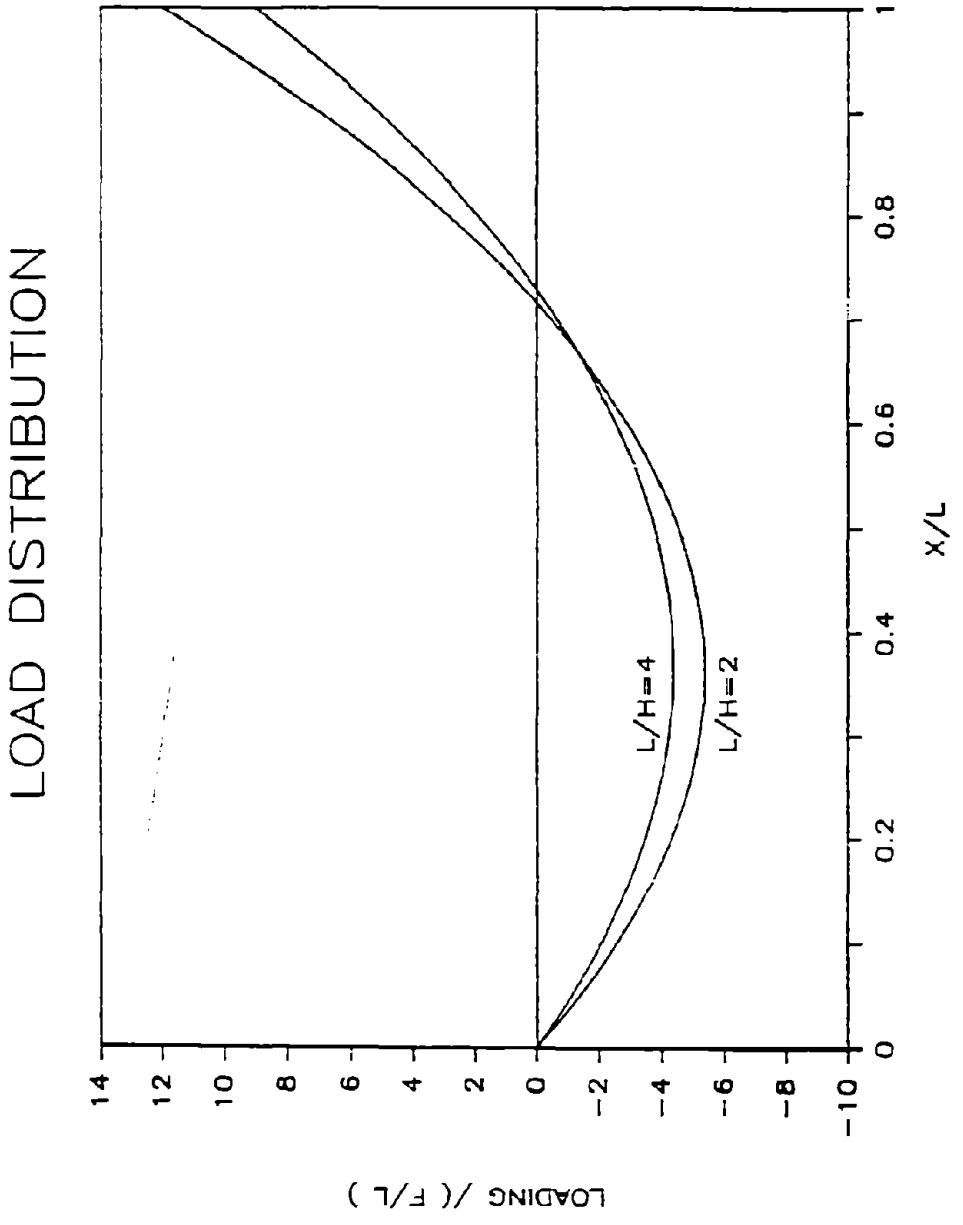

Figure 56. Loading on guardrail posts.

8. Impact Attenuators

The purpose of an impact attenuator is to arrest or redirect an errant vehicle. The discussion in this section will focus on the arresting requirement. Impact attenuators are usually used to shield man-made objects such as bridge piers, median barrier ends, and gore sites. The major design constraint is the space available for the installation of the attenuator. The design requirements for impact attenuators have been traditionally limited to the arresting of vehicles in the passenger car weight range at speeds up to 60 mi/h. Presently this weight range is bounded by the mini-sized cars weighing 1800 lb and by the full-sized sedans weighing 4500 lb.

Two types of impact attenuators will be investigated in this section. The first type is called a resistive attenuator. This type of attenuator requires a back-up structure to carry the force generated during the impact. The second type of attenuator is called inertial. Inertial attenuators do not require a back-up structure. The impact force is generated by accelerating the material of the impact attenuator.

a. Resistive Attenuators

(1) Constant Force Resistive Attenuators. To investigate the tradeoffs in the design of impact attenuators consider the case where the retarding force generated by the attenuator is a constant force level. One design approach would be to design the system based on the heaviest vehicle and the maximum speed. The design would be based on equating the work done on the vehicle to the change in kinetic energy of the vehicle. The equation for the system would be:

$$\int_0^T F\,dx = 0.5\,M_v\,(V_o^2 - V_f^2) \qquad (114)$$

where M_v = Mass of the vehicle
V_o = Impact speed
V_f = Final speed
X = Crush distance

Based on a total arresting of the vehicle, V_f would be equal to zero and the equation becomes:

$$\int_0^{X_{max}} F\,dx = 0.5\,M\,V_o^2 \qquad (115)$$

For a speed of 60 mi/h and a vehicle weight of 4500 lb, the kinetic energy of the vehicle at impact is 541,622 ft-lb. Since the attenuator retarding force is a constant, the equation for the system becomes:

$$F_c\,X_{max} = 541{,}622 \qquad (116)$$

where F_c = retarding force of attenuator
X_{max} = Length over which the attenuator can provide the force F_c

Given a maximum available length L for the impact attenuator, the value of X_{max} will usually be somewhat less than L to account for the crushed slug of attenuator material built up in front of the vehicle. For this design, it is assumed that the value of X_{max} is 90 percent of the total available length. The system equation becomes:

$$F_c\,(0.9\,L) = 541{,}622 \qquad (117)$$

For the design investigation, a value of 25.5 ft will be assumed for the total available length. The value of the required retarding force is given by:

$$F_c = [\ 541,622/(.9\ 25.5)\ ] \qquad (118)$$
$$F_c = 23,600$$

For the 4500 lb vehicle, this corresponds to a constant deceleration level of 5.24 G's.

To access the performance of the system, the delta V and the ridedown parameters must be calculated. Based on a 2-ft flail space, the value of delta V will be given by equation:

$$\text{delta } V = \sqrt{2\ g\ D_o} \qquad (119)$$
$$= \sqrt{2\ (5.24)(32.17)\ 2}$$
$$= 25.96 \text{ ft/sec}$$

where D_o = flail space = 2-ft
g = constant deceleration level
(ft/sec/sec)

The impact between the interior of the vehicle and the occupant would occur at time T_i given by equation:

$$T_i = \sqrt{2\ D_o\ /g} \qquad (120)$$
$$= 0.154 \text{ sec}$$

The time required to arrest the vehicle can be calculated from momentum considerations based on the equation:

$$\int_0^T F\ dt = M\ V_o \qquad (121)$$

$$F_c\ T = (4500/32.17)(88)$$
$$T = 12,309/23,600$$
$$T = 0.522 \text{ seconds}$$

The ridedown acceleration would be the 5.24 G deceleration level. The predicted level of delta V is below the NCHRP recommended value of 30 ft/sec. The value of ridedown is below the NCHRP recommended level of 15 G.

The impact of the small car (1800 lb) will produce a more violent impact. The performance parameters for the small car can be calculated in a similar fashion to the large car. The constant deceleration level for the small car is 13.1 G's. Table 12 summarizes the impact and performance parameters for the small car and the large car at speeds of 60 mi/h and 45 mi/h. The delta V for the small car impact is greater than the 30 ft/sec recommended level and is even greater then the 40 ft/sec design limit given in NCHRP 230.

An interesting result from the values in table 12 is that the impact at 45 mi/h is as severe as the impact at 60 mi/h. The result of the design investigation is that a constant force attenuator system based on an available length of 25.5 ft will not produce acceptable performance. In the above analysis the crush on the vehicle was not considered. If the crush of the vehicle is considered, the effective stopping distance is increased by the crush distance of the vehicle but there is little change in the performance parameters.

(2) Shaped Force/Deflection Resistive Barriers. The next design approach is to investigate the effect of shaping the force deformation curve to provide lower forces during the initial displacement and then to increase the force with increased deflection. There are obviously many ways in which the force deformation curve could be shaped. For the present analysis, the peak force on the large car will be limited to 15 G's for an impact speed of 60 mi/h. The initial force level will be set to a force level corresponding to 7 G's for the small car (12,600 lb). The shape of the force deformation curve is shown

Table 12. Attenuator performance.

CONSTANT FORCE-DEFLECTION ATTENUATOR

VEHICLE WEIGHT	IMPACT SPEED	DELTA V	RIDE DOWN	DEFLECT	PEAK FORCE	TI	T	PASS FAIL
lb	mi/h	ft/sec	G'S	ft	kips	sec	sec	
4500	60	26.0	5.2	22.9	23.6	0.154	0.522	P
4500	45	26.0	5.2	12.9	23.6	0.154	0.391	P
1800	60	41.1	13.1	9.2	23.6	0.097	0.209	F
1800	45	41.1	13.1	5.2	23.6	0.097	0.142	F

SHAPED FORCE-DEFLECTION ATTENUATOR

VEHICLE WEIGHT	IMPACT SPEED	DELTA V	RIDE DOWN	DEFLECT	PEAK FORCE	TI	T	
4500	60	21.0	15.0	22.9	67.5	0.209	0.383	P
4500	45	19.0	9.2	18.6	41.5	0.210	0.444	P
1800	60	30.0	14.4	16.0	26.0	0.133	0.319	P
1800	45	30.0	7.0	9.6	12.6	0.133	0.293	P

CONSTANT FORCE WITH DAMPING ATTENUATOR

VEHICLE WEIGHT	IMPACT SPEED	DELTA V	RIDE DOWN	DEFLECT	PEAK FORCE	TI	T	
4500	60	28.8	6.0	22.7	38.0	0.125	0.755	P
4500	45	25.5	4.4	15.7	29.8	0.145	0.655	P
1800	60	42.0	12.4	9.0	38.0	0.095	0.265	F
1800	45	37.8	8.7	6.3	29.8	0.080	0.300	F

CONSTANT FORCE WITH DAMPING ATTENUATOR
(CRUSH OF CAR INCLUDED)

VEHICLE WEIGHT	IMPACT SPEED	DELTA V	RIDE DOWN	DEFLECT	PEAK FORCE	TI	T	
4500	60	29.3	5.8	22.4	35.8	0.141	0.755	P
4500	45	25.5	4.4	15.5	28.0	0.155	0.685	P
1800	60	43.0	11.5	8.8	33.5	0.095	0.320	F
1800	45	37.1	8.4	6.0	26.2	0.105	0.285	F

in figure 57. The 12,600 pound force level is maintained for a distance of 13.75 feet and then the force increases linearly with increased deflection. The area under the force deformation curve represents the change in kinetic energy of the vehicle. The area under the curve for a displacement of 22.95 feet (90 percent of the available length) is exactly equal to the kinetic energy of the large car with an impact speed of 60 mi/h.

The calculation of the impact parameters and performance parameters is more complicated than for the case of constant deceleration but the basic concepts are the same. A BASIC computer program (25 lines) was written to calculate the impact and performance parameters. The results are given in table 12. Acceptable performance is shown at 45 and 60 mi/h for both the large car and the small car.

(3) Constant Force with Damping Resistive Attenuators. Damping devices are often used in engineering applications. These devices provide a resistive force proportional to the rate of deformation. To explore the effect of adding damping to the resistive force of an attenuator, the model shown in figure 58 was used. The equation of motion for the vehicle is given by:

$$M_v \ddot{X} = -c \dot{X} - K \qquad (122)$$

where X = displacement of the vehicle
M_v = Mass of the vehicle
c = Damping coefficient
pounds/foot/second
K = Constant retarding force for attenuator

The solution to this equation is given by:

$$X = A \exp[-(c/M_v)t] + B - (k/c)t \qquad (123)$$

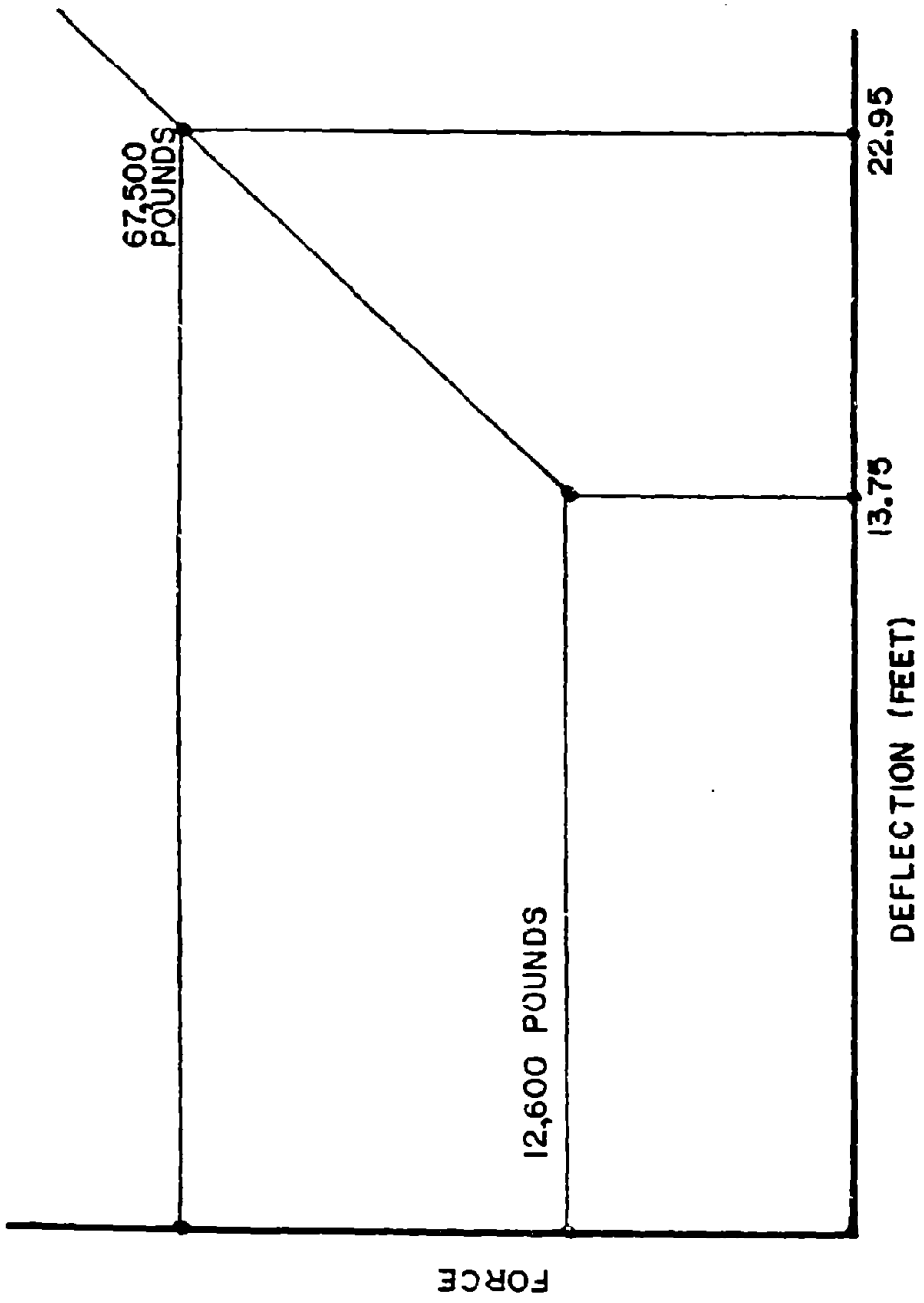

Figure 57. Force deflection characteristics of shaped impact attenuator.

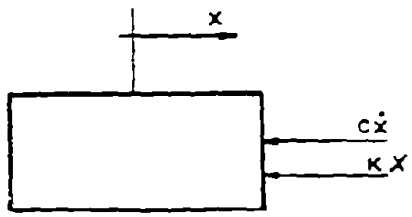

Figure 58. Damping Force Model.

where A= constant to be determined from initial conditions
B= constant to be determined from initial conditions
t= Time after impact
$\exp(t) = e^t$
$= (2.713)^t$

based on the initial conditions of no initial displacement and an initial speed of V_o, the value of A and B are given by:

$$A = [V_o + (k/c)](M_v/c) \qquad (124)$$

$$B = 0 \qquad (125)$$

Using value of c= 375 lb/ft/sec and K= 5,000 lb, the values in table 12 were determined. These values indicate that an attenuator based on this model would produce high peak forces on the vehicle. When compared to the example of the constant force attenuator discussed above, the performance is slightly worse at 60 mi/h and slightly better at 45 mi/h.

To explore the effect of the crush of the vehicle, a BASIC program was written which included the crush characteristics of the vehicle. The results of this program are given in table 12.

The crush stiffness of the car was 20,000 lb/ft. Comparison of these results with the case where vehicle crush was not considered indicate that delta V and ridedown acceleration are not significantly changed but that the peak force is slightly reduced.

b. Inertial Attenuators

Inertial attenuators do not require a back-up structure to develop the retarding force. The retarding force is generated by accelerating the material of the attenuator. A sand barrel attenuator system will be used as an example of this type of system.

A typical sand barrel array is shown in figure 59. It consists of 15 barrels positioned in triangular shape. The amount of sand in each barrel varies with position in the array. The first barrel in the array contains 400 lb of sand while the barrels in the back row contain 2100 lb of sand. The barrel are usually cylindrical in shape with a diameter of 3-ft and a height of approximately 4-ft.

The design of sand barrel attenuator systems is based on a conservation of linear momentum. Consider the case of a single barrel/vehicle impact. The initial linear momentum of the system is given by the product of the vehicle mass and impact velocity. After the vehicle has traveled a distance equal to the diameter of the barrel, the momentum of the system is redistributed. Some of the momentum is still in the vehicle but some of the momentum is now in moving sand. The equation for momentum transfer is given by:

$$M_v V_o = M_v V_f + M_s U \qquad (126)$$

where M_v = Mass of vehicle

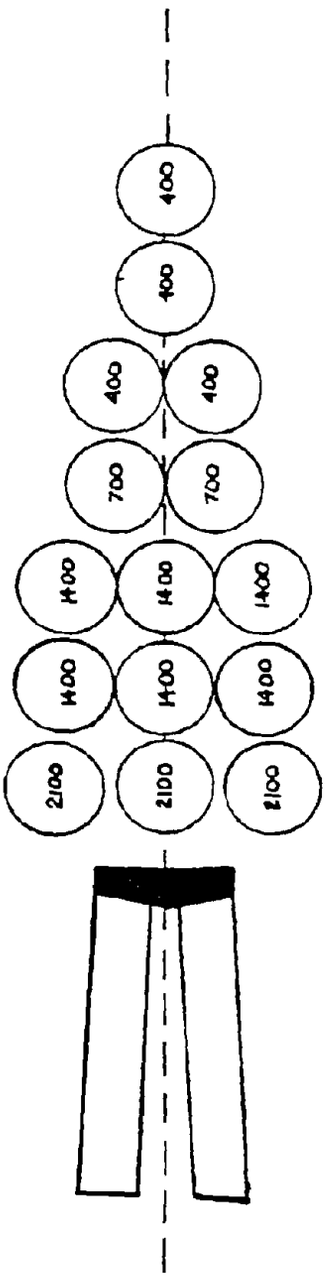

Figure 59. Typical sand barrel configuration.

M_s = Mass of sand
V_o = Impact speed
V_f = post impact of vehicle
U = post impact velocity of sand

An assumption of the design process is that the velocity of the sand is equal to the velocity of the vehicle at the completion of the impact. Using this assumption and the conservation of linear momentum, the relationship between the initial speed and the final speed is given by:

$$V_f = [\ M_v/(M_v+M_s)]\ V_o \qquad (\ 127\ )$$

This expression can be used to express the change in velocity experienced by the vehicle during impact:

$$\text{delta } V = [\ M_s/(M_v+M_s)]\ V_o \qquad (\ 128\ )$$

Assuming a constant acceleration during impact, the average speed is given by:

$$V_{ave} = 0.5\ (\ V_o+\ V_f\ ) \qquad (\ 129\ )$$

The duration of the impact is related to the diameter of the barrel and the average velocity by:

$$V_{ave}\ T = D \qquad (\ 130\ )$$

where T = duration of impact
D = diameter of barrel

The constant deceleration level is given by the expression:

$$A_c = [\ V_o^2 - V_f^2\ ]/(2\ D) \qquad (\ 131\ )$$

The design of a sand barrel array is based on applying this equation to the sequential impacts between the vehicle and the barrels of the array. Note that this approach will never stop the vehicle but just continue to reduce the velocity by the factor $[M_s/(M_v+M_s)]$ which is always less than one. The vehicle will be assumed to stop when the velocity approaches 5 mi/h.

The design procedure for the sand barrel attenuator system is based on the conservation of linear momentum. It is interesting to also use an energy approach to examine the performance. For the case of a single barrel, the initial kinetic energy of the vehicle/barrel system is based on the kinetic energy of the vehicle. The kinetic energy of the system after impact is the sum of the kinetic energy of the vehicle and the kinetic energy of the sand. If the sand had only a velocity component in the the initial direction of the vehicle motion, the kinetic energy of the system would be:

$$K.E. = 0.5\ M_v\ V_f^2 + 0.5\ M_s\ V_f^2 \qquad (132)$$

Using the relationship between V_o and V_f, this expression becomes

$$K.E. = 0.5\ M_v\ V_o^2\ [\ M_v/(\ M_v+M_s)\ ] \qquad (133)$$

The first term of this expression is equal to the initial kinetic energy. The second term will always have a value less than one. This means that the system has decreased in energy during the impact.

How is this loss of energy explained? To address this question consider the simple model shown in figure 60. The sand barrel mass is divided into two parts. The velocity of the sand now has a component perpendicular to the initial direction of travel of the vehicle (x-direction). The design procedure is based on conservation of momentum in the x-direction. If the velocity

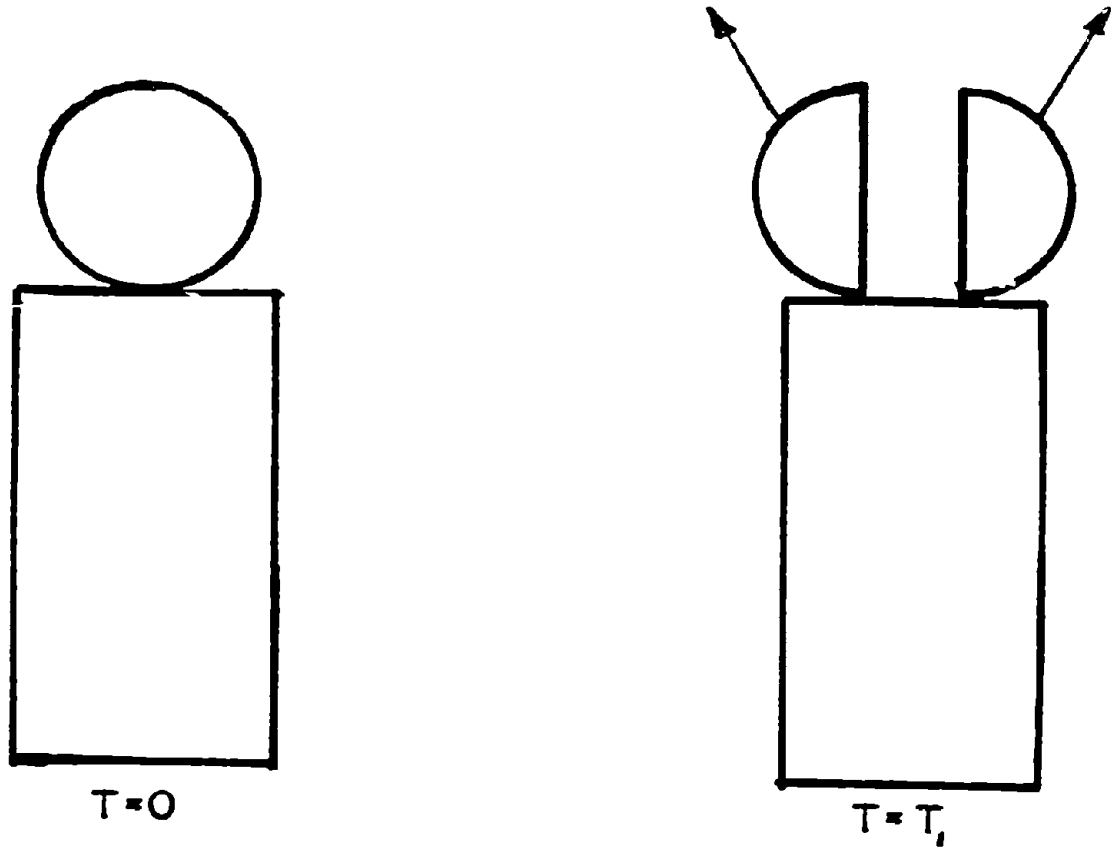

Figure 60. Sand barrel kinetic energy model.

components in the y-direction have the same magnitude but are in opposite directions, then the net momentum in the y-direction will be zero. Now the expression for the kinetic energy of the system after impact contains additional terms to account for the velocity of the sand in the y-direction. The expression for the kinetic energy of the system after impact is given by:

$$K.E. = 0.5\ M_v\ V_f^2 + 0.5\ M_s\ V_f^2 + 0.5\ M_s\ V_l^2 \qquad (134)$$

Using the relationship between V_o and V_f, this expression can be rewritten as:

$$K.E. = 0.5\ M_v\ V_o^2\ [\ (M_v/(M_v+M_s) + (V_l/V_o)^2 (M_s/M_v)\ ] \qquad (135)$$

The first term in the expression is the initial kinetic energy of the system. If the total energy of the system is to be explained by the kinetic energy of the vehicle and the sand only then the term in the square brackets must be equal to one. This implies that :

$$V_l = V_o \sqrt{M_v/(M_v+M_s)} \qquad (136)$$

The longitudinal velocity component of the sand at the end of the impact is given by:

$$V_f = M_v/(M_v + M_s) \qquad (137)$$

Thus the lateral component of velocity will always be higher than the longitudinal component. This implies that direction of motion of the sand (see figure 60) be at an angle of 45 degrees or more.

The energy analysis of the sand barrel system points to the importance of the barrels being frangible so that the sand can be accelerated in both the x and y directions.

As an example of the use of the design procedure for impact attenuators, consider the case of a head-on impact into the array of sand barrels shown in figure 59. The separation of the barrels is 0.5-ft in the longitudinal direction. The barrels have a diameter of 3-ft. A clearance of 1.5-ft is provided between the face of the gore and the backside of the last row of barrels.

The total impact is considered a sequence of seven impacts defined by table 13. The number of barrels impacted is based on the width of the vehicle being approximately 7.5 ft.

Table 13. Sand barrel attenuator.

Row	Sand Weight	Description
1	400	one 400 # barrel
2	400	one 400 # barrel
3	800	two 400 # barrels
4	1400	two 700 # barrels
5	2800	center 1400 # barrel plus one half of each outside 1400 # barrel
6	2800	center 1400 # barrel plus one half of each outside 1400 # barrel
7	4200	center 2100 # barrel plus one half of each outside 2100 # barrel

The results of applying the design process to impacts of a large car at 60 mi/h and 45 mi/h are given in table 14. Table 15 gives similar results for the small car. Table 16 provides the

Table 14. Sand barrel performance with a 4,500 lb vehicle.

4500 lb VEHICLE AT 60 mi/h

ROW	SAND WEIGHT	INITIAL SPEED	FINAL SPEED	G's	TIME START	TIME STOP
1	400	60.0	55.1	6.3	0.000	0.036
2	400	55.1	50.6	5.3	0.041	0.080
3	800	50.6	43.0	8.0	0.087	0.131
4	1400	43.0	32.8	8.6	0.139	0.193
5	2800	32.8	20.2	7.4	0.203	0.280
6	2800	20.2	12.5	2.8	0.297	0.422
7	4200	12.5	6.4	1.3	0.450	0.666

4500 lb VEHICLE AT 45 mi/h

ROW	SAND WEIGHT	INITIAL SPEED	FINAL SPEED	G's	TIME START	TIME STOP
1	400	45.0	41.3	3.5	0.000	0.047
2	400	41.3	50.6	5.3	0.041	0.080
3	800	50.6	43.0	8.0	0.087	0.131
4	1400	43.0	32.8	8.6	0.139	0.193
5	2800	32.8	20.2	7.4	0.203	0.280
6	2800	20.2	12.5	2.8	0.297	0.422
7	4200	12.5	6.4	1.3	0.450	0.666

Table 15. Sand barrel performance with 1800lb vehicle.

1800 lb VEHICLE AT 60 mi/h

ROW	SAND WEIGHT	INITIAL SPEED	FINAL SPEED	G's	TIME START	TIME STOP
1	400	60.0	55.1	6.3	0.000	0.036
2	400	55.1	50.6	5.3	0.041	0.080
3	800	50.6	43.0	8.0	0.087	0.131
4	1400	43.0	32.8	8.6	0.139	0.193
5	2800	32.8	20.2	7.4	0.203	0.280
6	2800	20.2	12.5	2.8	0.297	0.422
7	4200	12.5	6.4	1.3	0.450	0.666

1800 lb VEHICLE AT 45 mi/h

ROW	SAND WEIGHT	INITIAL SPEED	FINAL SPEED	G's	TIME START	TIME STOP
1	400	45.0	41.3	3.5	0.000	0.047
2	400	41.3	50.6	5.3	0.041	0.080
3	800	50.6	43.0	8.0	0.087	0.131
4	1400	43.0	32.8	8.6	0.139	0.193
5	2800	32.8	20.2	7.4	0.203	0.280
6	2800	20.2	12.5	2.8	0.297	0.422
7	4200	12.5	6.4	1.3	0.450	0.666

Table 16. Sand barrel attenuator performance.

VEHICLE WEIGHT	IMPACT SPEED	DELTA V	RIDE DOWN	DEFLEC-TION*	PEAK FORCE	TI	T*	PASS FAIL
lb	mi/h	ft/sec	G	ft	kips	sec	sec	
4500	60	28.0	8.6	25.5	38.7	0.150	0.666	P
4500	45	21.0	4.8	24.0	21.6	0.200	0.888	P
1800	60	32.2	9.4	19.0	16.9	0.109	0.530	F
1800	45	24.1	5.3	17.0	9.5	0.145	0.633	P

* Since the vehicle speed is never reduced to zero based on the momentum transfer, the deflection and impact duration are based on slowing the vehicle to approximately 5 mi/h.

human injury descriptors for the sand attenuator system. The system does not pass the NCHRP 230 criteria for the small car impact at 60 mi/h. However, the delta V is only 32.2 ft/sec.

9.Breakaway Hardware

Breakaway hardware is used to connect sign and luminaire supports to their foundations. The design requirements are twofold. First the breakaway must support the sign or luminaire support under non-impact conditions. The worst case loading for this condition is usually due to the wind. Second the breakaway hardware must release under impact loading at a low force level. These requirements appear to conflict but a suitable compromise can be obtained in most cases.

The design of a breakaway luminaire configuration will be used as the design example in this section.

The procedure for estimating the loads produced by the wind is defined in the AASHTO publication "Standard Specifications for Structural Supports for Highway Signs, Luminaires and Traffic Signals." For luminaire supports which are less than 50 ft, the pressure produced by the wind is estimated by:

$$P = 0.00256\ (1.3\ V_w)^2\ C_d\ C_h \qquad (\ 138\ )$$

where P = Wind Pressure (lb/ft^2)

V_w = Maximum wind speed based on 25 year mean recurrence interval (mi/h)

C_d = Drag coefficient

C_h = Coefficient of height

For the continental United States, the maximum wind speed is 100 mi/h with more typical values of 60 to 80 mi/h. The pressure acts on the projected area of the luminaire,mast arm and support to produce a shear force and moment at the base of the support. Values for the shear and moment at the base are given in table 17 for a 40-ft, a 30-ft, and a 20-ft luminaire support. The dimensions of the support are typical of an aluminum support

Table 17. Shear and moment calculations.

40 FOOT POLE

TOP DIAMETER	=	6	in			
BOTTOM DIAMETER	=	10	in			
LENGTH	=	40	ft			
WIND VELOCITY	=	100	mi/h	PRESSURE	43.26	lb/ft*ft

	CROSS SECTIONAL AREA	CENTROID FROM BASE	HEIGHT COEFF.	DRAG COEFF.	SHEAR	MOMENT
	ft*ft	ft			lb	lb*ft
POLE	26.67	18.33	1.00	1.10	1,269	23,266
MAST ARM/LUMINAIRE	2.00	40.50	1.10	1.00	95	3,855
				TOTAL	1,364	27,121

30 FOOT POLE

TOP DIAMETER	=	5.4	in			
BOTTOM DIAMETER	=	8.4	in			
LENGTH	=	30	ft			
WIND VELOCITY	=	100	mi/h	PRESSURE	43.26	lb/ft*ft

	CROSS SECTIONAL AREA	CENTROID FROM BASE	HEIGHT COEFF.	DRAG COEFF.	SHEAR	MOMENT
POLE	17.25	13.91	0.80	1.10	657	9,137
MAST ARM/LUMINAIRE	2.00	30.50	1.10	1.00	95	2,903
				TOTAL	752	12,040

20 FOOT POLE

TOP DIAMETER	=	4.8	in			
BOTTOM DIAMETER	=	6.8	in			
LENGTH	=	20	ft			
WIND VELOCITY	=	100	mi/h	PRESSURE	43.26	lb/ft*ft

	CROSS SECTIONAL AREA	CENTROID FROM BASE	HEIGHT COEFF.	DRAG COEFF.	SHEAR	MOMENT
POLE	9.67	9.43	0.80	1.10	368	3,469
MAST ARM/LUMINAIRE	2.00	20.50	1.10	1.00	95	1,951
				TOTAL	463	5,420

which provide more projected area than steel poles. For simplicity, the area associated with the mast arm and luminaire is taken as 2-ft^2 with a drag coefficient of 1.1. The values given in table 17 indicate that the shear force varies from 600 to 1,500 lb while the moment varies from 8,000 to 33,000 ft-lb.

The impact loading is applied near the base of the support. The effective moment arm is 18-in to 24-in above the base. For an impact loading of 15,000 lb (corresponding to approximately 1-ft of vehicle crush), the shear force is 15,000 lb while the moment is 30,000 ft-lb based on a 2-ft moment arm.

Comparing the shear and moment produced by the wind and by impact indicates that the moments produced at the base are of the same magnitude but that the shear force is 10 times higher for impact conditions. This distinction is the basis for the design of breakaway hardware.

The physics of the impact of a vehicle with a breakaway device will be analyzed using a 3 phase description of the impact. The first phase is defined by the vehicle crushing and the luminaire support remaining relatively rigid. This phase lasts until the impact force just initiates a failure of the breakaway hardware. The second and third phases start at the initiation of the failure. Phase 2 is associated with the completion of the breakaway of the base. Phase 3 is associated with the acceleration of the luminaire support resulting in the support rotating and translating.

Figure 61 shows a typical time history of the impact force and the base force. Assuming the luminaire support is rigid up to the point of breakaway, the impact force and the shear at the base are identical up to time t_1. After t_1, the shear force in the base starts to decrease since the breakaway device has lost its integrity. The impact force on the other hand can continue to increase due to the inertia of the pole. The breakaway is completed at time t_2 as indicated by the base force going to zero. The impact force will continue until the pole is

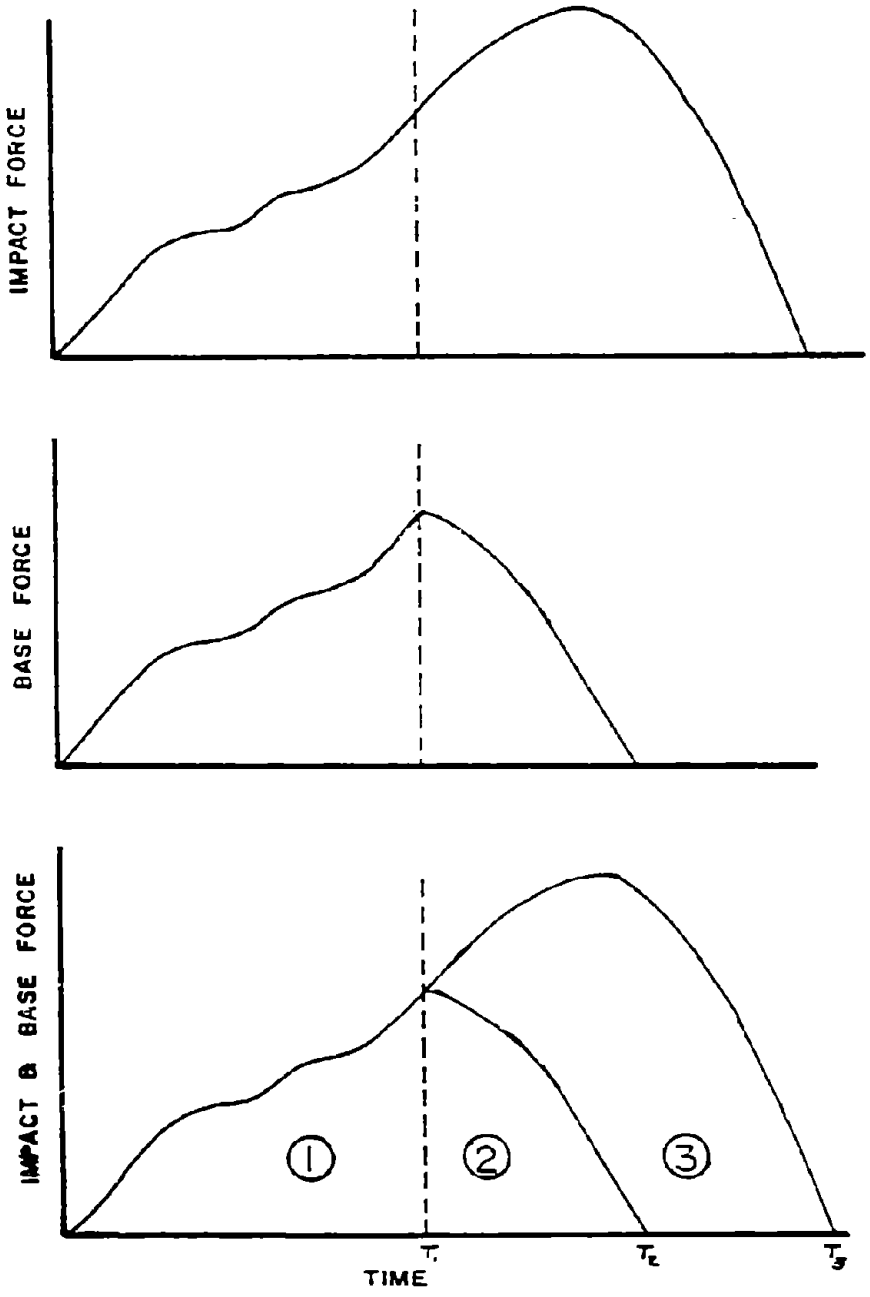

Figure 61. Force time plot for impact force and base force.

accelerated in translation and rotation resulting in separation of the vehicle and the pole.

The duration of the impact t_3 can be estimated by the distance traveled by the vehicle while in contact with the pole. This is usually a distance of 3 or 4-ft. Using a distance of 4-ft and the impact speed of the vehicle, t_3 is estimated by:

$$t_3 = 4/V_o \qquad (139)$$

For a 20 mi/h impact, this is time of 0.136 sec while for a 60 mi/h impact the duration is 0.045 sec. These durations are less than or about equal to the time required for the passenger to contact the interior of the vehicle based on a 2-ft flail space. Typically the impact between the vehicle and the support is completed before the occupant impacts the interior of the vehicle. This implies that the ridedown acceleration is zero and that the delta V is equal to the velocity change experienced by the vehicle during impact. The velocity change experienced by the vehicle during impact can be calculated based on momentum considerations from the equation:

$$M_v \, DV = \int_0^{t_3} F_i \, dt \qquad (140)$$

where M_v = Mass of vehicle
F_i = Impact force
DV = Velocity change

The analysis of the impact based on the 3 phase approach can be expressed by separating the integral into three integrals as expressed by:

$$M_v \text{ delta } V = \int_0^{t_3} F_i \, dt - \int_0^{t_3} F_s \, dt + \int_0^{t_3} F_s \, dt$$

$$M_v \text{ delta } V = \int_{\emptyset}^{t_3} F_i \, dt + \int_{\emptyset}^{t_3} (F_i - F_s) \, dt + \int_{\emptyset}^{t_3} F_s \, dt \quad (141)$$

Since the base force is equal to zero for times greater than t_2, the expression becomes:

$$M_v \, DV_1 = \int_{t_\emptyset}^{t_1} F_i \, dt + \int_{t_1}^{t_3} (F_i - F_s) \, dt + \int_{t_1}^{t_2} F_s \, dt \quad (142)$$

These three integrals represent the momentum change associated with the three phases of the impact described above.

a. Phase 1.

The first phase is characterized by crushing of the vehicle. During this phase the kinetic energy of the vehicle is decreased by the work done in crushing the vehicle. The work done in crushing the vehicle is given by:

$$\int_{\emptyset}^{X} F_c \, dx = M_v \, [\, V_o^2 - V_1^2 \,] \quad (143)$$

where V_1 = Velocity of vehicle at the end of phase 1

The limit of integration X is defined by the displacement required to produce a force equal to the breakaway force, F_b. The time integral defining phase 1 is given by:

$$\int_{\emptyset}^{t_1} F_i \, dt = M_v \, (V_o - V_1) \quad (144)$$
$$= M_v \, DV_1$$

The procedure used to evaluate this integral is based on knowing

the crush characteristics of the vehicle. Based on these characteristics, the work done to achieve the breakaway force can be calculated and equated to the change in kinetic energy. This will provide the value of V_1 and the value of the phase 1 momentum integral can be calculated.

To gain insight into this process and to estimate the value of the phase 1 integral, we will assume that the force deflection characteristics of the vehicle are linear. The work done to achieve a force, F_b , is given by:

$$\int_{\emptyset}^{X} F_i \, dx = \int_{\emptyset}^{(F_b/k)} K \, x \, dx \qquad (145)$$

$$= F_b^2/(2\ K)$$

where K = stiffness of vehicle (lb/ft)

The change in kinetic energy can be expressed in terms o $DV_1 = (V_o - V_1)$ and the impact speed by:

$$\emptyset.5 M_v\ V_o^{\,2} - \emptyset.5\ M_v\ [V_o^2 - DV_1^2] = \emptyset.5\ M_v\ [2\ DV_1\ V_o - DV_1^2] \qquad (146)$$

Equating these terms, we have:

$$F_b^2/(\ 2\ K\ ) = \emptyset.5\ M_v\ (\ 2\ DV_1 - DV_1^2\ ) \qquad (147)$$

This is a quadratic equation in DV_1. The solution for DV_1 is given by:

$$DV_1 = V_o[\ 1 - \sqrt{1 - F_b^2/(\ K\ V_o\ M_v)}\ ] \qquad (148)$$

For small values of:

$$F_b^2 / (K\ V_o\ M_v) \qquad (149)$$

this expression can be approximated by:

$$DV_1 = F_b^2/(2\ M_v\ K\ V_o) \qquad (150)$$

Table 18 provides values for the delta V for 20 mi/h and 60 mi/h impact speeds and four levels of breakaway force. The approximation expression for delta V provides a good estimate of the true value of delta V for all cases in table 17 except for the low speed impact of the light vehicle. This condition produces the largest Phase 1 velocity change.

b. Phase 2

The phase 2 integral is given by:

$$\int_{t_1}^{t_2} F_s\ dt \qquad (151)$$

The physics of this phase are dominated by the failure mode of the breakaway device. The failure mode of the breakaway device is idealized as shown in figure 62. The area under the force deformation curve is called the breakaway fracture energy (BFE). An estimate of the BFE is given by:

$$BFE = 0.5\ F_b\ D_{max} \qquad (152)$$

where D_{max} = Maximum displacement of base before complete failure

The exact value of the BFE depends on the shape of the force deflection curve. The value of D_{max} is usually small, not more

Table 18. Phase 1 velocity change.

VEHICLE WEIGHT	IMPACT SPEED	BREAKAWAY FORCE LEVEL	DELTA V APPROX.	DELTA V EXACT
lb	mi/h	lb	ft/sec	ft/sec
1800	20	15,000	3.8	4.1
1800	20	20,000	6.8	7.8
1800	20	25,000	10.6	13.8
1800	20	30,000	15.2	29.3
1800	60	15,000	1.3	1.3
1800	60	20,000	2.3	2.3
1800	60	25,000	3.5	3.6
1800	60	30,000	5.1	5.2
4500	20	15,000	1.5	1.6
4500	20	20,000	2.7	2.8
4500	20	25,000	4.2	4.6
4500	20	30,000	6.1	6.9
4500	60	15,000	0.5	0.5
4500	60	20,000	0.9	0.9
4500	60	25,000	1.4	1.4
4500	60	30,000	2.0	2.1

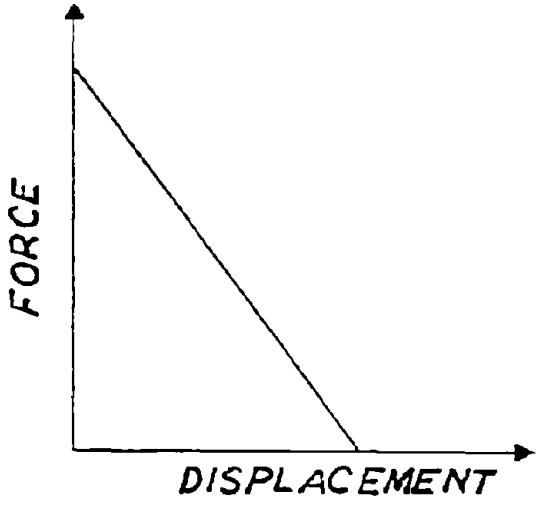

Figure 62. Failure mode of breakaway base.

than 2-in. For D_{max} = 2-in and a F_b = 24,000 lb, the BFE is estimated to be 2,000 ft-lb. This compares to a kinetic energy value of 24,072 ft-lb for an 18,000 lb vehicle at 20 mi/h. A breakaway device should have a low value of BFE to minimize the phase 2 velocity change. This requires that the base be "brittle" in the sense that once the failure is initiated, a small deflection of the base will result in complete separation.

The evaluation of the phase 2 time integral is difficult since during the time period t_1 to t_2 both the inertia of the pole and the base shear force limit the motion of the pole. The velocity of the pole is assumed to be zero at time t_1. To evaluate the integral, the velocity time history of the base is required. We will assume that the velocity of the base at time t_2 is given by:

$$\dot{D}_b(t_2) = m\ V_1 \qquad (153)$$

We will further assume that the base velocity is a linear

function of time in the interval t_1 to t_2 as given by the expression:

$$\dot{D}_b\ (t) = (t-t_1)/(t_2-t_1)\ mV_1 \qquad (\ 154\ )$$

The phase 2 integral can then be written as:

$$\int_{\emptyset}^{D_{max}} (F_s/\ \dot{D})\ dD \qquad (\ 155\ )$$

Evaluating this integral, we have:

$$\int_{t_1}^{t_2} F_s\ dt = \frac{\sqrt{D_{max}}}{m\ V_1} \int_{\emptyset}^{D_{max}} \frac{F_s(D)}{\sqrt{D}}\ dD \qquad (\ 156\ )$$

For the case of a triangular force deformation curve as given by:

$$F_s(D) = F_b\ [\ 1 - (D/D_{max})\ ] \qquad (\ 157\ )$$

The integral becomes:

$$\int_{t_1}^{t_2} F_s\ dt = (4\ F_b\ D_{max})/(3\ m\ V_1) \qquad (\ 158\ )$$

The BFE for a triangular force deformation curve is given by:

$$BFE_t = \emptyset.5\ F_b\ D_{max} \qquad (\ 159\ )$$

Using this expression for BFE, the time integral for phase 2 is given by:

$$\int_{t_1}^{t_2} F_s\ dt = (8\ BFE_t)/(3\ m\ V_1) \qquad (\ 160\ )$$

Thus the phase 2 velocity change is proportional to the BFE and inversely proportional to the speed obtained by the base at the

completion of breakaway.

c. Phase 3

The phase 3 integral is defined by:

$$\int_{t_1}^{t_3} (F_i - F_s)\, dt \qquad (161)$$

This impulse causes the pole to rotate and translate. The translational speed of the pole is given by:

$$\int_{t_1}^{t_3} (F_i - F_s)\, dt = M_p \dot{X}_p \qquad (162)$$

The rotation of the pole is given by:

$$\int_{t_1}^{t_3} D_o F_i\, dt - \int_{t_1}^{t_3} (D_o + z) F_s\, dt = I_p \dot{\theta}_p \qquad (163)$$

where D_o = distance from pole CG to impact point
(D_o+z) = distance from pole CG to base of pole
z = distance from impact point to the base of the pole

The value of D_o is approximately one half the height of the pole, while the value of z is on the order of 1.5 ft. We will assume, to facilitate the analysis that the moment arm for the base shear can be approximated by D_o with only a small error in estimating the angular momentum of the pole. The velocity at the impact point is given by:

$$V_i = \dot{X}_p + D_o \dot{\theta}_p \qquad (164)$$
$$= (R^2+D_o^2)/(M_p R^2) \int_{t_1}^{t_3} (F_i - F_s)\, dt$$

Now the velocity of the pole at the impact point must be greater than the speed of the car for separation. Assuming that the speed at the time of separation is e V_2, the value of e will always be greater than 1. A typical value e from field tests is 1.3 V_2. The resulting value for the phase 3 time integral is:

$$\int_{t_1}^{t_3} F_i - F_s \, dt = e \, V_2 \, M_p \, [\, R^2/(R^2 + D_o^2)] \qquad (165)$$

As discussed in section 3, a value of e equal to 1.3 indicates a loss of energy during the momentum transfer process.

Consider the force deformation curve shown in figure 62. The crush of the car continues after breakaway (point A) up to the maximum force level (point B). The crush force then decreases as the vehicle "springs back" recovering some of the crush distance. At point C, the pole is separated from the vehicle. The energy absorbed by the vehicle during phases 2 and 3 is indicated by the crosshatched area in the figure. This is a major mechanism for the energy dissipation during phases 2 and 3.

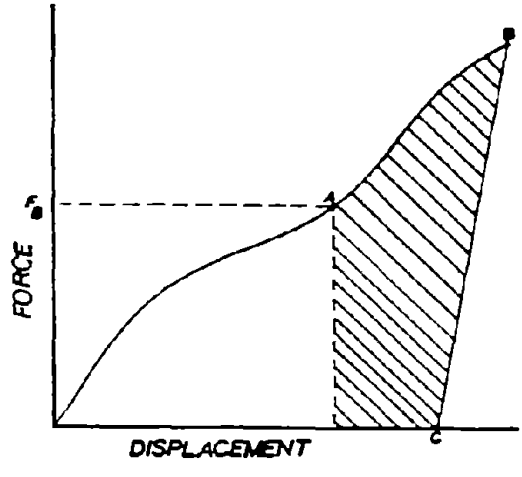

Figure 62. Vehicle crush.

The results of the analysis provide the values for the vehicle velocity change during the impact. In summary, these velocity changes are given by:

$$DV_1 = V_o - V_o \quad 1-[F_b^2/(K\ M_v\ V_o^2)] \qquad (166)$$

$$DV_2 = (8\ BFE)/[m\ (V_o-DV_1)\ M_v] \qquad (167)$$

$$DV_3 = e\ (V_o-DV_1-DV_2)(M_p/M_v)[R^2/(R^2+D_o^2)] \qquad (168)$$

Figure 64 is a plot of total delta V for the case of an 1,800 lb vehicle impacting a 40-ft pole weighing 417 lb. In this plot the BFE is zero and two breakaway force levels are shown 15,000 and 20,000 lb. The stiffness of the vehicle is 18,000 lb/ft. The curve for the 15,000 lb breakaway force is smooth for the speed range 10 to 60 mi/h. However the curve for the 20,000 lb force shows a sharp peak at about 14 mi/h. This is a result of the vehicle being brought to a stop at speeds below 14 mi/h. The delta V values are below the 15 ft/sec level recommended by NCHRP 230 for the impact speed range of 20 mi/h to 60 mi/hr. However the maximum delta V for the 20,000 lb breakaway force is 19 ft/sec at 14 mi/h.

Figure 65 includes the effect of BFE. The BFE is based on the breakaway force level, a maximum displacement of 2-in and a value of m equal to 0.5. Now both the 15,000 and the 20,000 lb breakaway levels show the peaking characteristic. The velocity change for the 20,000 breakaway level is 18 ft/sec while the velocity change for the 15,000 lb breakaway force is 12 ft/sec.

Figure 66 shows the velocity change for a 15,000 lb breakaway force and a BFE of 1,250 ft-lb. Two curves are shown. The lower curve is for a vehicle stiffness of 18,000 lb/ft while the top curve is for a stiffness of 10,000 lb/ft. This is a large variation in vehicle stiffness.

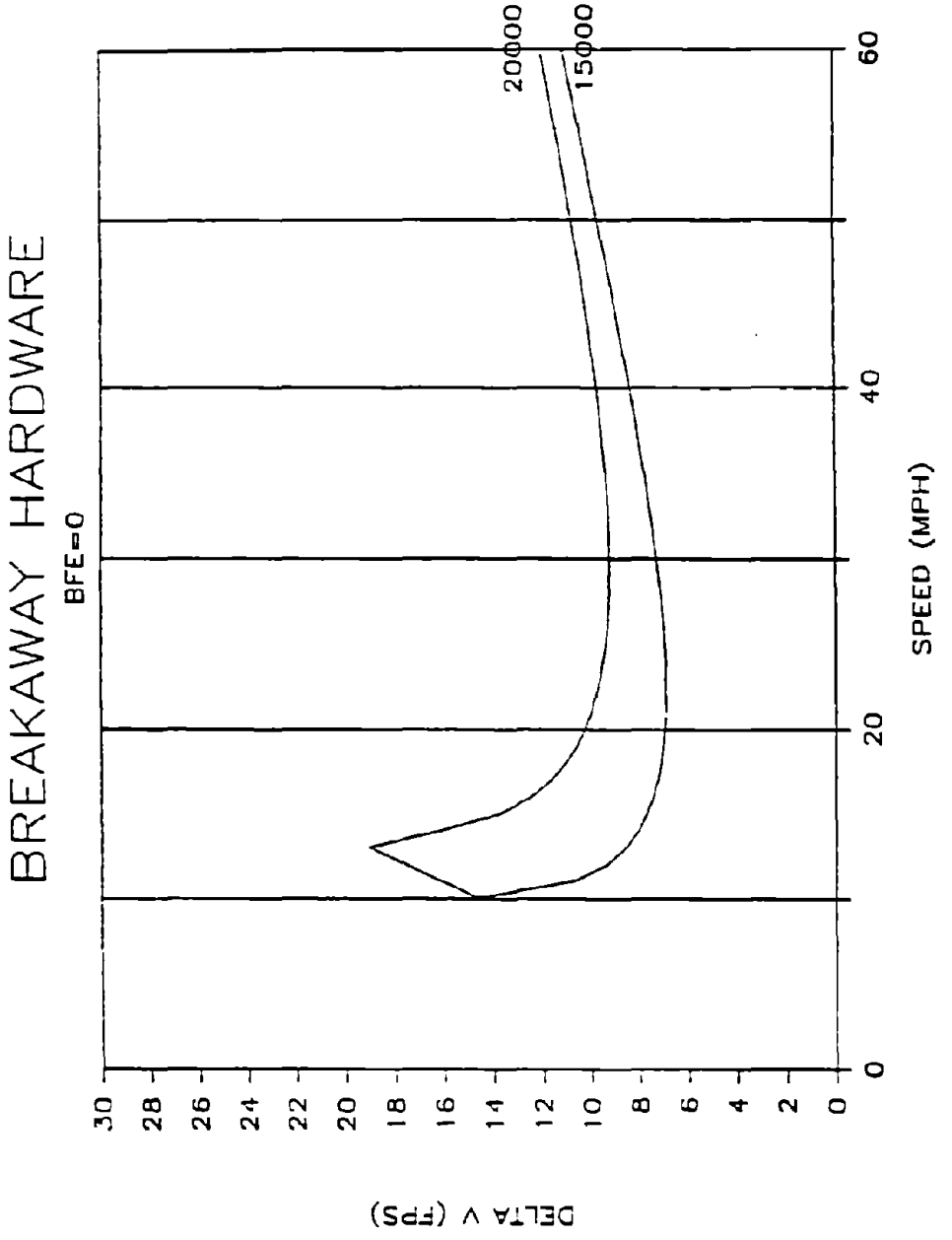

Figure 64. Delta V versus speed for breakaway forces of 15,000 and 20,000 lb.

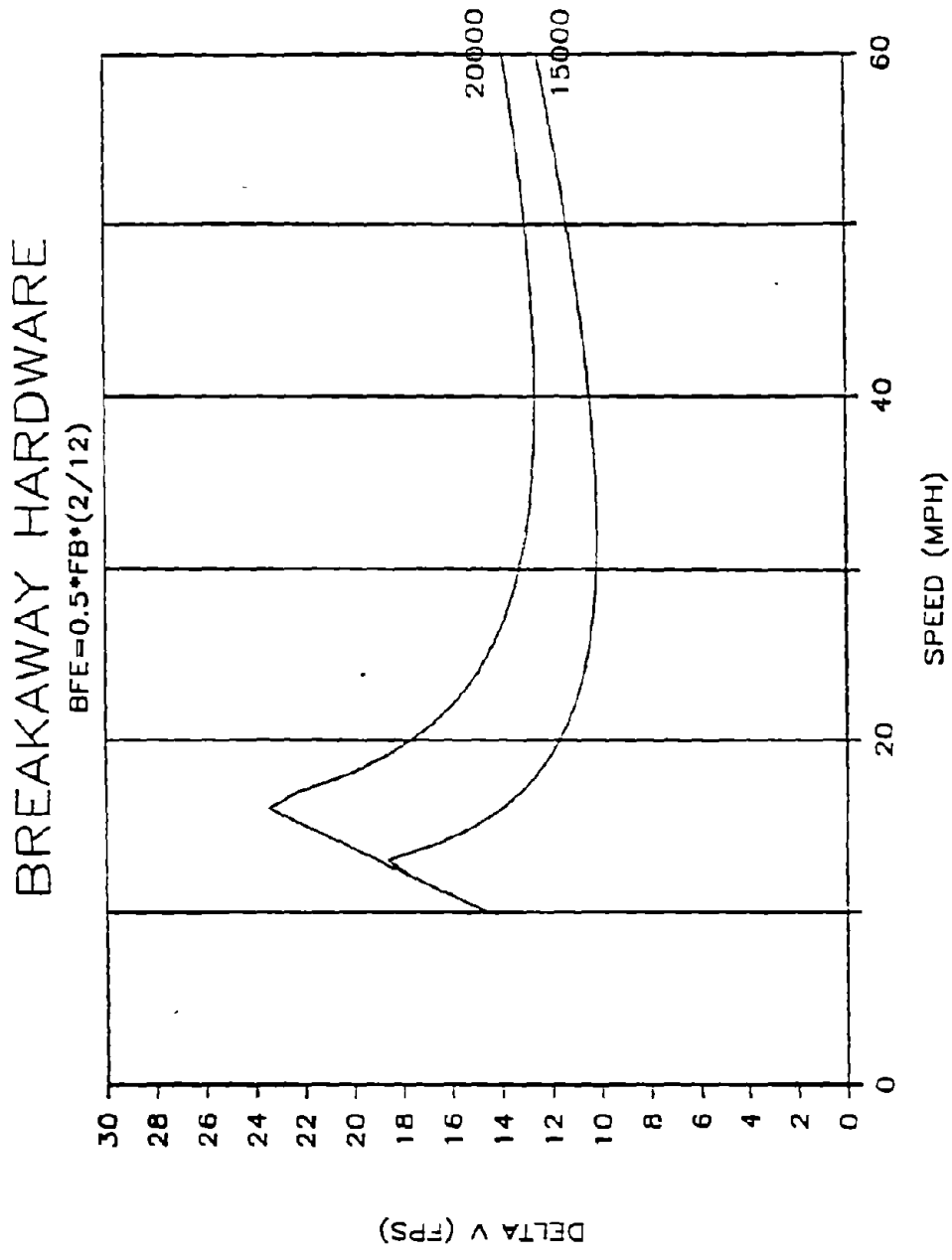

Figure 65. Delta V versus speed including BFE.

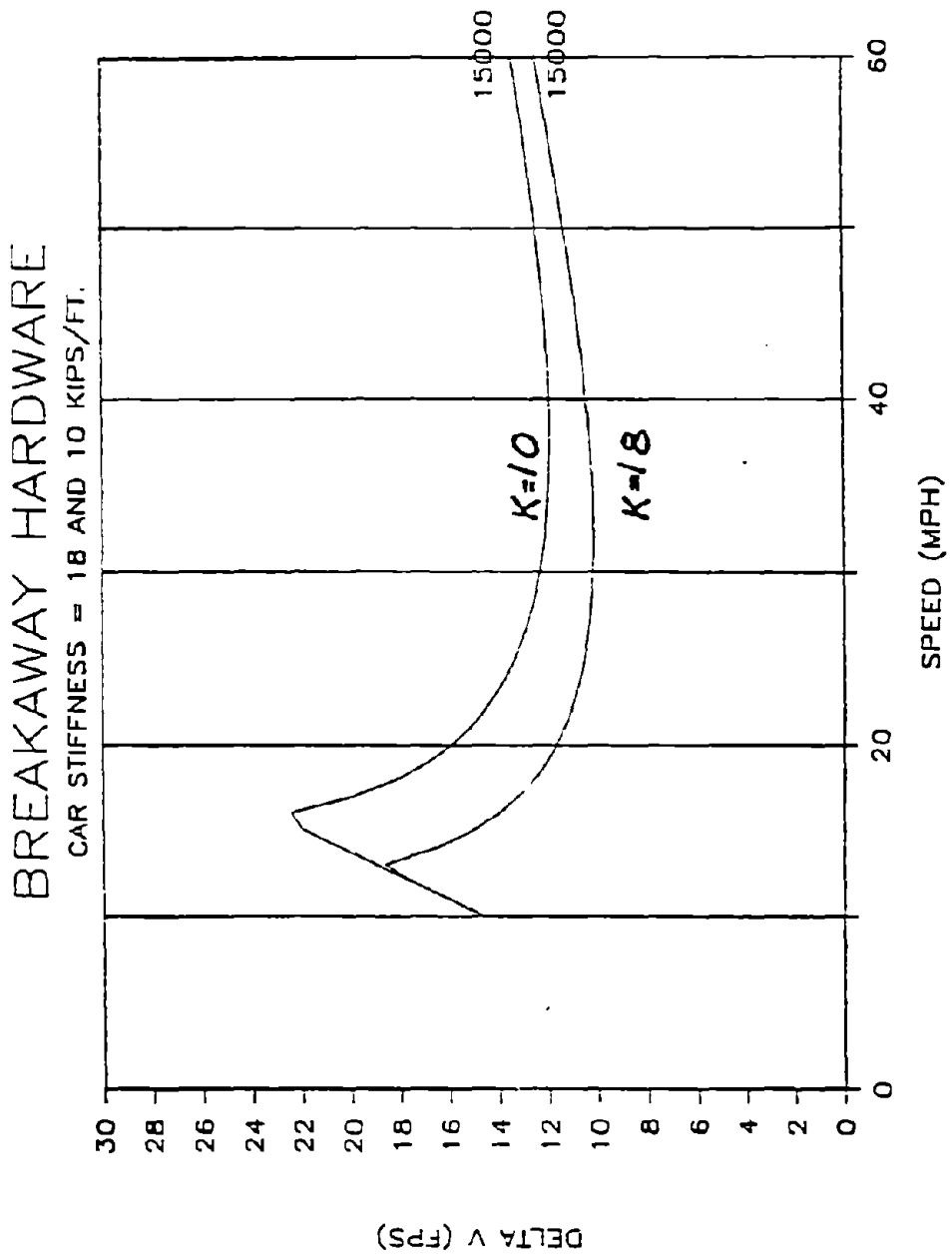

Figure 66. Delta V versus speed for car stiffness of 18 kips/ft and 10 kips/ft.

10. Longitudinal Barriers

The primary purpose of a longitudinal barrier is to safely redirect an errant vehicle. Two major questions in the design of longitudinal barriers are:

1. What strength is required ?
2. What height is required ?

These two questions will be addressed in this section for a barrier with a vertical face.

a. Strength

In NCHRP Report 86, " Tentative Service Requirements for Bridge Rail Systems", a simple mathematical model of a vehicle impacting a longitudinal barrier is developed. This model (the Olson model) estimates the average force acting on the vehicle during the phase of the impact which begins with the initial impact and ends with the vehicle parallel to the longitudinal barrier. Figure 67 shows the geometry on which the model is based.

NCHPR 86 lists the following assumptions on which the model is based:

1. The lateral and longitudinal vehicle decelerations are constant during the time interval required for the vehicle to become parallel to the undeformed barrier.
2. Vertical and rotational accelerations of the vehicle are neglected.
3. The lateral component of velocity is zero after the vehicle is redirected parallel to the barrier railing.
4. The vehicle is not snagged by the barrier railing as it is being redirected.

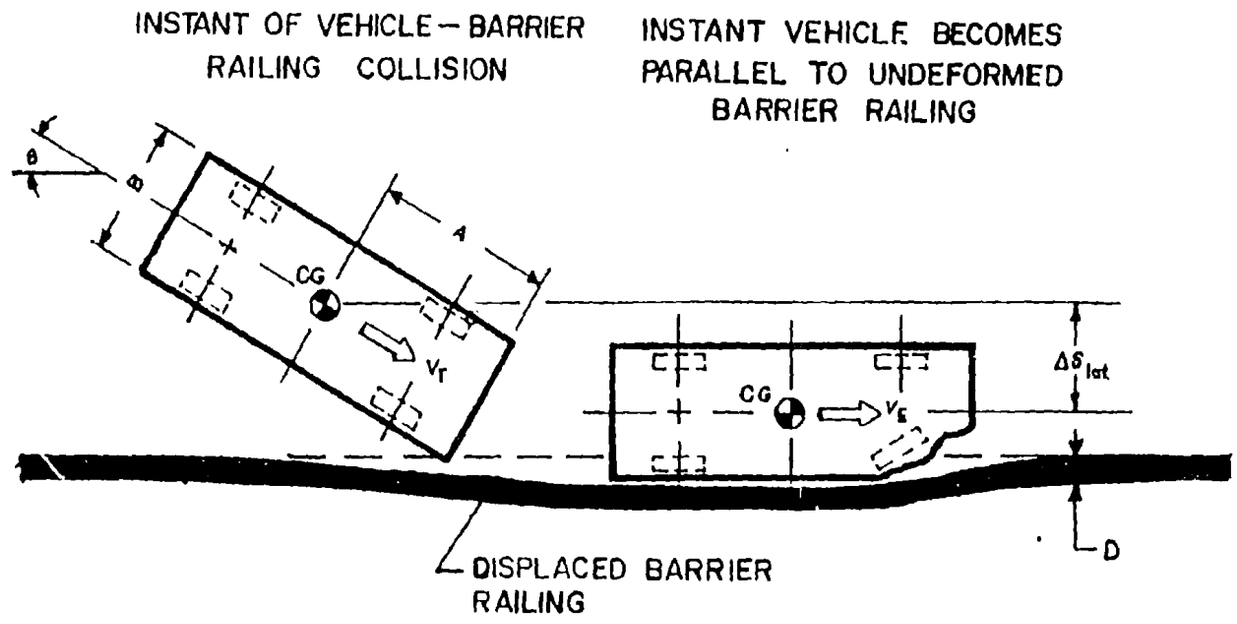

Figure 67. Olson model.

5. Deformation of the vehicle occurs in the area of impact, but the center of mass of the vehicle is not thereby changed appreciably.
6. The mass center of the vehicle moves as if the entire mass were concentrated at that point.
7. A barrier may be rigid or it may be flexible.
8. The friction forces developed between the vehicle tires and roadway surface are neglected.
9. The barrier railing system does not contain discontinuities (jutting curbs, etc.) which might produce abrupt vertical movement of the vehicle.

The lateral displacement (displacement perpendicular to the face of the barrier) of the vehicle during the interval t_o=Ø to t_p is given by:

$$S_{lat}\ [t_o,t_p] = A \sin \Theta - .5\ B\ [1 - \cos \Theta] + D \qquad (\ 169\ )$$

where A = Longitudinal distance from vehicle front end to the vehicle CG
B = Width of the vehicle
Θ = Impact angle
D = Lateral deflection of the barrier

The average lateral velocity of the vehicle in the interval $[t_o,t_p]$ is given by:

$$V_{ave} = S_{lat}/(t_p-t_o) \qquad (\ 170\ )$$

At the beginning of the impact, the component of velocity into the barrier is given by:

$$V_{lat} = V_o \sin \Theta \qquad (\ 171\ )$$

while at time t_p, the lateral velocity is zero. If we assume that the deceleration is constant during the interval t_o to t_p, the average velocity is given by:

$$V_{ave} = 0.5\ V_o \sin\theta \qquad (172)$$

The time required to move the distance S_{lat} is given by:

$$t_p = 2\ S_{lat}/(V_o \sin\theta) \qquad (173)$$

The constant deceleration level (measured in G's) is given by:

$$G = \frac{V_o \sin\theta}{g\ (t_p - t_o)} \qquad (174)$$

where g = acceleration of gravity.

Combining the above expressions, we can express the deceleration level in terms of the impact conditions, vehicle parameters, and barrier deflection by the expression:

$$G = \frac{V_o^2 \sin^2\theta}{2\ g\ [\ A \sin\theta - .5\ B\ (1 - \cos\theta) + D\ ]} \qquad (175)$$

The average lateral force on the barrier during the interval t_o to t_p is given by:

$$F_{ave} = W\ G_{ave} \qquad (176)$$

The longitudinal force (force along the barrier) can be estimated by assuming that it is frictional and related to the normal force

by:

$$F_{long} = m\, F_{lat} \qquad (177)$$

where m = coefficient of friction.

The velocity component parallel to the barrier at the time of impact is given by:

$$V_o \cos \Theta \qquad (178)$$

The momentum change in the longitudinal direction is given by:

$$M\, V_o \cos \Theta - M\, V_p = \int_{\emptyset}^{t_p} F_{long}\, dt \qquad (179)$$

$$= M\, V_o \sin \Theta\, m$$

This expression can be rewritten to provide:

$$V_p = V_o\, [\cos \Theta - m \sin \Theta] \qquad (180)$$

This expression indicates that the loss of speed during the phase of the impact which brings the vehicle parallel to the barrier is dependent only on the friction coefficient, impact angle and impact speed.

The change in kinetic energy of the vehicle is given by:

$$\emptyset.5\, M\, V_o^2 - \emptyset.5\, M\, V_p^2 = \emptyset.5\, M\, V_o^2 [\, 1 - (\cos \Theta - m \sin \Theta)^2]$$

(181)

This expression indicates that the change in kinetic energy is a function of the friction, impact speed and impact angle only.

The distance traveled along the rail is given by the product

of the average longitudinal speed and t_p. The expression for distance traveled is given by:

$$D_t = t_p \ (V_o \cos \theta + V_p)/2 \qquad (182)$$
$$= 2 \ S_{lat} \ (\cot \theta - .5 \ m)$$

This expression indicates that the distance traveled is a function of the vehicle characteristics, impact angle, and friction but not the impact speed.

Results of this model are shown in tables 19 to 22 for ten vehicles. The weights of these vehicles range from 2,000 lb to 30,000 lb. Each table represents a different set of initial impact conditions.

The redirection of a vehicle by a longitudinal barrier is a complex process. This model is quite simple. The model does, however, provide a good estimate of the impact parameters. The assumption of a constant lateral force is an obvious simplification. Test results indicate that the 50 millisecond lateral acceleration levels (i.e. estimates of the peak accelerations) reported are 1.7 to 6 times the levels predicted by the formula. For automobiles, the factor is typically 1.7 to 2.0 for rigid barrier tests. For large single unit vehicles, the higher values are calculated. However, the model does provide an estimate of the "best" that can be expected in the sense of constant redirection force.

b. Height

If a barrier does not have sufficient strength, the vehicle might penetrate the barrier. If the barrier does not have sufficient height, the vehicle might rollover the barrier. In many cases, the lack of sufficient rail height results in a rollover after the the vehicle is redirected back towards the roadway.

Table 19. Olson model results for 60 mi/h and no barrier deflection.

BARRIER DEFLECTION = 0
COEFFICIENT OF FRICTION = 0.2
Vo = 60 MPH
IMPACT ANGLE 20 DEGREES

WEIGHT	A	HALF WIDTH	DS	Tp	Glat	LATERAL FORCE	ENERGY LOSS	WORK DONE (LONG)	WORK DONE (LAT)	TRAVEL LENGTH ALONG RAIL
lb	ft	ft	ft	sec	G's	lb	ft-lb	ft-lb	ft-lb	ft
2,000	5.4	2.8	1.76	0.117	8.0	15,962	57,973	29,818	28,155	9.3
2,750	6.0	3.0	1.96	0.130	7.2	19,736	79,714	41,000	38,713	10.4
3,635	7.2	3.3	2.36	0.157	6.0	21,643	105,367	54,195	51,172	12.5
4,500	7.2	3.3	2.36	0.157	6.0	25,793	130,440	67,091	63,349	12.5
4,000	8.3	2.8	2.76	0.183	5.1	20,434	115,947	59,637	56,310	14.6
5,500	9.1	3.3	3.01	0.200	4.7	25,687	159,427	82,001	77,426	16.0
7,000	9.9	3.3	3.29	0.218	4.3	29,972	202,907	104,364	98,543	17.4
8,000	9.9	3.8	3.27	0.217	4.3	34,412	231,894	119,274	112,620	17.3
17,500	16.5	3.8	5.53	0.367	2.5	44,550	507,268	260,911	246,357	29.3
30,000	19.3	4.0	6.48	0.431	2.2	65,174	869,602	447,276	422,326	34.3

FOR ALL VEHICLES
SPEED AT TIME Tp = 52.3 MPH
PERCENT ENERGY DISSIPATED = 24.1%

Table 20. Olson model results for 60 mi/h and 2-ft barrier deflection.

BARRIER DEFLECTION = 2
COEFFICIENT OF FRICTION = 0.2
Vo = 60 MPH
IMPACT ANGLE 20 DEGREES

WEIGHT	A	HALF WIDTH	DS	Tp	Glat	LATERAL FORCE	ENERGY LOSS	WORK DONE (LONG)	WORK DONE (LAT)	TRAVEL LENGTH ALONG RAIL
lb	ft	ft	ft	sec	G's	lb	ft-lb	ft-lb	ft-lb	ft
2,000	5.4	2.8	3.76	0.250	3.7	7,480	57,973	29,818	28,155	19.9
2,750	6.0	3.0	3.96	0.263	3.6	9,772	79,714	41,000	38,713	21.0
3,635	7.2	3.3	4.36	0.290	3.2	11,725	105,367	54,195	51,172	23.1
4,500	7.2	3.3	4.36	0.290	3.2	14,515	130,440	67,091	63,349	23.1
4,000	8.3	2.8	4.76	0.316	3.0	11,941	115,947	59,637	56,310	25.2
5,500	9.1	3.3	5.01	0.333	2.8	15,441	159,427	82,001	77,426	26.6
7,000	9.9	3.3	5.29	0.351	2.7	18,636	202,907	104,364	98,543	28.0
8,000	9.9	3.8	5.27	0.350	2.7	21,359	231,894	119,274	112,620	27.9
17,500	16.5	3.8	7.53	0.500	1.9	32,717	507,268	260,911	246,357	39.9
30,000	19.3	4.0	8.48	0.564	1.7	49,803	869,602	447,276	422,326	44.9

FOR ALL VEHICLES
SPEED AT TIME Tp = 52.3 MPH
PERCENT ENERGY DISSIPATED = 24.18

Table 21. Olson model results for 40 mi/h and no barrier deflection.

BARRIER DEFLECTION = 0
COEFFICIENT OF FRICTION = 0.2
Vo = 40 MPH
IMPACT ANGLE 20 DEGREES

WEIGHT	A	HALF WIDTH	DS	Tp	Glat	LATERAL FORCE	ENERGY LOSS	WORK DONE (LONG)	WORK DONE (LAT)	TRAVEL LENGTH ALONG RAIL
lb	ft	ft	ft	sec	G's	lb	ft-lb	ft-lb	ft-lb	ft
2,000	5.4	2.8	1.76	0.176	3.5	7,094	25,766	13,253	12,513	9.3
2,750	6.0	3.0	1.96	0.196	3.2	8,772	35,428	18,222	17,206	10.4
3,635	7.2	3.3	2.36	0.236	2.6	9,619	46,830	24,087	22,743	12.5
4,500	7.2	3.3	2.36	0.236	2.6	11,908	57,973	29,818	28,155	12.5
4,000	6.3	2.8	2.76	0.275	2.3	9,082	51,532	26,505	25,027	14.6
5,500	9.1	3.3	3.01	0.300	2.1	11,417	70,856	36,445	34,412	16.0
7,000	9.9	3.3	3.29	0.328	1.9	13,321	90,181	46,384	43,797	17.4
8,000	9.9	3.8	3.27	0.326	1.9	15,294	103,964	53,011	50,053	17.3
17,500	16.5	3.8	5.53	0.551	1.1	19,800	225,452	115,961	109,492	29.3
30,000	19.3	4.0	6.48	0.646	1.0	28,966	386,490	198,789	187,700	34.3

FOR ALL VEHICLES
SPEED AT TIME Tp = 34.9 MPH
PERCENT ENERGY DISSIPATED = 24.1%

Table 22. Olson model results for 40 mi/h and 2-ft barrier deflection.

BARRIER DEFLECTION = 2
COEFFICIENT OF FRICTION = 0.2
Vo = 40 MPH
IMPACT ANGLE 20 DEGREES

WEIGHT	A	HALF WIDTH	DS	Tp	Glat	LATERAL FORCE	ENERGY LOSS	WORK DONE (LONG)	WORK DONE (LAT)	TRAVEL LENGTH ALONG RAIL
lb	ft	ft	ft	sec	G's	lb	ft-lb	ft-lb	ft-lb	ft
2,000	5.4	2.8	3.76	0.375	1.7	3,225	25,766	13,253	12,513	19.9
2,750	6.0	3.0	3.96	0.395	1.6	4,343	35,428	18,222	17,206	21.0
3,635	7.2	3.3	4.36	0.435	1.4	5,211	46,830	24,087	22,743	23.1
4,500	7.2	3.3	4.36	0.435	1.4	6,451	57,973	29,818	28,155	23.1
4,000	8.3	2.8	4.76	0.474	1.3	5,263	51,532	26,505	25,027	25.2
5,500	9.1	3.3	5.01	0.500	1.2	6,863	70,856	36,445	34,412	26.6
7,000	9.9	3.3	5.29	0.527	1.2	8,283	90,181	46,384	43,797	28.0
8,000	9.9	3.8	5.27	0.526	1.2	9,493	103,064	53,011	50,053	27.9
17,500	16.5	3.8	7.53	0.751	0.8	14,541	225,452	115,961	109,492	39.9
30,000	19.3	4.0	8.48	0.845	0.7	22,135	336,490	198,789	187,700	44.9

FOR ALL VEHICLES
SPEED AT TIME Tp = 34.9 MPH
PERCENT ENERGY DISSIPATED = 24.1%

In this section, four scenarios that describe the possible roll behavior of a vehicle will be discussed. These four scenarios are:

1. Stable Behavior (all four tires remain on the ground)
2. Unstable Behavior (vehicle does not rollover but the outside wheels leave the ground)
3. Roll-over to the road side of the barrier
4. Roll-over to the rail side of the barrier

To investigate the first scenario, consider the simple model described in figure 68. The vehicle is considered to be in equilibrium. The horizontal force acting at the CG represents the inertial force on the vehicle. The horizontal force opposing this force represents the force developed by the barrier. The weight of the vehicle is opposed by vertical forces at the wheels. The sum of these forces is equal to the weight of the vehicle. The distribution of the weight will be adjusted to counter the moment produced by the inertial force and the rail force.

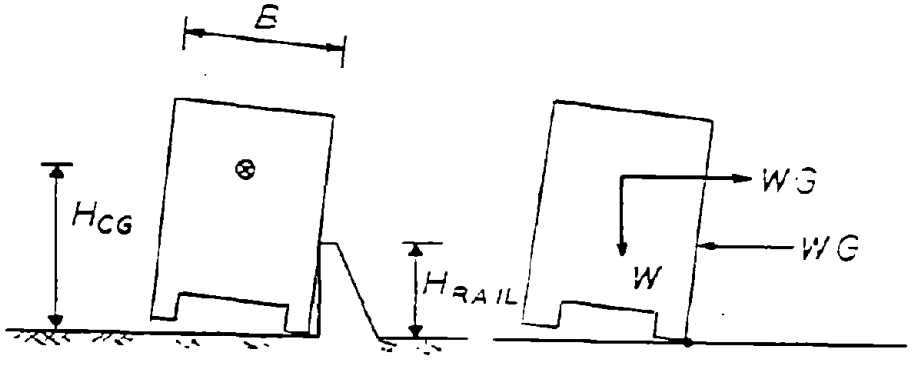

Figure 68. Wheel lift model.

When the outside wheel just starts to lift from the ground, the summation of moments provides:

$$W\ G\ H_{cg} - W\ G\ H_{rail} - W\ (B/2) = \emptyset \qquad (183)$$

where W = Weight of the vehicle
G = Lateral acceleration of the vehicle (g's) required to lift the outside wheel
H_{cg} = Height of the vehicle CG
H_{rail} = Height of the rail
B = Width of the vehicle

The expression for G is given by:

$$G = \frac{B}{2\ (H_{cg} - H_{rail})} \qquad (184)$$

The greater the rail height deficiency ($H_{cg} - H_{rail}$), the lower the value of lateral acceleration required to lift the wheels from the ground. As an example, consider the case of a bus with a CG height of 50-in. If the rail height is 32-in and the bus width 92-in, the lateral acceleration required to lift the outside wheels is:

$$G = (92/2)/(50-32) \qquad (185)$$
$$= 2.55 \text{ g's}$$

Next we will investigate scenario three, roll-over to the road side of the rail. The approach is to calculate the angular impulse generated during the impact which results in a roll rate of the vehicle. The kinetic energy associated with this roll rate

will than be compared with the potential energy that can be stored by the increase in the height of the CG. If the kinetic energy is greater than available potential energy, the vehicle will roll over. If the kinetic energy is less than the available potential energy, the roll rate will be decreased to zero and the weight of the vehicle will cause the vehicle to rotate back to a stable position.

To estimate the roll rate generated during the impact, an impulse momentum approach is taken. The linear impulse required to reduce the lateral momentum to zero is given by:

$$\int_{0}^{T} F \, dt = M \, V_o \sin \Theta \qquad (186)$$

where F = Lateral impact force
M = Mass of the vehicle
V_o = Impact speed
Θ = Impact angle

Assuming that the impact force acts at the top of the rail, the angular impulse is related to the linear impulse by the rail height deficiency. The angular momentum of the vehicle is given by:

$$I_{roll} \dot{\Theta} = (H_{cg} - H_{rail}) \, M \, V_o \sin \Theta \qquad (187)$$

$$= M \, R^2 \dot{\Theta}$$

where I_{roll} = Roll moment of inertia of the vehicle
R = Radius of gyration

Note that this expression neglects the weight of the vehicle which tends to oppose roll motion. The expression therefore tends to overestimate the roll rate. However the moment arm is is taken at the top of the rail which provides a minimum estimate of the

moment arm. If a barrier deflects during an impact, the expression will tend to further overestimate the roll rate. The resulting expression for the roll rate is given by:

$$\dot{\theta} = \frac{(H_{CG} - H_{rail})\ V_o \sin\theta}{R^2} \qquad (188)$$

The kinetic energy is given by:

$$KE_{roll} = 0.5\ M\ R^2\ \dot{\theta}^2 \qquad (189)$$

$$= \frac{M\ V_o^2 \sin^2\theta\ (H_{cg} - H_{rail})^2}{2\ R^2}$$

The potential energy available is based on the maximum raise of the CG during the roll motion. Figure 69 shows the geometry when the CG is just above the inside tire. The rise in the CG is given by:

$$X = \sqrt{H_{cg}^2 + (B/2)^2} - H_{cg} \qquad (190)$$

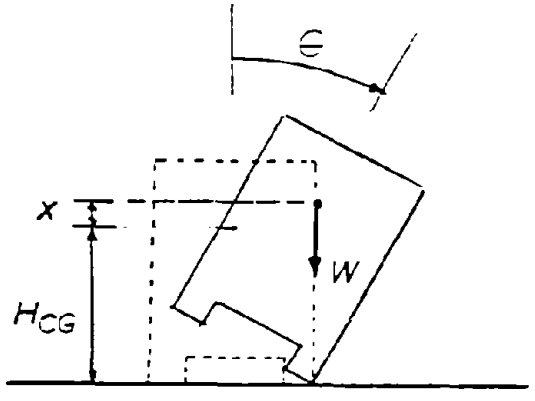

Figure 69. Vehicle at critical roll angle.

The maximum potential energy gained by the vehicle in the roll motion is W X. If the kinetic energy and the potential energy are equated, the resulting equation defines the speed at which the vehicle becomes unstable. This velocity is called the critical velocity. It is defined by the equation:

$$V_{cr} = \frac{R\sqrt{2\,g\,X}}{\sin\Theta\,(H_{cg} - H_{rail})} \qquad (191)$$

Figure 70 shows a plot of the critical velocity as a function of the vehicle CG height for a 32-in rail height. The values for vehicle width and radius of gyration used to generate this plot are:

$$B = 8 \text{ ft} \qquad (192)$$

$$R = .5\sqrt{H_{cg}^2 + (B/2)^2} \qquad (193)$$

Figure 71 shows a similar plot with the barrier height equal to 45-in.

Scenario four describes the case where the vehicle rolls over the barrier. This scenario is similar to scenario three but now the vehicle rotates about the top of the rail. Figure 72 shows the geometry for this motion. The roll moment of inertia for this motion using the parallel axis theorem is given by:

$$I_{rail} = I_{roll}(cg) + M\,d^2 \qquad (194)$$

$$\text{where} \quad d = \sqrt{(h_{cg} - H_{rail})^2 + (B/2)^2}$$

The radius of gyration for the rail rollover mode is given by:

$$R_r = \sqrt{R^2 + (H_{cg} - H_{rail})^2 + (B/2)^2} \qquad (195)$$

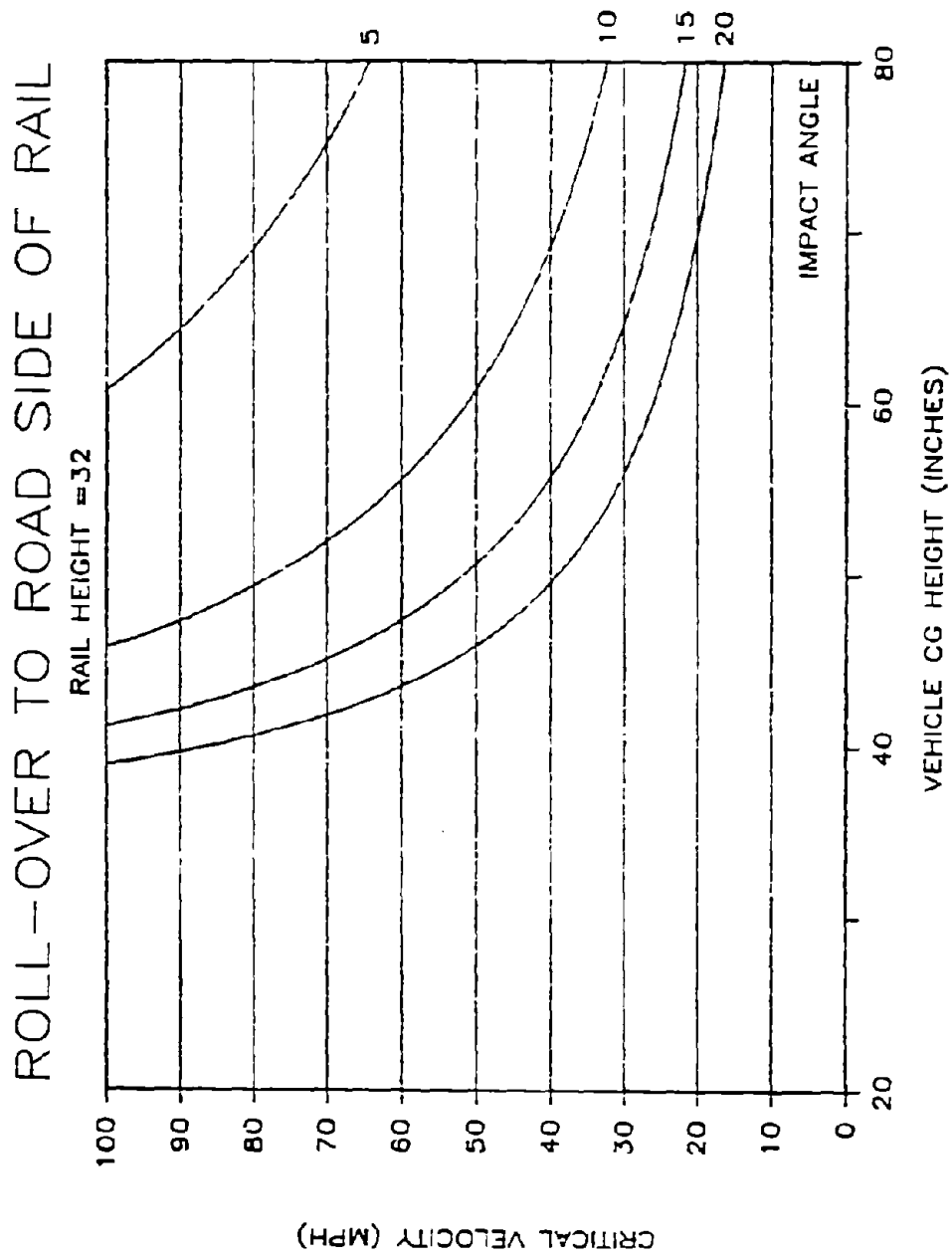

Figure 70. Predicted roll over to the road side of the rail for 32-in high barrier.

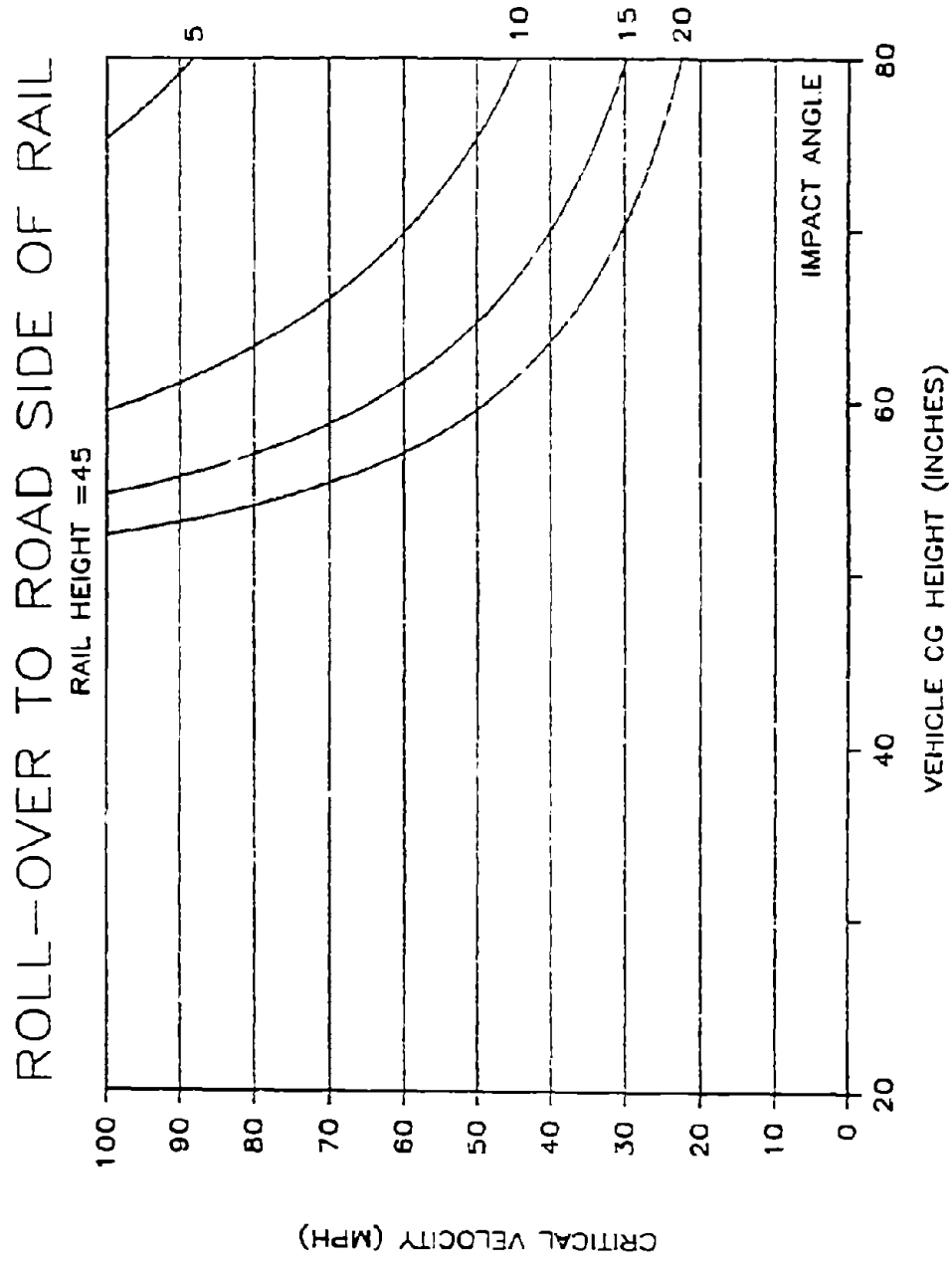

Figure 71. Predicted roll over to the road side of the rail for 45-in high barrier.

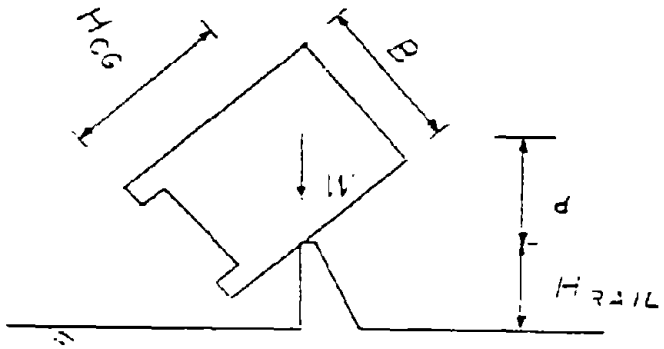

Figure 72. Rail rollover geometry.

The maximum increase in height that the CG can achieve is given by:

$$X_r = H_{rail} + d - H_{cg} \qquad (196)$$

The expression for the critical velocity becomes:

$$V_{cr} = \frac{R_r \sqrt{2 g X_r}}{\sin \Theta \, (H_{cg} - H_{rail})} \qquad (197)$$

Figure 73 shows a plot of the critical velocity as a function of the vehicle CG height for a rail height of 32-in. Figure 74 shows a similar plot for a 45-in rail.

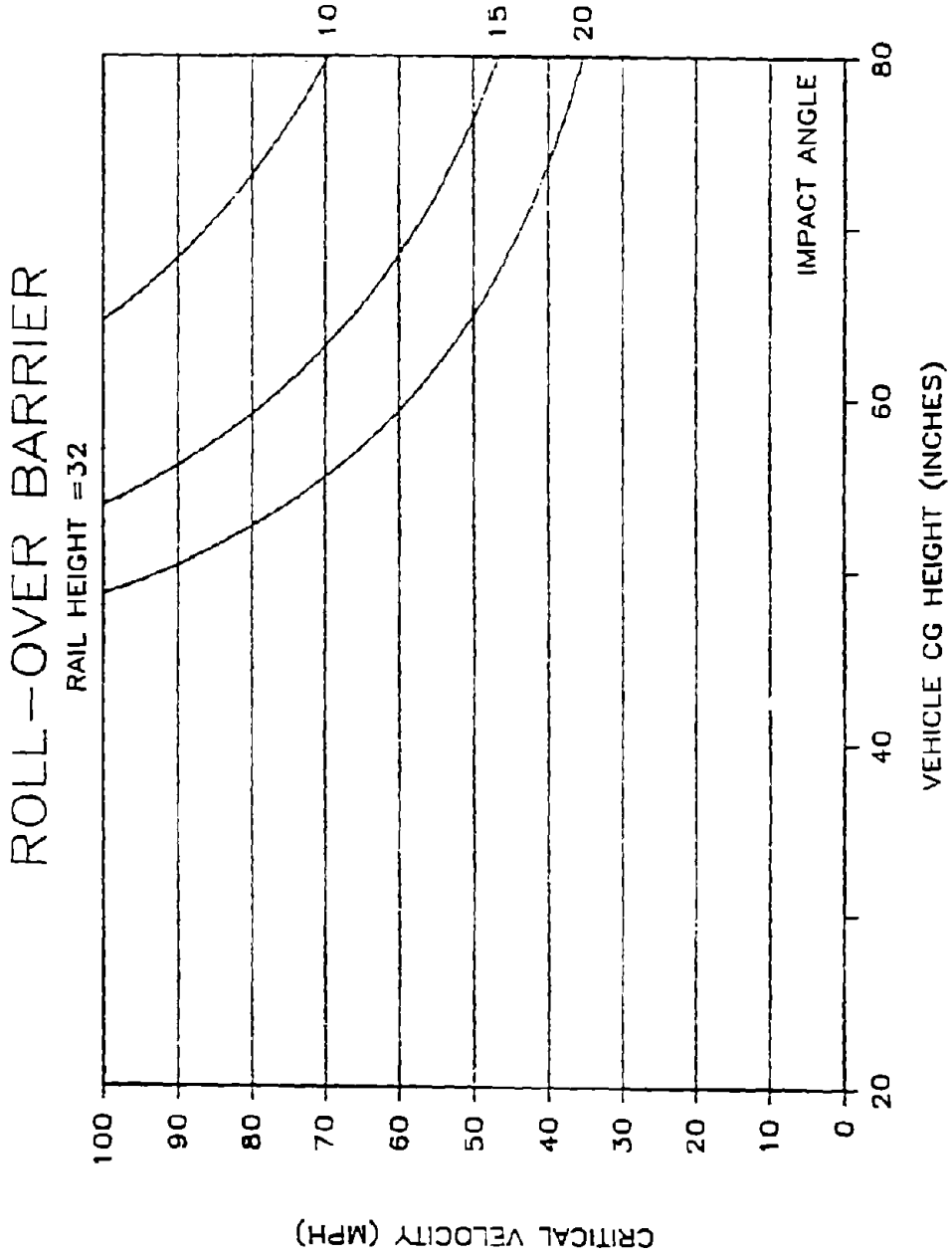

Figure 73. Predicted rollover of the barrier for a 32-in barrier.

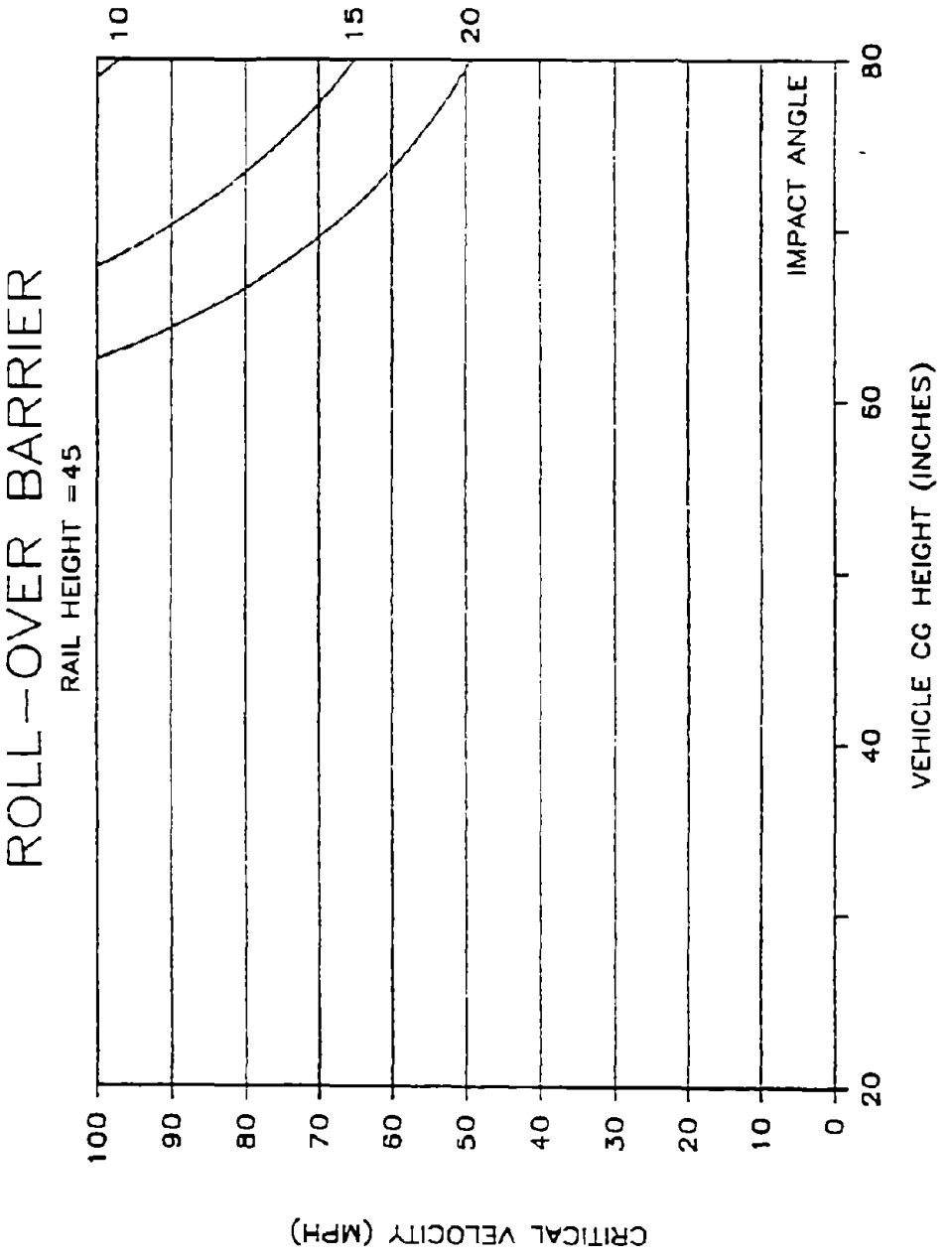

Figure 74. Predicted rollover of the barrier for a 45-in barrier.

Appendix A

CONVERSION FACTORS

To convert from	to	multiply by
foot	meter	0.3048
inch	meter	0.0254
mile	meter	1609.
slug	kilogram	14.59
horsepower	watt	745.7
horsepower	foot pounds/sec	550.
miles/hour	kilometers/hour	1.609
pound force	newton	4.448
foot pound	joule	1.355
pound/ft^2	pascal	47.88

REFERENCES

(1) Robert Olson, Edward R. Post, and William F. McFarland, "Tentative Service Requirements for Bridge Rail Systems," Highway Research Board, 1970.

(2) Peter M. Riede, Ronald L. Leffert, and William A. Cobb, "Typical Vehicle Parameters for Dynamic Studies Revised for the 1980's," Society of Automotive Engineers, Inc., 1984.

(3) J. Hinch, D. Sawyer, D. Stout, G. Manhard, and R. Owings, "Impact Attenuators A Current Engineering Evaluation," Final Report Contract DTFH 61-83-C-00140, December 1985.

(4) J. Hinch, G. Manhard, D. Stout, and R. Owings, "Laboratory Procedures to Determine the Breakaway Behavior of Luminaire Supports in Minisized Vehicle Collisions, Vol. 1," Final Report Contract DTFH61-C-81-00036, March 1986.

(5) J. Hinch, G. Manhard, D. Stout, and R. Owings, "Laboratory Procedures to Determine the Breakaway Behavior of Luminaire Supports in Minisized Vehicle Collisions, Vol. 2," Final Report Contract DTFH61-C-81-00036, March 1986.

(6) J. Hinch, G. Manhard, D. Stout, and R. Owings, "Laboratory Procedures to Determine the Breakaway Behavior of Luminaire Supports in Minisized Vehicle Collisions, Vol. 3," Final Report Contract DTFH61-C-81-00036, March 1986.

(7) Jerry B. Marion, Classical Dynamics of Particles and Systems, (New York: Academic Press, 1965).

(8) Irving H. Shames, Engineering Mechanics Statics, (Englewood Cliffs, New Jersey: Prentice-Hall, Inc., 1959).

(9) AASHTO Subcommittee on Bridges and Structures, "Standard Specifications for Structural Supports for Highway Signs, Luminaires and Traffic Signals," Washington, D.C.: American Association of State Highway and Transportation Officials, 1975.

(10) Raymond P. Owings, Ph.D. and Clarence Cantor, "Simplified Analysis of Vehicle Change in Momentum During Impact with a Breakaway Support," Paper presented at the 55th Annual meeting of the Transportation Research Board.

(11) Jarvis D. Michie, "Recommend Procedures for the Safety Performance Evaluation of Highway Appurtenances," NCHRP 230, March 1981.

(12) AASHTO, "A Policy on Geometric Design of Highways and Streets," Washington, D.C., 1984.

(13) SAE Recommended Practice, "Instrumentation for Impact Tests," SAE J211a

(14) Tom Grubbs, "Laboratory Procedures for: FMVSS 208 Occupant Crash Protection, FMVSS 301 Fuel System Integrity and Part 572 Anthropomorhic Test Dummy," NHTSA TP-208-03